Molecular alterations in muscle wasting and cachexia: therapeutic approaches in animal models

Alba Chacón Cabrera

Director:

Dr. Esther Barreiro

Tutor:

Prof. Dr. Joaquim Gea

UPF Doctoral Thesis / 2016

Department of Experimental and Health Sciences

upf. Universitat Pompeu Fabra Barcelona

“Nothing in life is to be feared, it is only to be understood. Now is the time to understand more, so that we may fear less.”

Marie Curie

Agradecimientos

Esta tesis ha sido el resultado del esfuerzo de muchos. A cada una de estas persones tengo que agradecerles la dedicación, la paciencia, el apoyo, la experiencia y los consejos que me han ofrecido. Gracias por formar parte de esta etapa.

Esther, Quim, Juana, Diego, Jose Yélamos, Ana, Mercè, Anna, Maria, Ester, Mònica, Carme, Clara, Laura, Conchi, Isa, Elena, Estefania, Mireia, Eugenia, Carles, Loli, Eladio, Isa, Loli, Patri, Tina, Carles, Mireia, Marcos, Mar, Alba, Rubén, Pau, Martina.

TABLE OF CONTENTS

ABSTRACT

Cachexia and muscle deconditioning, which are the major comorbidities in patients with chronic diseases including lung cancer (LC), impair disease prognosis. Several biological mechanisms are involved in these two muscle wasting conditions but current treatment options are limited. **Hypothesis:** the biological mechanisms involved in muscle wasting and dysfunction may differ between muscle deconditioning and LC induced cachexia in mice. We also hypothesized that the profile of molecular events implicated in disuse muscle atrophy and muscle recovery, may be different between early and late phases in gastrocnemius of mice exposed to hindlimb unloading. Pharmacological inhibition of MAPK, NF-kB, and proteasome, and the deficiency of either PARP-1 or PARP-2 proteins may revert impaired muscle mass and force in cachectic animals. **Objectives:** to explore the differences in the biological mechanisms potentially involved in muscle wasting and dysfunction in LC cancer cachexia and disuse muscle atrophy. To establish the temporal sequence of the molecular events involved in skeletal muscle mass loss during limb muscle unloading and reloading. To investigate several pharmacological strategies potentially beneficial for cachexia treatment. **Methods**: muscle mass, structure and function, muscle proteolysis, muscle anabolism, signaling pathways, and epigenetic markers were evaluated in 1) the diaphragm and gastrocnemius of LC cachectic mice: wild type, Parp-$1^{-/-}$ and Parp-$2^{-/-}$; 2) in gastrocnemius of mice exposed to different periods of hindlimb immobilization and recovery. **Results**: In LC cachectic wild type mice: muscle proteolysis, MAPK, NF-κB, and protein acetylation were increased, while muscle structure and function, muscle anabolism, microRNAs, myogenic transcription factors and hystone deacetylases were decreased. After late-time points of hindlimb immobilization, muscle structure and function, and muscle anabolism were decreased, whereas FoxO signaling and proteolysis were increased. Muscle reloading improved the alterations seen during immobilization, especially during late phases. Pharmacological inhibition of NF-κB and MAPK, and PARP-1 and -2 deficiencies improved muscle mass and force through a decrease in protein oxidation and catabolism, together with a greater content of contractile and functional proteins. **Conclusions**: Molecular mechanisms involved in muscle

mass loss and dysfunction are slightly different depending on the underlying condition (cancer or disuse). During disuse muscle atrophy, biological mechanisms are characterized by a differential expression profile between early- and late-phases, being the latter a crucial stage for muscle recovery. NF-κB and MAPK inhibitors, as well as available PARP inhibitors, may have potential clinical applicability for cancer cachexia treatment.

RESUMEN

La caquexia y el decondicionamiento muscular, los cuales son las mayores comorbilidades en pacientes con enfermedades crónicas tales como el cáncer de pulmón (CP), empeoran el pronóstico de la enfermedad. Diversos mecanismos biológicos están involucrados en estas dos condiciones de desgaste muscular pero las opciones actuales de tratamiento son limitadas. **Hipótesis:** los mecanismos biológicos implicados en la pérdida de masa y función muscular podrían diferir entre el decondicionamiento muscular y la caquexia inducida por CP en ratones. El perfil de eventos moleculares involucrados en el desuso y en la regeneración muscular, podrían ser diferentes entre las etapas tempranas y tardías en el gastrocnemio de ratones expuestos a inmovilización de la extremidad posterior. La inhibición farmacológica de MAPK, NF-kB, y el proteosoma, y la deficiencia de las proteínas PARP-1 o PARP-2 podrían revertir la pérdida de masa y fuerza de los músculos en los animales caquécticos. **Objetivos:** explorar las diferencias en los mecanismos biológicos potencialmente implicados en la perdida y disfunción muscular en la caquexia por CP y en el decondicionamiento muscular. Establecer la secuencia temporal de eventos biológicos involucrados en la pérdida de masa muscular durante la descarga y recarga del músculo de las extremidades. Investigar diferentes estrategias farmacológicas potencialmente beneficiosas para el tratamiento de la caquexia. **Métodos**: la masa, estructura y función de los músculos, la proteólisis y el anabolismo muscular, vías de señalización, y marcadores epigenéticos fueron evaluados en 1) el diafragma y gastrocnemio de ratones con caquexia por CP: *wild type,* Parp-$1^{-/-}$ y Parp-$2^{-/-}$; 2) en el gastrocnemio de ratones expuestos a diferentes periodos de inmovilización y recarga. **Resultados**: en los animales *wild type* caquécticos: la proteólisis, MAPK, NF-κB, y la acetilación proteica aumentaron, mientras que la estructura, función, anabolismo, microRNAs, factores de transcripción miogénicos, y las histonas deacetilasas disminuyeron. Después de periodos tardíos de inmovilización de las extremidades posteriores, la estructura, función, y el anabolismo muscular disminuyeron, mientras que FoxO y la proteólisis se incrementaron. Tras la recarga muscular, las alteraciones observadas durante la inmovilización mejoraron, especialmente durante las

fases finales. La inhibición farmacológica de NF-kB y MAPK, y la deficiencia de PARP-1 o -2 mejoraron la masa y fuerza muscular mediante la disminución de la oxidación y el catabolismo proteico, junto con un mayor contenido de proteínas contráctiles y funcionales. **Conclusiones**: Los mecanismos moleculares implicados en la pérdida de masa y función muscular son ligeramente diferentes dependiendo de la enfermedad subyacente (cáncer o desuso). Durante el desuso, dichos mecanismos se caracterizan por un perfil de expresión diferencial entre fases de inmovilización tempranas y tardías, siendo estas últimas cruciales para la recuperación muscular. El tratamiento con inhibidores de NF-kB y MAPK, así como los inhibidores de PARP disponibles, pueden tener potencial aplicabilidad clínica para el tratamiento de la caquexia por cáncer.

PREFACE

Scientific collaborations

In the current thesis, the investigations have been conducted in the Muscle Wasting and Cachexia in Chronic Respiratory Diseases and Lung Cancer Research group, Institute of Medical Research of Hospital del Mar (IMIM)-Hospital del Mar, Barcelona, Spain, and Department of Health Sciences (CEXS), Universitat Pompeu Fabra (UPF), Barcelona, Spain. Moreover, three of the five studies have been performed in collaboration with researchers from other departments and centers as described below.

Study #1 was conducted in collaboration with the Research Area Institute of Oncology 'Angel H. Roffo', University of Buenos Aires, Buenos Aires, Argentina, and the Department of Biomedical Sciences, University of Padova, Dubelcco Telethon Institute, Venetian Institute of Molecular Medicine, Padova, Italy.

Study #2 was conducted in collaboration with the Cancer Research Program-Immunology, *Hospital del Mar* Medical Research Institute (IMIM)-*Hospital del Mar*, Barcelona, Spain.

Study #3 was conducted in collaboration with the Cancer Research Program-Immunology, *Hospital del Mar* Medical Research Institute (IMIM)-*Hospital del Mar*, Barcelona, Spain, and the *Unitat de Patologia Neuromuscular i Mitocondrial, Hospital Universitari Vall d'Hebron Institut de Recerca (VHIR), Universitat Autònoma de Barcelona.*

Publications

Some of the studies included in the current thesis have already published in international journals:

Study #1

Chacon-Cabrera A, Fermoselle C, Urtreger AJ, Mateu-Jimenez M, Diament MJ, de Kier Joffé ED, Sandri M, Barreiro E. Pharmacological strategies in lung cancer-induced cachexia: effects on muscle proteolysis, autophagy, structure, and weakness.

J Cell Physiol. 2014;229(11):1660-72.

Study #2

Chacon-Cabrera A, Fermoselle C, Salmela I, Yelamos J, Barreiro E. MicroRNA expression and protein acetylation pattern in respiratory and limb muscles of Parp-1(-/-) and Parp-2(-/-) mice with lung cancer cachexia.
Biochim Biophys Acta. 2015;1850(12):2530-43.

In addition, results corresponding to studies #3, #4 and #5 have been recently submitted:

Study #3

Chacon-Cabrera A, Fermoselle C, García-Arumi E, Andreu AL, Yelamos J, Barreiro E. Deficiency of either PARP-1 or PARP-2 improves protein anabolism and catabolism, phenotype, ad function in respirator and limb muscles of lung cancer cachectic mice.
Submitted J Cell Physiol.

Study #4

Chacon-Cabrera A, Lund-Palau E, Gea J, Barreiro E. Time-course of muscle mass loss, damage, and proteolysis in gastrocnemius following unloading and reloading: implications in chronic diseases.
Submitted PLoS One.

Study #5

Chacon-Cabrera A, Lund-Palau E, Gea J, Barreiro E. Short- and long-term hindlimb immobilization and reloading: profile of epigenetic events in gastrocnemius.
Submitted J Cell Physiol.

Communications

Some of the results included in the current thesis, as well as those from other studies that are not part of the Ph.D thesis, have been previously presented in the form of an abstract or oral communication at several national and international conferences.

1- Chacon-Cabrera A, Rojas Y, Nin N, Martínez-Caro L, Gea J, Esteban A, Barreiro E, Lorente JA.

Efectos de la ventilación mecánica en los músculos respiratorios y periféricos de ratas con y sin sepsis.

V Jornadas de Formación del CIBERES (Abstract book, page 34), Bunyola, Mallorca, Illes Balears, Spain, October 2012.

2- Chacon-Cabrera A, Fermoselle C, Urteger AJ., Mateu-Jimenez M, Diament MJ., Bal De Kier Joffé ED., Sandri M, Barreiro E.

Pharmacological strategies in lung cancer-induced cachexia: effects on muscle proteolysis, autophagy, structure, and weakness.

XVII Jornadas de Formación del CIBERES (Abstract book, page 18), Valladoild, Spain, October 2014.

3- Chacon-Cabrera A, Fermoselle C, Salmela I, Yelamos J, Barreiro E.

MicroRNA and protein acetylation expression in respiratory and limb muscles of Parp-1-/- and Parp-2-/- mice with lung cancer cachexia.

The 6th EMBO Meeting (Abstract book, page 95), Birmingham, UK, September 2015.

4- Chacon-Cabrera A, Fermoselle C, Salmela I, Yelamos J, Barreiro E.

MicroRNA and protein acetylation expression in respiratory and limb muscles of Parp-1-/- and Parp-2-/- mice with lung cancer cachexia.

XVIII Jornadas de Formación del CIBERES (Abstract book, page 29), Valladoild, Spain, October 2015.

Funding

The research studies inlcuded in the current Ph.D thesis have been supported by:

CIBERES; FIS 11/02029; FIS 12/02534; FIS 14/00713; 2009-SGR-393; SEPAR 2010; SEPAR 2013; FUCAP 2011; FUCAP 2012; and Fundació La Marató de TV3 (MTV3-07-1010 and MTV3-2013-4130).

The binding of the present doctoral thesis has been funded by “Fundació IMIM”.

Acknowledgements

I am grateful to Ms. Mònica Vilà, Isabel Fabra-Heredia, Mireia Solà-Colom, Eugènia Serramontmany, Estefania Carrillo, and Elena Lund-Palau for their help with part of the laboratory experiments.

ABBREVIATIONS

AcFoxO: acetylated forkhead box O

ActRIIB: activin receptor type-IIB

ADP: adenosine diphosphate

Akt: RAC-alpha serine/threonine-protein kinase

ATP: adenosine triphosphate

Bax: Bcl-associated X

Bcl-2: B-cell lymphoma 2

C8-20S: C8 alpha-subunit of the 20S proteasome

CAIII: carbonic anhydrase III

CK: creatine kinase

CoA: coenzyme A

COPD: chronic obstructive pulmonary disease

CSA: cross-sectional area

DGCR8: Drosha associated with Pasha

DNA: deoxyribonucleic acid

E1: ubiqiutin-activating enzyme

E2: ubiquitin-conjugating enzyme

E3: ubiquitin-ligase enzyme

eIF3F: eukariotic translation initiation factor 3 subunit F

ELISA: enzyme-linked immunosorbent assay

ERK: extracellular signal-regulated kinases

FAD: flavin adenine dinucleotide

FoxO: forkhead box O class

GDF: growth and differentiation factor

HAT: histone acetyltransferase

HDAC: histone deacetylase

HNE: hydroxynonenal

I: immobilization

INF-γ: interferon-gamma

IGF-1: insulin-like growth factor 1

IkB-α: nuclear factor kappa-light-chain-enhancer of activated B cells inhibitor-alpha

IL-1β: interleukin-1-beta

IL-6: interleukin-6

JNK: c-Jun NH_2-terminal kinase

LC: lung cancer

LC3: light chain-3

MAFbx: muscle atrophy F box

MAPK: mitogen-activated protein kinase

MDA: malondialdehyde

MEF2: myocyte enhancer factor 2

miR: microRNA

miRNA: microRNA

MRF: myogenic regulatory factor

mRNA: messenger ribonucleic acid

mtDNA: mitochondrial deoxyribonucleic acid

mTOR: mammalian target of rapamycin

MuRF1: muscle ring finger protein 1

MyHC: myosin heavy chain

MyoD: myogenic differentiation

NAD: nicotinamide adenine dinucleotide

nDNA: nuclear deoxyribonucleic acid

NF-kB: nuclear factor kappa-light-chain-enhancer of activated B cells

NT: nitrotyrosine

p70S6K: 70 protein S6 kinase

PARP: Poly-ADP ribose polymerase

Pax7: Paired Box 7

pERK: phosphorylated extracellular signal-regulated kinase

PET: positron emission tomography

pFoxO: phosphorylated forkhead box O

PGC1-α: peroxisome proliferator-activated receptor-γ coactivator 1-alpha

PI3K: phosphoinositide 3-kinase

p-mTOR: phosphorylated mammalian target of rapamycin

p-p70S6K: phosphorylated 70 protein S6 kinase

PTEN: Phosphatase and tensin homolog

qRT-PCR: quantitative reverse transcription - polymerase chain reaction

R: recovery

RISC: ribonucleic acid-induced silencing complex

RNA: ribonucleic acid

RNS: reactive nitrogen species

ROS: reactive oxygen species

SIRT1: silent information regulator 1

SMAD: similar to mothers against decapentaplegic

SOD: superoxide dismutase

SRF: serum response factor

TGF-β: transforming growth factor-beta

TNF-α: tumour necrosis factor-alpha

TRIM32: Tripartite motif-containing protein 32

TUNEL: Terminal deoxynucleotidyl transferase-mediated dUTP nick-end labeling

UPF: Universitat Pompeu Fabra

UPS: ubiquitin-proteasome system

XPO5: exportin-5

YY1: yin yang 1

INTRODUCTION

In this section the main concepts that comprise the current thesis are defined, including muscle wasting and dysfunction, which are the major comorbidities associated with chronic diseases and several conditions in humans. Cancer induced cachexia and disuse muscle atrophy are the two conditions studied in this thesis. In the first place skeletal muscles are introduced, since are the target organs analyzed in this investigation. Secondly, biological mechanisms involved in the process of muscle dysfunction and muscle mass loss in cancer-induced cachexia and disuse muscle atrophy are also described in this section.

1- Skeletal muscles

Around 40% of the total body weight is comprised of skeletal muscle, which is a specialized tissue with the capacity to contract and relax and it is essential to generate movements that allow the development of physiological activities such as maintain posture, breathing, walking or running. Thus, these organs need to be in optimal conditions to perform their vital functions (1, 2).

1.1- Muscle structure and organization

Skeletal muscles are composed of a group of fibers, called muscle fascicles, which are formed by muscle cells or muscle fibers that are organized with their longitudinal axes in parallel (1, 2). Each skeletal muscle fiber is surrounded by a cell membrane known as sarcolemma, and has a cytoplasm named sarcoplasm. Within the sarcoplasm of muscle cells are located multiple nuclei for each muscle fiber, mitochondria, and the main intracellular structures in striated muscles, the myofibrils (figure 1) (1-3). Every myofibril is formed by different types of proteins: the muscle contractile proteins actin and myosin, the regulatory proteins tropomyosin and troponin, and the accessory proteins titin and nebulin (2). While actin is grouped forming clusters in order to constitute the thin filaments, myosin molecules are joined together forming the thick filaments (figure 2) (1, 4).

The disposition of thick and thin filaments in a myofibril originates a repeating pattern of light and dark bands, characteristic of the skeletal muscle (1, 2, 4, 5). One repeating unit of the pattern forms a sarcomere, which is the

contractile unit of striated muscles and consists of various distinct regions. Each sarcomere is delimited by two dense protein regions named **Z-discs**. The area between the Z-discs alternates light bands and dark bands, known as **I** and **A bands** respectively. I bands only has thin filaments, while A bands contains thick filaments. Both myosin and actin filaments are overlapped in external regions of A bands, whereas the central region (**H zone**) only contains myosin. In the middle of H zone is located the **M line**, where the thick filaments are attached (1-3, 5, 6).

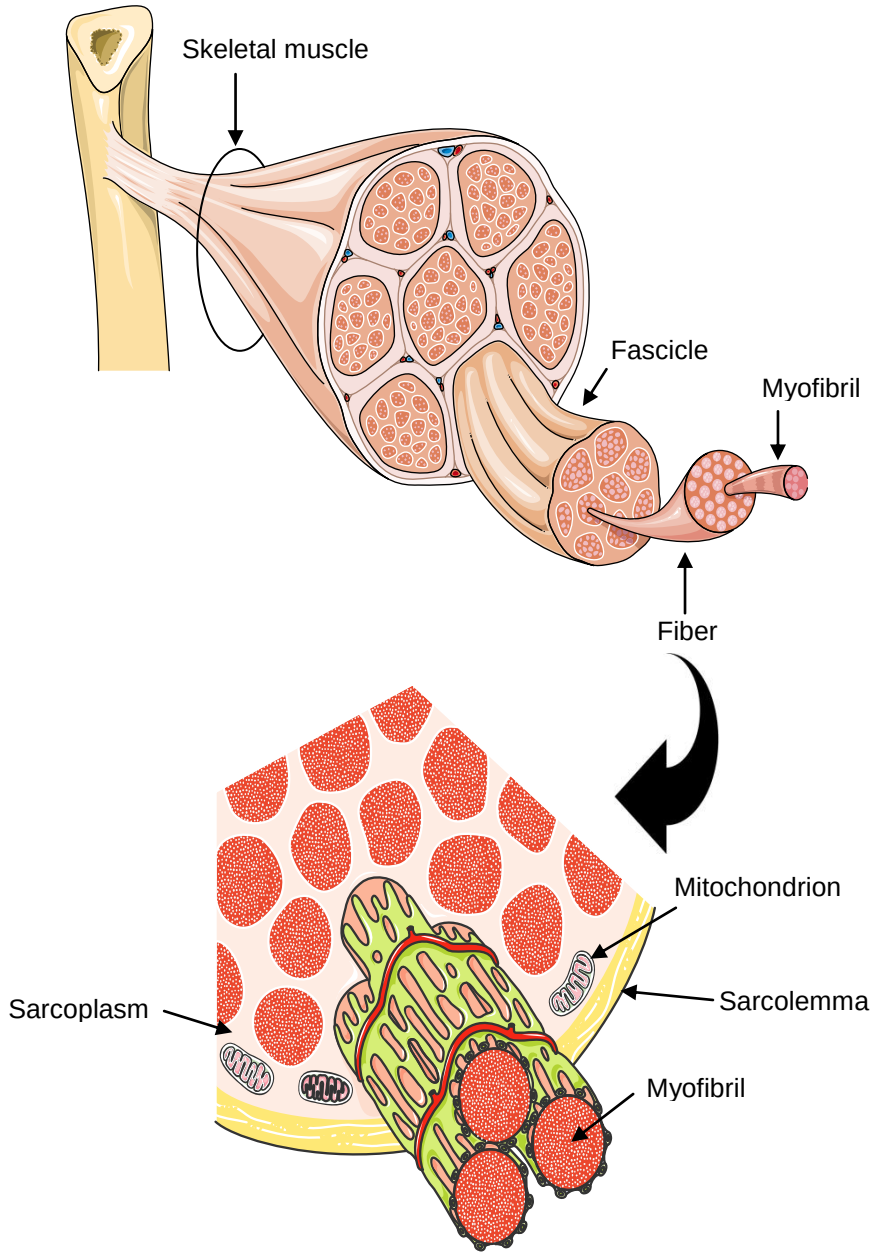

Figure 1. Skeletal muscle structure and organization. Figure was produced using Servier Medical Art (http://www.servier.com).

Furthermore, there are other proteins that also contribute to the stability and structure of the sarcomere. Titin is a big protein that expands from M line to Z disc and acts maintaining the myosin filaments centered on the sarcomere, while nebulin regulates thin filament longitude during sarcomere assembly (2, 6).

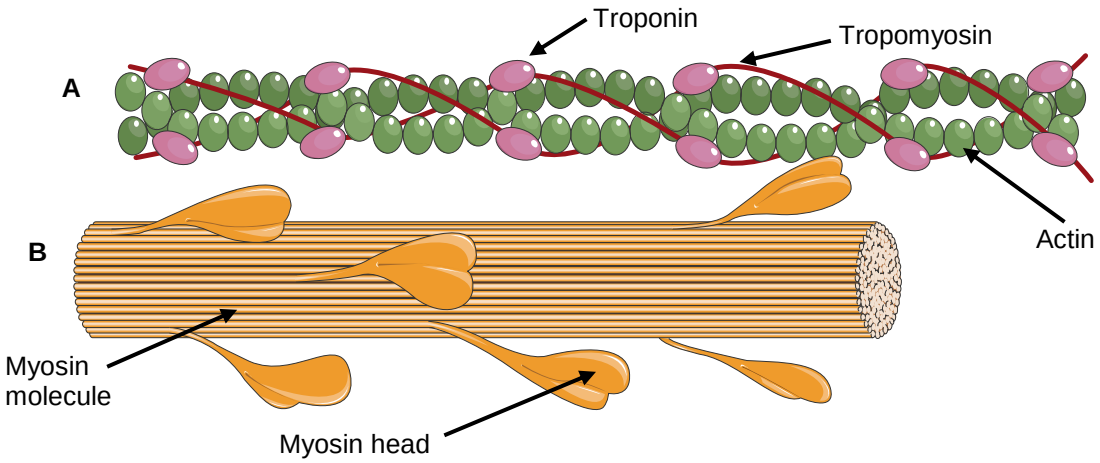

Figure 2. Thin (A) and thick (B) filaments of a muscle myofibril. Figure was produced using Servier Medical Art (http://www.servier.com).

1.2- Fiber type composition

Myosin is the most abundant protein in the skeletal muscle and has the ability to create movement and generate force through actin-myosin cross-bridge mechanism.

Several isoforms of myosin take place in different types of muscle and contribute to determine the muscle's speed and contraction. Each fiber type confers to the muscle different structural and functional properties. In this regard, each muscle can perform different activities depending on the fiber type composition. Proportions and sizes of each muscle fiber type can change in response to different conditions such as exercise, training and environmental factors, which regulate muscle phenotype with the purpose of adapt to the different functional requirements (1, 5, 7, 8).

Muscle fibers can be classified into three main types according to the morphological, biochemical, physiological and metabolic characteristics as showed in the following table (Table 1) (1, 2, 5, 8):

	Type I	Type IIa	Type IIb
METABOLIC CHARACTERISTICS			
Twitch speed	Slow	Fast	Very fast
Myosin ATPase activity	Slow	Fast	Very Fast
Metabolism	Oxidative; aerobic	Oxidative glycolytic; aerobic	Glycolytic; anaerobic
Myoglobin content	High	Medium	Low
Endurance	Fatigue-resistant	Moderately fatigue-resistant	fatigable
STRUCTURAL CHARACTERISTICS			
Color	Dark red	Red	White
Mitochondrial density	High	Medium	Low
Fiber diameter	Small	Medium	Large
ACTIVITIES BEST STUDIED FOR			
Use	Endurance-type activities: running a marathon, maintaining posture	Sprinting, walking	Short-term intense or powerful movements: jumping

Table 1. Characteristics of skeletal muscle fiber types (1, 5, 7).

The **type I** muscle fibers are the slow-twitch fibers, characterized by forming part of red muscles, color given by its high myoglobin content. This type of

fibers has an oxidative metabolism owing to the elevated mitochondrial content that makes it fatigue resistant (8, 9). Both **type IIa** and **type IIb** muscle fibers are the fast-twitch fibers, which are found in the white muscles (low myoglobin content) and are characterized for having a glycolytic metabolism. **Type IIa** fibers possess high mitochondrial content that confers them an oxidative-glycolytic metabolism, which make them fatigue resistant, but less than type I fibers (5, 8, 9). However, **type IIb** fibers have low mitochondrial content and they do not have oxidative metabolism. This type of fibers has exclusively glycolytic metabolism that make them easily fatigable (1, 5, 9).

As previously mentioned, every muscle in our body is composed by proportions of each fiber type in order to perform a given function. Moreover, the distribution pattern of muscle fiber types varies between species. For example, the diaphragm, a respiratory muscle exposed to continuous involuntary contractions, is considered a faster muscle in rodents than in humans (10). In this manner, this respiratory muscle contains 10% of type I fibers and 90% of type II fibers in mice (11), weather in humans the proportions are around 30% of type I and 70% of type II fibers (12).

In contrast, limb muscles are subjected to voluntary contractions that allow the generation of daily life movements. Gastrocnemius, the most representative limb muscle in rodents, is essentially involved in running, jumping and other "fast" movements of limbs, and for this reason it contains a high proportion of fast-twitch fibers. By contrary, soleus muscle which is closely connected to the gastrocnemius and it is implicated in standing and walking, is characterized by containing a higher proportion of slow-twitch fibers (13-15).

1.3- Energy production in muscles

Muscles need energy constantly in order to contract, to generate force and to produce movement. ATP is the energy source of muscle physiology and it is synthesized by different pathways depending on muscle demands (1, 15):

- **Direct phosphorylation:** for short-duration exercise (15 seconds), ATP is formed from creatine phosphate and ADP by the enzyme creatine kinase (CK). ATP generated from this pathway is very limited, so when the muscle

activity is prolonged (30-40 seconds), ATP is synthesized by anaerobic metabolism (5, 15).

- **Anaerobic pathway (glycolysis and lactic acid formation):** in the cytosol, each glucose molecule is converted in two pyruvate molecules, two ATP, and two NADH through the glycolysis. Owing to the lack of oxygen, piruvate is converted into lactate by the action of the enzyme lactate dehydrogenase (5, 6, 15).

- **Aerobic pathway:** for prolonged-duration exercise (hours) and under adequate oxygen conditions, the pyruvate obtained in the glycolysis is conducted inside the mitochondria and converted to acetyl coenzyme A (CoA). The acyl unit of acetyl CoA then is incorporated into the citric acid cycle where is combined with oxaloacetate to produce citrate. Each completed cycle releases two molecules carbon dioxide and produces one ATP, three NADH, and one $FADH_2$ (1, 2, 5).

  In the next step of the aerobic metabolism, NADH and $FADH_2$ transport their electrons to the electron transport system, located in the inner mitochondrial membrane. Energy from electrons moving along the electron transport system pumps protons from the mitochondrial matrix to intermembrane space, generating a proton concentration gradient. Then, protons move back across the membrane to the matrix, via ATP synthase (4-6).

  The synthesis of ATP through the electron transport system is known as oxidative phosphorylation and has a net energy yield of thirty-two molecules of ATP for each molecules of glucose (5, 6).

2- Muscle dysfunction and muscle wasting

Strength and endurance are the main functional properties of the muscle. Strength is the capacity of the muscle to generate force through muscle contractions, while endurance is the ability of the muscle to maintain that force for a long period of time. Strength depends on muscle mass, whereas endurance depends on the proportion of type I fibers, which are the most fatigue-resistant (16, 17).

Skeletal muscle dysfunction is an alteration of normal muscular activity, and it is characterized by a decline in strength and/or endurance of the affected muscles, which may lead to muscle weakness and fatigue (16, 17). Muscle dysfunction may be associated with **muscle wasting,** defined as muscle mass loss. Moreover, muscle wasting may also be part of cachexia, which is defined as a multifactorial syndrome characterized by an ongoing loss of both adipose and skeletal muscle tissue, as well as loss of visceral tissue, together with a reduced muscle strength and endurance, weakness and fatigue. This wasting syndrome is presented as a complication of chronic or end-stage malignant diseases such as cancer (18-21).

Muscle dysfunction and wasting are comorbidities associated with several respiratory diseases including chronic obstructive pulmonary disease (COPD), and lung cancer (LC) (16, 20, 21). Moreover, these patients may also undergo disuse muscle atrophy caused by prolonged bed rest, or due to limited exercise capacity as a consequence of the underlying disease (22, 23). The alteration of normal muscle function, as well as the presence of muscle mass loss due to these diseases or conditions impairs the quality of life of these patients, and getting worse the prognosis of the disease (19-21, 24).

2.1- Conditions associated with muscle dysfunction and wasting

2.1.1- Lung cancer

Cancer is one of the main conditions associated with muscle dysfunction and muscle wasting. Lung cancer is the most common cause of cancer death worldwide, with about 1,500,000 deaths annually (25). It has been reported that more than half of patients with this tumor type, among others, usually show an important weight loss, including skeletal muscle wasting and develop cachexia, which impairs the quality of life of these patients (26-30). A recent study of our group has been shown that vastus lateralis of lung cancer cachectic patients exhibited a reduction in type II fibers size, together with an increase in muscle structural abnormalities impairing the exercise capacity and quadriceps muscle force in these patients (16).

In addition, cancer cachexia is related to a reduced tolerance to anticancer therapy and a reduced survival (31) being the cause of death in 20-40% of cancer patients (20, 28).

In this regard, due to the great impact of cachexia in lung cancer prognosis, therapeutic targets to prevent or treat cachexia are necessary, but no effective treatment is currently available. Sulfasalazine and Bortezomib are drugs already approved for use in patients for treatment of rheumatoid arthritis and multiple myeloma, respectively (32, 33). These drugs act by inhibiting certain biological mechanisms (described in section 2.2) also involved in the development of cancer-induced cachexia, but nevertheless its effects on this disease remain unknown. Before designing studies in patients, especially with regard to therapeutic interventions, is essential the use of experimental animal models, which simulate human diseases and test the effects of therapeutic strategies. In our group it has been performed several animal models of cancer-induced cachexia in order to explore the effects of this disease on respiratory and peripheral muscles (34, 35). In this regard, already exist experimental validation of animal models for studying paraneoplastic syndromes of cancer, as well as the potential treatments.

2.1.2- Disuse

Muscle wasting can also take place in absence of the disease, during extended periods of muscle disuse including physical inactivity, chronic bed rest, when a single limb is immobilized, and spaceflight.

Disuse muscle atrophy can lead to a significant decrease in muscle mass and strength, thus impairing physiological function of respiratory or limb muscles (23, 36-38).

As to study the mechanisms responsible for disuse muscle atrophy in humans is very complex, numerous experimental animal models have been designed with the aim to simulate the different conditions that cause disuse muscle atrophy in humans. For example, tail suspension is an animal model based on unloading hindlimb muscles, which is suitable for studying microgravity-induced atrophy due to spaceflight (39). Denervation is an efficient method for simulating the pathology of trauma in which nerve functions have been affected (40). In order to mimic muscle atrophy due to prolonged bed rest

or limb cast, the most effective animal model is the hindlimb immobilization (22, 23, 41, 42).

Although the different conditions of disuse muscle atrophy share the common feature in loss of muscle mass, differences in how this muscle loss occurs may exist. Disuse muscle atrophy due to physical inactivity or limb cast is characterized by a rapid atrophy of slow-twitch muscles such as soleus muscle, and fibers size reduction of limb muscles (22, 37, 43). However, exist some controversy regarding to the fiber type proportions during disuse muscle atrophy. On the one hand, studies performed in hindlimb immobilized rats between 4 and 8 weeks have been reported that there is frequently a switch of the muscle fiber-type composition, giving rise a transition of slow to fast myosin isoform expression in gastrocnemius and soleus muscles (44). On the other hand, some studies have been shown that in soleus muscle of rats exposed to 14 days of spaceflight, fiber proportions were maintained despite the existence of a tendency of type I fibers shift to a type II fibers (45). The reasons of these contradictory results could be due to the use of different experimental models of disuse muscle atrophy, or owing to the immobilization period.

Muscle activity after the immobilization period, results in a gradual increase of muscle mass and force production (22, 46). Several studies have been shown that after 7 days of hindlimb immobilization followed by 11 days of recovery period, there is a progressive increase in protein synthesis and muscle function, as well as increased expression of genes involved in energy metabolism in the mouse gastrocnemius muscle (22, 23).

2.2- Biological mechanisms involved in muscle dysfunction and mass loss in different models

2.2.1- Oxidative and nitrosative stress

Reactive oxygen species (ROS) and reactive nitrogen species (RNS) are highly reactive molecules that are produced at low levels within skeletal muscle fibers, playing a positive role in muscle contraction and muscle force production (35, 47, 48). In order to maintain the constitutive levels of ROS and RNS inside the muscle cells, some intracellular antioxidant enzymes act neutralizing the increased levels of these reactive species (49). These antioxidant enzymes including catalase, cytosolic superoxide dismutase (SOD1), and mitochondrial

superoxide dismutase (SOD2), are highly expressed within skeletal muscles (48). However, when the increased levels of ROS and RNS cannot be neutralized by the antioxidant agents, occurs a phenomenon named oxidative and nitrosative stress (48, 50, 51). These excessive levels of ROS and RNS can exert injurious effects in muscle proteins, membrane lipids and even nucleic acids (DNA) (52). Proteins, including structural proteins of skeletal muscle are the major targets of ROS and RNS, leading to the alteration on its function as well as an increase of its degradation, contributing to muscle mass loss and muscle dysfunction (53). Quantification of carbonyl groups, which appear as a result of the oxidation of some amino acids, is a good marker to explore protein oxidation (48, 53). In addition, final products of lipid peroxidation such as malondialdehyde (MDA), 4-hydroxy-2-onenal (HNE), and 3-nitrotyrosine (NT) formation from the reaction of peroxynitrite and tyrosine, are important markers of oxidative and nitrosative stress (48, 50, 53, 54).

Consistent evidence of our group showed that redox imbalance is involved in muscle wasting and dysfunction in both respiratory and limb muscles of COPD patients (48, 51, 53), as well as COPD patients with lung cancer (16), and cancer cachectic animals (35, 48, 50). In addition, several studies have been demonstrated the implication of oxidative and nitrosative stress in disuse muscle atrophy (43, 55-57).

2.2.2- Inflammation

Inflammation is a protective biological response of our body against aggressions of foreign agents, with the aim to destroy, defend or isolate these external agents and repairs the tissue damage. In this manner, inflammatory response is a beneficial pathological process for our body due to the limitation of the pathogen action. During the inflammatory process, host cells, proteins, and other mediators are activated and they travel through the blood vessels towards the site of damage, where release different substances such as cytokines in order to eliminate the injurious stimuli and to initiate the tissue healing process (2, 5). Nevertheless, an exaggerated or persistent inflammatory process may become harmful (58). Excessive inflammatory mediators can exert adverse effects in systemic circulation, arriving at organs and tissues, including

muscles, damaging muscle structure and altering the muscle contraction, leading to their dysfunction (59, 60).

Both local and systemic inflammation can take place in skeletal muscle wasting and dysfunction. During the systemic inflammation response, proinflammatory cytokines such as TNF-α, interleukin-1-beta (IL-1β, IL-6, and interferon gamma (IFNγ) are produced. These cytokines are shown to be involved in muscle wasting diseases including cancer cachexia, by activating intracellular signaling pathways that enhance protein degradation through the activation of catabolic pathways, leading to muscle atrophy and dysfunction (16, 61-64). Nonetheless, as previously described, muscle inflammation seems to be a less predominant event in muscle wasting diseases (16, 65, 66).

However, muscle atrophy during immobilization takes place in the presence of local inflammation (22, 23), while in the rehabilitation after muscle disuse, inflammation response decreases and return to basal levels (23).

2.2.3- Cell signaling pathways

Cell signaling is a part of complex system that has the function of communicate information (signals) within the cell in order to regulate cellular activities. Signal transduction take place when an extracellular or intracellular stimulus activates a specific receptor situated on the membrane cell or inside the cell. In turn, this receptor triggers a number of biochemical events inside the cell, producing a response. This signal transduction process normally involves multiple steps, amplifying the signal response. In this manner one signaling molecule can originate more than one cellular response (67, 68).

Oxidative and nitrosative stress, and inflammation, act as activators of a great number of signaling pathways that in turn, stimulate the activity of different effectors promoting skeletal muscle atrophy and dysfunction, by an imbalance between the rate of protein synthesis (anabolism) and degradation (catabolism), being the latter the predominant (50, 51, 69). Mitogen-activated protein kinase (MAPK), nuclear factor-KappaB (NF-kB), and forkhead box O class (FoxO) are the main signaling pathways involved in muscle mass loss associated to different diseases and conditions (70-72).

2.2.3.1- Mitogen-activated protein kinase (MAPK) pathway

MAPK is a family of proteins composed by four subgroups of signaling proteins, each one sensitive to a given stimulus and specialized in a determinate response in skeletal muscle: the extracellular signal-regulated kinases (ERKs) 1 and 2 (ERK1/2); the p38 MAPK, the c-Jun NH_2-terminal kinase (JNK); and the ERK5 or big MAPK (71, 73).

All of these MAPK proteins are stimulated by cytokines, growth factors, and cellular stress and then, through phosphorylation interact with other proteins or transcription factors forming a signaling cascade which is involved in multiple biologic processes such as cell proliferation, differentiation, hypertrophy, apoptosis, and inflammation (70).

In skeletal muscle, these MAPKs are important regulators in muscle fiber phenotype, muscle mass maintenance, and muscle diseases. The upregulation of these pathways is shown to be involved in skeletal muscle atrophy diseases by stimulating expression of protein degradation (E3 ligase atrogin1/MAFbx and muscle RING-finger protein-1 (MuRF1), and the consequently activation of ubiquitin-proteasome system. In addition, MAPKs can promote the transcription of genes implicated in apoptosis and autophagy, participating by this way in muscle wasting through both, the ubiquitin-proteasome and autophagy-lysosome dependent proteolytic mechanisms (74-79).

2.2.3.2- Nuclear Factor-kappaB (NF-kB) pathway

NF-kB is an important protein complex that, in response to oxidative stress and proinflammatory cytokines, regulates the transcription of genes involved in apoptosis, inflammation, differentiation, cachexia, muscle mass loss, and disuse atrophy in skeletal muscle (16, 80-82). NF-kB family is formed by five different proteins: p50, p52, p65, Rel B and c-Rel (83). In order to facilitate binding of NF-kB to DNA and regulate gene expression, two of these proteins must form a dimmer. Is well known that the dimmer p50-p65 is in charge of the majority activity of NF-kB in skeletal muscle (84).

When the tissue is not submitted to any stimuli, NF-kB is found in the nucleus attached to its inhibitor IkappaB-alpha (IkB-α). However, under various stimuli, Ikappa kinase (IKK) is activated and therefore phosphorylates IkB-α, which is ubiquitinated and degraded via proteasome. Exclusively only NF-kB

complexes without their IkB-α inhibitory can translocate into the nucleus and regulate gene expression and consequently mediate multiple signaling pathways such as apoptosis, inflammation and differentiation (83, 85).

2.2.3.3- Forkhead box O family (FoxO) pathway

Forkhead box transcription factors are a family of proteins characterized by having a conserved DNA-binding domain named the “forkhead box”. Mammals have four different members of the FoxO family: FoxO1, FoxO3, FoxO4, and FoxO6, all of them regulate cell growth, cell proliferation, cell differentiation, and cell longevity by up-regulating genes involved in energy metabolism, apoptosis, and cell cycle arrest (86, 87).

FoxO transcription factors are regulated by different stimuli, such as IGF-I, cytokines, and oxidative stress. These triggers control FoxO activity by post-translational modifications, such as phosphorylation, acetylation, ubiquitination, and methylation, which allow FoxO movement between the cytoplasm and the nucleus (88).

Several studies, some of our group, have shown that FoxO transcription factors are important mediators of muscle mass loss associated with cancer-cachexia, COPD, hindlimb suspension and denervation (12, 16, 89-91). It has been reported that the activation of FoxO transcription factors carries to an increase expression of the muscle-specific ubiqutin ligases and the autophagy related genes, which in turn upregulate the ubiquitin-proteasome system and autophagy (12, 16, 71, 79).

2.2.3.4- Myostatin/ActivinIIB pathway

Myostatin or growth and differentiation factor-8 (GDF-8), is a member of the transforming growth factor (TGF) family of proteins that is highly expressed in skeletal muscle. Myostatin inhibits muscle growth and differentiation in the process of myogenesis, being an important negative regulator of muscle mass (92, 93). Myostatin regulates muscle growth by binding to the activin IIB membrane receptor (ActRIIB), resulting in the phosphorylation of the Similar to Mothers Against Decapentaplegic 2 and 3 (Smad2/3) transcription factors, and inhibiting transcription genes including myogenin, which is essential for skeletal muscle differentiation (94, 95). Moreover, myostatin is also involved in the

regulation of different signaling pathways such as MAPK pathway, which block the myogenesis responsible genes (96, 97). In addition, increased myostatin expression inhibits Akt signaling leading to a decreased protein synthesis (97, 98). The myostatin-activin receptors binding also induces the activation of FoxO transcription factors, allowing the transcription of MuRF1 and atrogin-1 which promote the ubiquitination of muscle structural proteins including myosin, leading to skeletal muscle wasting (99).

Increased myostatin levels has been shown to be involved in muscle wasting diseases and conditions including cancer cachexia, and inactivity-induced muscle atrophy (96, 100).

2.2.3.5- The Phosphatidylinositol-3kinase/RAC-alpha serine/threonine-protein kinase /mammalian target of rapamycin/70 protein S6 kinase (PI3K/Akt/mTOR/p70S6K) pathway

In muscles, the balance between protein synthesis and degradation allows the proper muscle mass maintenance and a good response to different conditions including exercise, and environmental factors. However, an imbalance between the rate of protein catabolism and anabolism, in the favor of the first one, can lead to muscle wasting diseases (101).

Protein synthesis, also known as protein anabolism, is essential for body muscle development, strength growth and muscle mass recovery (102, 103). The PI3K/Akt/mTOR/p70S6K pathway is the main regulator of protein anabolism. It is mainly activated by insulin-like growth factor-1 (IGF-1), which when is attached to its receptor triggers the activation of PI3K. This kinase phosphorylates and activates Akt, which, in turn promotes the stimulation of the mammalian target of rapamycin (mTOR) (21, 104). The activation of mTOR results in the phosphorylation and activation of p70S6K, which induces phosphorylation of S6 ribosomal protein, leading to the protein synthesis at the ribosome (103, 105, 106). Moreover, Akt activation also results in inhibition of protein degradation by phosphorylating and thus repressing the transcription factors of the FoxO family proteins. This way, FoxO members are unable to enter the nucleus and to induce transcription of the muscle specific ubiquitin ligases (MAFbx/Atrogin-1 and MuRF1) and autophagic related genes such as autophagy protein microtubule-associated protein 1 light chain-3 (LC3) (21, 89,

90, 107). Despite increased protein catabolism has been extensively shown in different muscle wasting conditions, a decrease of protein synthesis has also been demonstrated in several muscle wasting conditions, contributing to the imbalance between protein synthesis and degradation (108).

2.2.4- Proteolytic systems

Protein catabolism, also named protein degradation or proteolysis, is an important regulator of many physiological and cellular processes, along with preventing the accumulation of unnecessary or damaged proteins in cells, including in muscle cells. The proteolytic process, consist in the break of proteins into smaller amino acids by the hydrolysis of the peptide bond, mainly through enzymes called proteases (109).

However, an increased protein catabolism has been presented to be a relevant mechanism of muscle mass loss in cancer-induced cachexia and disuse muscle atrophy, among other muscle wasting diseases (16, 20, 110). The following proteolytic pathways are involved in protein degradation in skeletal muscle: autophagy, calpain system, caspase-mediated apoptosis, and the ubiquitin-proteasome system, being the latter the main mechanism implicated in the muscle wasting and dysfunction by the degradation of contractile proteins (20, 31, 111, 112).

2.2.4.1- Ubiquitin-proteasome system

The ubiquitin-proteasome system (UPS) is the principal mechanism of protein degradation in the mammalian cells. In UPS, proteins have to be marked with multiple ubiquitin molecules in order to be degraded. This process can be summarized in three consecutive steps, each one regulated by different enzymes, the ubiquitin-activating E1, the ubiquitin-conjugating E2, and the ubiquitin-ligase E3 (69, 113):

1) The ubiquitin activation: ubiquitin molecules are activated by the E1 enzyme in an ATP-dependent process.

2) The ubiquitin conjugation: E2 enzyme catalyzes the transfer of ubiquitin activated molecule from E1 to the active site of E2. $E2_{14K}$ is an E2 enzyme that regulates the ubiquitin conjugation of skeletal muscle proteins.

3) The ubiquitin ligation: E2 enzyme carries the ubiquitin unit to the ubiquitin-ligase enzyme E3 that is bound to a protein substrate. In this final step, the protein receives the ubiquitin molecule, which after several cycles of ubiquitination, will have a long ubiquitin chain. The muscle specific E3 ligases atrogin-1 (also named muscle atrophy F box, MAFbx), and the muscle ring finger-1 (MuRF1) play an important role in skeletal muscle atrophy (114, 115). In addition, tripartite motif-containing protein 32 (TRIM32) is an E3 ubiquitin ligase expressed in skeletal muscles that also is involved in the ubiquitination process of skeletal muscle proteins (116).

Proteins marked with polyubiquitin can be recognized and therefore degraded through the 26S proteasome complex, which is composed by the regulatory subunit 19S, and the catalytic subunit 20S (67, 117).

2.2.4.2- Autophagy

Autophagy is a proteolytic mechanism which degrades cellular components, even proteins, through enzymes contained within the lysosomes. During this process, target proteins are surrounded by a vesicle named autophagosome. Then, the autophagosome fuses with the lysosome, which degrades and recycles its content (118, 119).

Autophagy takes place constitutively in order to maintain an anabolic and catabolic balance in the cell. Nevertheless, upregulate autophagy activity can induce muscle protein degradation and therefore muscle mass loss. Akt signaling regulates the autophagy pathways in skeletal muscles by phosphorylation and inactivation of FoxO transcription factors, thus preventing the transcription of autophagy genes. Several autophagy enhancers, including beclin-1, microtubule-associated protein 1A/1B-light chain 3 (LC3), and p62 are shown to be involved in the process of muscle wasting in cachectic muscles of COPD patients (16), and in experimental models of cancer cachexia (71, 120).

2.2.4.3- Calpain-calpastatin system

Calpains are calcium cysteine proteases that are ubiquitously expressed in mammalian tissues. Calpains break directly the cytoskeletal proteins (titin and nebulin), resulting in the liberation of contractile proteins (actin and myosin) from the sarcomere, and the subsequent degradation by the proteasome

system (121, 122). The calpain proteolytic activity is regulated by the concentration of cytosolic calcium, or by the levels of its endogenous specific inhibitor, calpastatin (55).

Several studies have been reported that increased calpain levels are involved in the muscle wasting process in cancer cachexia and in disuse muscle atrophy (123, 124).

2.2.4.4- Caspase-mediated apoptosis

Apoptosis or programmed cell death is an important mechanism for maintaining cell community in tissues. Cells subjected to this process are characterized by have morphological changes, such as nuclear fragmentation or chromatin condensation, resulting in a cell fragments known as apoptotic bodies, which will be eliminated by phagocytic cells. This process of cell degradation is carried out by the proteases called caspases (125, 126). The apoptotic mechanism is regulated by proteins that either induce it (pro-apoptotic, i.e. Bcl-associated X, Bax) or inhibit it (anti-apoptotic, i.e. B-cell lymphoma 2, Bcl-2) (55).

Apoptosis takes place normally during development or aging, but under defective apoptotic conditions, this mechanisms can contributes to muscle wasting diseases including cachexia and disuse atrophy (124, 127-130).

2.2.5- Mitochondrial dysfunction

Mitochondria are cell organelles that have a key role in energy production in skeletal muscles as well as other tissues, through oxidative phosphorylation. In addition, these organelles are involved in muscle mass maintenance and loss in diseases. Alterations in muscle mitochondrial content and function are related with several muscle wasting diseases, including cancer cachexia (109, 131), and COPD (11, 132). Besides, some mitochondrial alterations can induce a greater generation of ROS in skeletal muscles, which could be implicated in a redox disbalance and an altered muscle function (11, 133). A recent study of our group has shown that both diaphragm and gastrocnemius muscles of LC cachectic mice exhibited an affected mitochondrial respiratory chain caused by a reduction of mitochondrial chain complexes activity (34). This mitochondrial dysfunction resulted in a reduced muscle mass and strength in those animals (34).

Moreover, mitochondrial DNA (mtDNA), which encodes thirteen proteins that are crucial for oxidative phosphorylation and ATP generation, can be damaged (10, 132, 134). Alterations or deficiencies in nuclear genes implicated in the mtDNA synthesis can compromise mitochondrial biogenesis in skeletal muscles and therefore inducing muscle loss (131).

2.2.6- Poly-ADP ribose polymerase (PARP)

PARP is a family of proteins involved in the regulation of several cellular processes, including DNA repair, cell death, inflammation, differentiation, and metabolism (135-138). Among the family of PARP proteins, PARP-1 and PARP-2 are extremely conserved proteins, that are ubiquitously expressed in mammalian tissues and are localized in the cell's nucleus (136). These proteins have greater activity in the cell. Concretely, PARP-1 is responsible for the 85%-90% of PARP activity, whereas the rest is predominating PARP-2 (136).

PARP-1 and PARP-2 use NAD^+ as a substrate to form polymers of ADP-ribose on other proteins and therefore are the major NAD^+ consumers in several cell types such as skeletal muscle cells (137, 139). In this regard, prolonged PARP activation can reduce the NAD^+ levels and, thereby to impair glycolysis compromising cell survival. In addition, a reduced glycolytic activity results in ATP depletion, and an impaired flow of glucose-derived components into the citric acid cycle, further compromising energy balance (140).

Aside from play a role in oxidative metabolism, PARP enzymes are also implicated in metabolic regulation by influencing mitochondrial function. Silent mating type information regulation 2 homolog-1 (SIRT1), a NAD^+-dependent type III deacetylase, regulates oxidative metabolism by the acetylation and regulation the activity of a number of enzymes and transcriptional regulators (141, 142). In skeletal muscle, SIRT1 is an important regulator of mitochondrial function (143). In fact, the activity of SIRT1 is controlled by the bioavailability of the substrate NAD^+. Evidences suggest that increased NAD^+ content results in a higher SIRT1activity (142). Thus SIRT1 acts as an intracellular sensor by increasing the mitochondrial biogenesis to achieve the energy requirements of the cell (144).

The NAD^+ dependence of PARP and SIRT1 suggests that these enzymes could compete for a limited NAD^+. Recent studies have demonstrated that the

genetic deletion of either Parp-1 or Parp-2, or through the pharmacological inhibition of PARP activity, intracellular NAD^+ levels can be elevated in skeletal muscle, and hence increasing SIRT1 activity and mitochondrial function (145, 146). Moreover, it has been shown that Parp-2 deletion increases SIRT1 expression and activity in cultured myotubes without changing NAD^+ levels, leading to an increased mitochondrial content (146). These results insinuate that PARP-2 behaves as a direct negative regulator of the SIRT1 promoter. Therefore, PARP may alter SIRT1 activity by reducing or not NAD^+ bioavailability.

PARP-1 and PARP-2 are also involved in tumorogenesis of some cancer types (147, 148) by altering the mechanisms of DNA repair, thereby stimulating tumor progression (147-150). In fact, the overexpression of PARP-1 is related with low survival rates in patients with breast cancer (151). A recent study of our group conducted in lung cancer Parp-$1^{-/-}$ and Parp-$2^{-/-}$ mice, showed that these animals exhibited a reduction in tumor weight and tumor cell proliferation through an increase in oxidative stress, apoptosis and autophagy (152). In addition, pharmacological inhibition of PARP-1 and PARP-2 has been shown to be a treatment option for several cancer types including lung cancer (153, 154).

Taking into account all these findings, PARP inhibitors could play a dual role as therapeutic agents: anti-tumoral and anti-cachectic.

2.2.7- Epigenetic events

Epigenetics are the functionally relevant modifications to the gene expression that do not implicate an alteration in the DNA sequence. These epigenetic modifications can induce changes in skeletal muscle plasticity in response to environmental stimuli, such as immobilization, as well as some diseases including COPD (155-158). Epigenetic regulation of gene expression includes several changes including protein acetylation and microRNAs (155, 159, 160).

Recent studies, some of our group, propose that these epigenetic modifications may play an important role in the loss of muscle mass and dysfunction (155-157).

2.2.7.1- Protein acetylation and deacetylation

Genes are packaged into the nucleus of our cells forming the chromatin. Chromatin is comprised by an octamer of protein histones (two of each of the core histones H2A, H2B, H3, and H4), which compact the DNA resulting in the functional basic unit of DNA package, the nucleosome (161). Chromatin structure can be modulated, leading to two different types of chromatin depending on the degree of its condensation. When chromatin is slightly compacted, genes are more accessible and therefore, they are transcriptionally active. In this case, chromatin is called euchromatin. However, heterochromatin is referred to a tightly packaged chromatin, which difficult the accessibility to the transcription factors, repressing gene transcription (161, 162).

Acetylation and deacetylation of histones are to mechanisms that control gene expression through modulation of chromatin structure. On the one hand, acetylation is a post-translational modification of histones that consists in the transference of the acetyl group from acetyl-CoA to a lysine residue. This modification leads to an opened chromatin (euchromatin) which is transcriptionally active. On the other hand, deacetylation reverses this action resulting in a closed chromatin (heterochromatin) that is transcriptionally inactive (155, 159, 161, 163).

Histone acetyltransferases (HATs) and histone deacetylases (HDACs) are two different groups of enzymes, which regulate this contrary process (155, 159, 161).

HATs, that are responsible of histone acetylation, are involved in the process of muscle wasting allowing the transcription of NF-kB and FoxO transcription factors, both implicated in protein degradation (163). By contrary, HDACs revert the acetylation process by removing acetyl groups of the lysine residues, thus preventing gene transcription. Exist 18 HDACs divided into four classes, being HDAC3 (a class I HDAC), HDAC4 (a class IIa HDAC), HDAC6 (a class IIb HDAC), and silent information regulator 1 (SIRT1) (a class III HDAC, also called sirtuins) the most important in the regulation of muscle mass (163-167).

Proteins other than histones, including transcription factors, can be acetylated or deacetylated in order to modify its function and turnover. This

reversible process is mediated by the enzymes HATs and HDACs that increase or decrease, respectively, the protein acetylation levels.

Concretely, HDAC3 and SIRT1 deacetylate p65 subunit, preventing the activity of transcription factor NF-κB, and thus impeding muscle atrophy (168, 169). In addition, SIRT1 acts blocking the transcription of FoxO genes leading to the inhibition of atrophy-related genes (atrogin-1 and MuRF-1) (170). Furthermore, SIRT1 enhances the peroxisome proliferator-activated receptor gamma coactivator 1-alpha (PGC-1α) (171), which induces fiber type switching from fast- to slow-twitch, and also impedes the transcription of FoxO genes (172). In this manner, SIRT1 prevents the muscle mass loss and promoting muscle growth (170, 173).

Furthermore, in the presence of an imbalance between protein acetylation and deacetylation, in favor of the first ones, proteins become hyperacetylated, being more susceptible to be degraded (163). In fact, HATs can act as ubiquitin ligases increasing the ubiquitin proteasome activity (174). Besides, excessive protein acetylation may be due to a deficient HDACs activity. A recent study has been reported that a reduced expression of HDAC6 and SIRT1 in muscles of septic rats contributes to muscle wasting (165).

In this regard, protein acetylation acts as an important regulator of muscle mass, contributing to the process of muscle wasting (163).

Moreover, acetylation and deacetylation also control the expression of myogenic transcription factors such as the myocyte enhancer factor-2 (MEF2) family (159). This family of transcription factors, which includes MEF2C and MEF2D, regulates muscle differentiation and muscle repair and are decreased in muscle wasting diseases and conditions (159, 175). In contrast, the transcription factor Yin Yang 1 (YY1), which inhibits myogenesis and muscle gene expression, is found to be increased in muscle wasting processes (176).

2.2.7.2- MicroRNAs

MicroRNAs (miRNAs) are non-coding ribonucleic acids of approximately 20-30 nucleotides of length that are involved in the regulation of gene expression. miRNAs repress protein translation or promote mRNA degradation by means of

base-pairing with complementary sequences of the mRNAs targets (177). A single miRNA have several targets (mRNA) and these in turn can be regulated by multiple miRNAs. In this manner, miRNAs are implicated in various processes such as the regulation of muscle mass and muscle phenotype (155, 178).

These small non-coding RNAs are firstly transcribed as long transcripts into the nucleus, which are named primary miRNAs (pri-miRNAs) (179). The ribonuclease (RNase) III endonuclease Drosha associated with Pasha (named DGCR8) splits the pri-miRNA into a smaller miRNA precursor (pre-miRNA). This pre-miRNA is transported from the nucleus towards the cytoplasm through exportin-5 (XPO5), where once there a second RNase III endonuclease cleaves the pre-miRNA in order to obtain two short (22 nucleotides) complementary molecules of miRNA. One strand of this miRNA duplex is degraded whereas the other one becomes in the mature miRNA, which is incorporated into the RNA-induced silencing complex (RISC) allowing the identification and binding to the complementary target mRNA. The union between the miRNA and the mRNA results in the degradation of the latter or the inhibition of protein translation (178, 180).

Numerous miRNAs are highly expressed in the skeletal muscle, some of them being muscle-specific miRNAs also known as myomiRs. miR-1, miR-133, and miR-206 are the most studied muscle-specific miRNAs since have an important relevance in muscle development, muscle mass, muscle fyber type, and muscle wasting conditions (156, 178, 181). In addition, non-muscle specific miRNAs including miR-486, are also expressed in skeletal muscles and are necessary for the regulation of muscle growth and homeostasis (182).

During development, myomiR regulation is directed by myogenic regulatory factors (MRFs), such as myogenin and myogenic differentiation 1 (MyoD), as well as serum response factor (SRF) and MEF2 (175, 183, 184). MicroRNAs miR-1 and miR-206 induce MEF2 expression by the repression of HDAC4 activity, promoting muscle differentiation, whereas miR-133 enhances myoblast proliferation by blocking the SFR and inhibiting myotube formation. However, miR-486 acts directly on the FoxO expression, decreasing its activity and thus

promoting protein synthesis and muscle growth, through the activation PI3K/Akt signaling (184, 185).

These miRNAs are shown to be involved in the process of muscle wasting during muscle related diseases and conditions. Concretely, a recent study has been reported that miR-1 expression is downregulated in the quadriceps of COPD patients, leading to its skeletal muscle dysfunction (186). In experimental models of disuse muscle atrophy, the gastrocnemius of mice exhibited a reduction of miR-206, whereas miR-1 and miR-133 levels showed a trend towards reduction. These results, together with the increase of muscle atrophy genes (atrogin-1 and myostatin) in the same muscle, contributed to the loss of muscle mass and force generation (114, 158). By contrary, pharmacologycal administration of miR-1, miR-133, and miR-206 into the injured tibialis improve mucle regeneration (187).

RATIONALE AND HYPOTHESIS

Skeletal muscle dysfunction and wasting are important systemic manifestations associated with chronic diseases such as lung cancer. In addition, muscle deconditioning takes place in patients with chronic illnesses, which have to rest for long periods of time, or have limited exercise capacity as a result of the underlying disease.

Evidence shows that muscle mass loss associated with these conditions occurs as a consequence of enhanced muscle proteolysis, mainly through the ubiquitin proteasome system, which is regulated by cell signalling pathways such as NF-kB and MAPK. However, *in vivo* studies demonstrating the effectiveness of the pharmacological inhibition of these pathways are still lacking.

Epigenetic mechanisms such as muscle-specific microRNAs, histone acetylation/deacetylation balance, and myogenic transcription factors which regulate muscle mass maintenance and muscle repair in several chronic respiratory diseases, could also be involved in the muscle wasting process during cancer cachexia and disuse muscle atrophy. Moreover, overexpression of PARP-1 and PARP-2 promotes carcinogesis and tumor progression, and impairs muscle metabolism affecting mitochondrial function, but their role in protein anabolism and catabolism, muscle mass, muscle function and other epigenetic mechanisms in *in vivo* models of cancer cachexia remains unclear.

Despite the knowledge of the molecular and cellular mechanisms involved in disuse muscle atrophy due to immobilization, the temporal sequence of different events is still undefined. Furthermore, the biological mechanisms involved in the recovery process of muscle mass and function after the immobilization period are also poorly understood.

In the current thesis, we hypothesized that the biological mechanisms involved in the process of muscle wasting and dysfunction may differ between disuse muscle atrophy and LC induced cachexia in mice. Moreover, we also hypothesized that the profile of molecular events implicated in deconditioning of skeletal muscles, as well as in the recovery process of muscle following immobilization may be different between early- and late-time points in limb muscles of mice exposed to hindlimb unloading. Finally, we also hypothesized

that pharmacological inhibition of MAPK, NF-kB, and proteasome mechanisms, as well as the deficiency of either PARP-1 or PARP-2 proteins may have beneficial effects on total body and muscle weights and force production in LC cachectic mice.

OBJECTIVES

The different objectives of each study have been defined in the corresponding articles and manuscripts.

In this regard, the specific objectives of each study were summarized as follows:

Objectives

Study #1: Pharmacological strategies in lung cancer-induced cachexia: effects on muscle proteolysis, autophagy, structure, and weakness

In the respiratory and limb muscles from lung cancer (LC) cachectic mice receiving concomitant treatment with MAPK, NF-kB, or proteasome inhibitors:

1) To assess physiological characteristics: body and muscles weights, limb muscle strength, and tumor size

2) To explore molecular mechanisms potentially involved in muscle wasting and dysfunction:

    - Redox balance: protein carbonylation and nitration, and antioxidant enzymes

    - Inflammation: tumor necrosis factor alpha (TNF-α), interferon gamma (IFNγ), interleukin 1 beta (IL-1β), and interleukin 6 (IL-6)

    - Proteolysis: tyrosine release

    - Proteolysis markers: E2 enzyme $E2_{14K,}$ E3-ligases (atrogin-1 and Murf-1), C8-20S, and total ubiquitinated proteins

    - Signaling pathways: MAPK, NF-kB, and FoxO

    - Autophagy: LC3, p62, and beclin-1

    - Muscle mass markers: myostatin and myogenin

3) To evaluate muscle contractile and functional proteins: actin, myosin, creatine kinase (CK), and carbonic anhydrase III (CAIII)

4) To analyze muscle structural characteristics:

    - Muscle phenotype: fiber size and composition

    - Muscle structural abnormalities

Study #2: MicroRNA expression and protein acetylation pattern in respiratory and limb muscles of Parp-1$^{-/-}$ and Parp-2$^{-/-}$ mice with lung cancer cachexia

In the diaphragm and gastrocnemius muscles of either Parp-1$^{-/-}$ or Parp-2$^{-/-}$ lung cancer (LC) cachectic mice:

1) To evaluate the effects of PARP-1 or PARP-2 selective deletions on body and muscle weights, and grip strength

2) To analyze the expression levels of several epigenetic modifications:

- Muscle-enriched microRNAs: miR-1, miR-133, miR-206, and miR-486
- Total protein hyperacetylation, acetialtion levels of FoxO1, FoxO3, and PGC1-α and levels of histone deacetylation (HDAC3, HDAC6, and SIRT1)

3) To determine the levels of myogenic transcription factors: MEF2C, MEFD2, and YY1

4) To assess the expression of downstream markers of myogenic transcription factors MEF2C, MEF2D, and YY1: α-actin, PGC1-α, and muscle CK

5) To analyze muscle phenotype: fiber size and composition

6) To explore potential correlations between physiological and molecular variables in cachectic wild type, Parp-1$^{-/-}$ and Parp-2$^{-/-}$ animals

In the subcutaneous tumor of wild type, Parp-1$^{-/-}$, and Parp-2$^{-/-}$ lung cancer (LC) cachectic mice:

1) To explore tumor size

2) To assess autophagy levels: LC3 and SIRT1

3) To evaluate apoptotic markers: Bcl-2 and Bax

4) To analyze tumor cell proliferation: Ki-67 levels

Objectives

Study #3: Muscle protein catabolism, phenotype, and function in respiratory and limb muscles in Parp-1$^{-/-}$ or Parp-2$^{-/-}$ mice with lung cancer cachexia

In the diaphragm and gastrocnemius muscles of either Parp-1$^{-/-}$or Parp-2$^{-/-}$ lung cancer (LC) cachectic mice:

1) To explore the effects of Parp-1 or Parp-2 selective deletions on body and muscle weights, and grip strength

2) To analyze Poly-ADP ribosylation activity

3) To assess molecular mechanisms potentially involved in muscle wasting and dysfunction:

- Redox balance: protein carbonylation and antioxidant enzymes
- Proteolysis: tyrosine release
- Signaling pathways: NF-kB
- Proteolysis markers: E3-ligases (atrogin-1, Murf-1, and TRIM32), C8-20S, and total ubiquitinated proteins

4) To determine levels of muscle anabolism: Akt/mTOR/p70S6K pathway and mitochondrial content

5) To evaluate muscle contractile proteins: actin and myosin

6) To analyze muscle structural characteristics:

- Muscle phenotype: fiber size and composition
- Muscle structural abnormalities

Study #4: Time-course of muscle mass loss, damage, and proteolysis in gastrocnemius following unloading and reloading: implications in chronic diseases

In the gastrocnemius muscle of mice exposed to a) different time-points of unilateral hindlimb immobilization or b) 7-days of unilateral hindlimb immobilization followed by different recovery periods:

1) To assess physiological characteristics: body and gastrocnemius weights, and limb muscle strength

2) To assess molecular mechanisms potentially involved in muscle wasting and dysfunction:

    - Proteolysis: tyrosine release

    - Proteolysis markers: proteasome activity, E3-ligases (atrogin-1, Murf-1, and TRIM32), C8-20S, and total ubiquitinated proteins

    - Markers of muscle atrophy: growth and differentiation factor 15 (GDF15)

3) To determine levels of muscle anabolism: Akt, p70S6K, and mitochondrial content

5) To evaluate muscle contractile and functional proteins: actin and myosin

6) To analyze muscle structural characteristics:

    - Muscle phenotype: fiber size and composition

    - Muscle structural abnormalities

In the blood of animals exposed to a) 1, 7, 15, and 30 days of immobilization and b) 7-days of unilateral hindlimb immobilization followed by 1, 15 and 30 days of recovery:

1) Muscle damage: troponin I

Study #5: Short- and long-term hindlimb immobilization and reloading: profile of epigenetic events in gastrocnemius

In the gastrocnemius muscle of mice exposed to a) different time-points of unilateral hindlimb immobilization or b) 7-days of unilateral hindlimb immobilization followed by different recovery periods:

1) To assess physiological characteristics: body and gastrocnemius weights, and limb muscle strength

2) To analyze the expression levels of several epigenetic modifications:

    - Muscle-enriched microRNAs: miR-1, miR-133, miR-206, and miR-486

    - Protein hyperacetylation, acetylated histone 3 (AcH3), and levels of histone deacetylation (HDAC3, HDAC6, and SIRT1)

    - Acetylated levels of FoxO, PGC1-α, and NF-kB

3) To determine the levels of myogenic transcription factors: Pax7, MEF2C, MEFD2, and PTEN

4) To analyze muscle phenotype: fiber size and composition

METHODS

The different methodologies used in the four studies are summarized below. Detailed information about the different materials and methods of each study is described in the corresponding online data supplement of the articles.

Animal models			
	Animal model	**laboratory-bred strain**	**Groups**
Study #1	Lung cancer cachexia	BALB/c mice	Control (N=10) LC-cachexia (N=10) LC-cachexia + Proteasome inhibitor (N=10) LC-cachexia + NF-kB inhibitor (N=10) LC-cachexia + MAPK inhibitor (N=10)
Studies #2 & #3	Lung cancer cachexia	BALB/c mice	Control wild type (N=12) LC-cachexia wild type (N=14) Control Parp-1$^{-/-}$ (N=8) LC-cachexia Parp-1$^{-/-}$ (N=12) Control Parp-2$^{-/-}$ (N=6) LC-cachexia Parp-2$^{-/-}$ (N=6)
Studies #4 & #5	Unilateral hindlimb immobilization	C57BL/6J mice	Non-immobilized (N=10) 1-day immobilized (N=10) 2-day immobilized (N=10) 3-day immobilized (N=10) 7-day immobilized (N=10) 15-day immobilized (N=10) 30-day immobilized (N=10) 1-day recovery (N=10) 3-day recovery (N=10) 7-day recovery (N=10) 15-day recovery (N=10) 30-day recovery (N=10)

Physiological evaluation	
Studies #1, #2 & #3	Body weight and limb strength Food intake measurements Tumor progression by positron emission tomography (PET) Muscles and tumor weights measurements
Studies #4 & #5	Body weight and limb strength Food intake measurements Gastrocnemius muscle weights

Samples			
	Muscles	Tumor	Blood
Studies #1 & #2	Diaphragm Gastrocnemius	Yes	No
Study #3	Diaphragm Gastrocnemius	No	No
Studies #4 & #5	Gastrocnemius	-	Yes

Molecular biology techniques		
Study #1	Immunoblotting of 1D electrophoresis	Protein carbonylation and nitration, and antioxidant enzymes Autophagy Signaling pathways Proteolysis Muscle contractile and functional proteins
	Tyrosine release assay	Protein catabolism
	Luciferase reporter gene assay	Transcriptional activity of NF-kB
	Cytokine enzyme-linked immunosorbent assay (ELISA)	Muscle levels of TNF-α, IFNγ, IL-1β, and IL-6
	Immunohistochemistry/ Hematoxilin and eosin staining Optical microscopy	Muscle fiber size and composition of type I and type II fibers Muscle damage
	Terminal deoxynucleotidyl transferase-mediated dUTP nick-end labeling (TUNEL) assay	Muscle apoptotic nuclei

Study #2	Trizol technique Taqman based qPCR reactions (real-time PCR)	Muscle RNA isolation MicroRNA expression: miR-1, miR-133, miR-206, miR-486
	Immunoblotting of 1D electrophoresis	Total protein acetylation levels Acetylated levels of FoxO1, FoxO3 and PGC1-α Histone deacetylases Muscle-specific transcription factors and their downstream targets Autophagy Apoptosis
	Immunohistochemistry & Optical microscopy	Muscle fiber size and composition of type I and type II fibers
Study #3	QIAmp DNA Mini Kit & absolute quantification by real-time PCR of DNAs	Muscle DNA isolation Mitochondrial DNA (mtDNA) copy number
	Immunoblotting of 1D electrophoresis	Protein carbonylation and antioxidant enzymes Proteolysis Muscle contractile and functional proteins Muscle anabolism Signaling pathways
	Tyrosine release assay	Protein catabolism
	Immunohistochemistry & Hematoxilin and eosin staining Optical microscopy	Muscle fiber size and composition of type I and type II fibers Muscle damage Poly ADP-ribosylation
	Terminal deoxynucleotidyl transferase-mediated dUTP nick-end labeling (TUNEL) assay	Muscle apoptotic nuclei

Study #4	Tyrosine release assay	Protein catabolism
	Proteasome activity assay	Protein degradation
	Immunoblotting of 1D electrophoresis	Proteolysis and atrophy Muscle anabolism Muscle contractile and functional proteins Total protein acetylation levels, histone deacetylases Muscle-specific transcription factors
	Cytokine enzyme-linked immunosorbent assay (ELISA)	Plasma levels of troponin I
	Immunohistochemistry & Hematoxilin and eosin staining Optical microscopy	Muscle fiber size and composition of type I and type II fibers Muscle damage
Study #5	Trizol technique Taqman based qPCR reactions (real-time PCR)	Muscle RNA isolation MicroRNA expression: miR-1, miR-133, miR-206, miR-486
	Immunoblotting of 1D electrophoresis	Histone deacetylases Downstream targets of epigenetic regulation Total protein acetylation levels Muscle-specific transcription factors and their downstream targets
	Immunohistochemistry & Optical microscopy	Muscle fiber size and composition of type I and type II fibers

Statistical analyses		
	Physiological and biological variables	**Correlations**
Study #1	ANOVA+*Tukey's* post hoc test	Pearson 's correlation coefficient
Study #2	ANOVA+ *Dunnett's* post hoc test Student's *T- test*	Pearson 's correlation coefficient
Study #3	ANOVA+ *Dunnett's* post hoc test	Pearson 's correlation coefficient
Studies #4 & #5	ANOVA+ *Dunnett's* post hoc test Student's *T- test*	-

RESULTS

1- Summary of main findings Study #1

In LC-cachectic mice compared to non-cachectic controls:

Body and muscle weights and muscle function

Body and muscle weights (diaphragm and gastrocnemius), and in limb strength were decreased.

Redox balance

Protein oxidation was increased while SOD2 levels were decreased in diaphragm and gastrocnemius muscles.

Inflammation

INF-γ levels were increased in the diaphragm, while TNF-α, IL-6 and IL-1β did not differ between groups in any of the study muscles.

Signaling pathways

Protein levels of NF-kB p50, p-NF-kB p50, NF-kB p65 and p38 were higher in both respiratory and limb muscles.

NF-kB transcriptional activity was higher in the gastrocnemius.

Protein levels of IkB and p-IkB were decreased in both muscles.

Proteolytic systems

Total protein degradation was increased in both diaphragm and gastrocnemius muscles.

Protein levels of $E2_{14k}$ were decreased only in the gastrocnemius.

Protein ubiquitination levels were greater in both muscles.

Muscle structural proteins

MyHC protein content was reduced in both muscles, while CK protein levels were decreased only in the gastrocnemius.

Muscle structure characteristics

Fiber type proportions did not differ between groups in any of the study muscles.

Type I and type II fiber sizes were reduced in both muscles.

The different treated groups of rodents compared to non-treated LC-cachectic animals:

Body and muscle weights and muscle function

NF-kB and MAPK inhibitors induced an increase in body and muscle weights (diaphragm and gastrocnemius), and an improvement of limb strength.

Subcutaneous tumor

All pharmacological treatments reduced subcutaneous tumor weight: proteasome inhibitor (18%), NF-kB inhibitor (27%) and MAPK inhibitor (60%).

Redox balance

Proteasome, NF-kB and MAPK inhibitors induced a reduction in protein oxidation in both muscles, and an increase in SOD2 content in the gastrocnemius.

Inflammation

Proteasome inhibitor reduced INF-γ, TNF-α, IL-6 and IL-1β levels in the gastrocnemius.

MAPK inhibitor induced a reduction of INF-γ, TNF-α and IL-6 in the diaphragm.

Signaling pathways

All three pharmacological treatments induced a reduction in total NF-kB p50 levels, and an increase in IkB and p-IkB protein content in both muscles.

NF-kB inhibitor reduced NF-kB p50, p-NF-kB p50, NF-kB p65 and p-NF-kB p65 levels in both muscles.

Proteasome and NF-kB inhibitors induced a decrease of NF-kB transcriptional activity in the gastrocnemius.

MAPK inhibitor induced a reduction in p38, ERK1/2 and pERK1/2 levels in both muscles.

Proteolytic systems

Proteasome, NF-kB, and MAPK inhibitors reduced total protein degradation in both muscles.

All three pharmacological treatments reduced $E2_{14k}$ protein content in the gastrocnemius.

Proteasome inhibitor reduced protein ubiquitination levels in both muscles, whereas NF-kB and MAPK inhibitors induced a decrease in that proteolytic marker only in gastrocnemius.

Muscle structural proteins

NF-kB and MAPK inhibitors increased MyHC protein levels, while the three pharmacological strategies caused an increase in CK protein content in the gastrocnemius.

Muscle structure characteristics

Proteasome and MAPK inhibitors increased type I fiber cross sectional area (CSA) in both muscles.

Chacon-Cabrera A, Fermoselle C, Urtreger AJ, Mateu-Jimenez M, Diament MJ, de Kier Joffé ED, Sandri M, Barreiro E. Pharmacological strategies in lung cancer-induced cachexia: effects on muscle proteolysis, autophagy, structure, and weakness. J Cell Physiol. 2014 Nov;229(11):1660-72. doi: 10.1002/jcp.24611.

2- Summary of main findings study #2

In LC-cachectic wild type mice compared to non-cachectic wild type controls:

Body and muscle weights and muscle function

Body and muscle weights (diaphragm and gastrocnemius), and in limb strength were decreased.

Muscle structure

Fiber type proportions did not differ between groups in any of the study muscles.

Type I and type II fiber sizes were reduced in both muscles.

Gastrocnemius type II fibers area and miR-133 levels were positively correlated.

MicroRNA expression

Expression levels of miR-1, miR-133, miR-206 and miR-486 were reduced in both diaphragm and gastrocnemius muscles.

Protein acetylation and histone deacetylase levels

Total protein acetylation levels were increased in both muscles.

Acetylated levels of FoxO1 were increased in the diaphragm, while acetylated FoxO3 protein content was increased in both muscles.

HDAC3, HDAC6 and SIRT1 protein content was reduced in both diaphragm and gastrocnemius muscles.

Myogenic transcription factors and downstream markers

MEF2C, MEF2D and YY1 levels were decreased in both muscles.

CK protein content was reduced in both muscles.

In LC-cachectic Parp-1$^{-/-}$ or Parp2$^{-/-}$ mice compared to LC-cachectic wild type animals:

Body and muscle weights and muscle function

Body and muscle weights (diaphragm and gastrocnemius), and in limb strength were improved.

Subcutaneous tumor

PARP-1 and PARP-2 deletions reduced subcutaneous tumor weight, increased apoptotic and autophagy levels, and reduced tumor cell proliferation.

Muscle structure

Type I and type II fiber sizes were improved in both muscles.

MicroRNA expression

Downregulation of miR-133, miR-206 and miR-486 was counterbalance especially in gastrocnemius of Parp-$1^{-/-}$ mice.

Protein acetylation and histone deacetylase levels

Increased protein acetylation was attenuated in both muscles by the improvement in HDAC3, SIRT1, and acetylated FoxO3 levels in both muscles, and acetylated FoxO1 levels in the diaphragm.

Myogenic transcription factors and downstream markers

Reduced MEF2C, MEF2D, were mitigated in both muscles.

CK protein content was improved in the gastrocnemius.

Chacon-Cabrera A, Fermoselle C, Salmela I, Yelamos J, Barreiro E. MicroRNA expression and protein acetylation pattern in respiratory and limb muscles of Parp-1(-/-) and Parp-2(-/-) mice with lung cancer cachexia. Biochim Biophys Acta. 2015 Dec;1850(12):2530-43. doi: 10.1016/j.bbagen.2015.09.020. Epub 2015 Oct 12.

3- Summary of main findings Study #3

In LC-cachectic wild type mice compared to non-cachectic controls:

Body and muscle weights and muscle function

Body and muscle weights (diaphragm and gastrocnemius), and in limb strength were decreased.

Muscle structure

Fiber type proportions did not differ between groups in any of the study muscles.

Type I and type II fiber sizes were reduced in both muscles.

Poly-ADP ribosylation

Levels of Poly-ADP ribosylation were increased in both muscles.

Redox balance

Protein oxidation was increased while SOD2 levels were decreased in diaphragm and gastrocnemius muscles.

Proteolytic systems

Total protein degradation was increased in both diaphragm and gastrocnemius muscles.

Total protein ubiquitination and protein content of 20S proteasome subunit C8 were greater in both muscles.

Levels of atrogin-1 were greater in both muscles.

Signaling markers in muscles

Activated levels of NF-kB p50 and NF-kB p65 were increased in both muscles.

Muscle anabolism

Activated levels of mTOR were reduced in both muscles.

Activated levels of p70S6K were decreased in the gastrocnemius.

Levels of mtDNA/nDNA were reduced in both muscles.

Muscle structural proteins

MyHC protein content was decreased in both muscles.

Muscle structure characteristics

Proportions of abnormal muscle fraction, including inflammatory cells and internal nuclei counts were increased in both respiratory and limb muscles.

Results

In LC-cachectic Parp-$1^{-/-}$ or $Parp2^{-/-}$ mice compared to LC cachectic wild type animals:

Body and muscle weights and muscle function

Body and muscle weights (diaphragm and gastrocnemius), and in limb strength were improved.

Muscle structure

Type I and type II fiber sizes were improved in both muscles.

Poly-ADP ribosylation

Increased Poly-ADP ribosylation levels were attenuated in both muscles.

Redox balance

Enhanced protein oxidation and reduced SOD2 levels were attenuated in both muscles.

Proteolytic systems

Enhanced protein catabolism by the activation of the ubiquitin-proteasome system (total protein ubiquitination, atrogin-1, and 20S proteasome C8 subunit) was mitigated in both diaphragm and gastrocnemius muscles.

Signaling markers in muscles

Increased activated levels of NF-kB p50 and NF-kB p65 were attenuated in both muscles.

Muscle anabolism

Activated levels of Akt, mTOR and p70S6K were partly improved in both muscles.

Levels of mtDNA/nDNA were only improved in both muscles of Parp-$1^{-/-}$ animals.

Muscle structural proteins

MyHC protein content was improved in the gastrocnemius of Parp-$1^{-/-}$ mice, and in both muscles of Parp-$2^{-/-}$ animals.

Muscle structure characteristics

Proportions of abnormal muscle fraction, inflammatory cells and internal nuclei did not differ in any muscle between groups.

MUSCLE PROTEIN CATABOLISM, PHENOTYPE, AND FUNCTION IN RESPIRATORY AND LIMB MUSCLES IN PARP-1$^{-/-}$ AND PARP-2$^{-/-}$ MICE WITH LUNG CANCER CACHEXIA

Alba Chacon-Cabrera[1,2], Clara Fermoselle[1], Elena García-Arumí[3,4], Antoni L. Andreu[3,4], Jose Yelamos[5,6], and Esther Barreiro[1,2]

[1]Pulmonology Department-Lung Cancer and Muscle Research group, IMIM-*Hospital del Mar*, Health and Experimental Sciences Department (CEXS), *Universitat Pompeu Fabra* (UPF), Barcelona Biomedical Research Park (PRBB), C/ Dr. Aiguader, 88, Barcelona.

[2]*Centro de Investigación en Red de Enfermedades Respiratorias* (CIBERES), *Instituto de Salud Carlos* III (ISCIII), Barcelona, Spain.

[3]*Unitat de Patologia Neuromuscular i Mitocondrial, Hospital Universitari Vall d'Hebron Institut de Recerca (VHIR), Universitat Autònoma de Barcelona.*

[4]*Centro de Investigación Biomédica en Red de Enfermedades Raras (CIBERER), ISCIII,* Barcelona, Spain.

[5]Cancer Research Program-Immunology, Hospital del Mar Medical Research Institute (IMIM)-Hospital del Mar, Barcelona, Spain

[6]*Centro de Investigación en Red de Enfermedades Hepáticas y Digestivas* (CIBERehd), *Instituto de Salud Carlos* III (ISCIII), Barcelona, Spain.

Corresponding author: Dr. Esther Barreiro, Pulmonology Department, IMIM-Hospital del Mar, PRBB, C/ Dr. Aiguader, 88, Barcelona, E-08003 Spain, Telephone: (+34) 93 316 0385, Fax: (+34) 93 316 0410, e-mail: ebarreiro@imim.es.

Running head: Cancer-induced cachexia in Parp-1 and -2 deficient mice

Word count: 5,515

ABSTRACT

Background: Muscle wasting and cachexia further impair disease prognosis, regardless of the underlying condition. Strategies to treat cachexia are still at its infancy. Enhanced muscle protein breakdown and ubiquitin-proteasome system are common features of cachexia associated with chronic conditions including lung cancer (LC). Poly(ADP-ribose) polymerases (PARP) may play a role in muscle metabolism and body composition. We hypothesized that protein catabolism, proteolytic markers, muscle fiber phenotype, and muscle anabolism may improve in respiratory and limb muscles of LC-cachectic Parp-1-deficient (Parp-$1^{-/-}$) and Parp-$2^{-/-}$ mice. **Methods:** Body and muscle weights, limb muscle force, muscle fiber phenotype, apoptotic nuclei, tyrosine release, total protein ubiquitination, muscle-specific E3 ligases, NF-κB signaling pathway, and markers of muscle anabolism (Akt, mTOR, p70S6K, and mitochondrial DNA) were evaluated in the diaphragm and gastrocnemius of LC (LP07 adenocarcinoma) bearing mice: wild type, Parp-$1^{-/-}$ and Parp-$2^{-/-}$. **Results:** Compared to wild type cachectic animals, in both respiratory and limb muscles of Parp-$1^{-/-}$ and Parp-$2^{-/-}$ cachectic mice: the characteristic enhanced protein catabolism (tyrosine release) via activation of the ubiquitin-proteasome system (total protein ubiquitination, atrogin-1, and 20S proteasome C8 subunit) was blunted, the reduction in contractile myosin and atrophy of the fibers was attenuated, while no effects were seen in other structural features (inflammatory cells, internal or apoptotic nuclei), and markers of muscle anabolism partly improved. **Conclusions:** These findings suggest that PARP-1 and -2 are likely to play a relevant role in muscle protein catabolism. Thus, the use of PARP inhibitors in patients with cancer cachexia warrants further attention.

Word count: 246

KEY WORDS: cancer-induced cachexia; muscle anabolism and catabolism; muscle atrophy and myosin loss; Parp-$1^{-/-}$ and Parp-$2^{-/-}$ mice; mitochondrial biogenesis.

Introduction

Muscle dysfunction and mass loss are common features of many chronic conditions. In advanced stages of respiratory and cardiac diseases and malignancies, the prevalence of muscle wasting and cachexia is very high (von and Anker, 2010;Diaz et al, 2014;Evans et al, 2008;Fearon et al, 2011;Leiro-Fernandez et al, 2014;Sanchez-Salcedo et al, 2015;Sanchez, 2015;Muscaritoli et al, 2006). Muscle mass loss and dysfunction have a great impact on the patients' quality of life as they severely compromise exercise tolerance. Additionally, muscle wasting and weakness were shown to negatively influence disease prognosis and survival (Evans et al, 2008;Muscaritoli et al, 2006;von and Anker, 2010;Diaz et al, 2014;Penalver Cuesta et al, 2015;Rodriguez et al, 2014;Sebio et al, 2015;Fearon et al, 2011).

Despite that growing evidence has shown that mechanisms such as oxidative stress, systemic inflammation, ubiquitin-proteasome system, metabolic derangements (Chacon-Cabrera et al, 2014;Fermoselle et al, 2011;Fermoselle et al, 2012;Puig-Vilanova et al, 2014), and myostatin (Fermoselle et al, 2011;Whittemore et al, 2003;Zhou et al, 2010) are involved in muscle wasting and cachexia, the contribution of other pathways that could have potential therapeutic implications remain to be fully identified. In this regard, it has been recently demonstrated (Chacon-Cabrera et al, 2014) that attenuation of mitogen-activated protein kinases (MAPK) and nuclear factor (NF)-κB signaling pathways induced beneficial effects on body and muscle weight loss in cancer-induced cachectic mice through the action of a cascade of molecular events.

Poly(adenosine diphosphate-ribose) polymerases (PARPs) consist of a family of proteins that catalytically cleave β-nicotinamide adenine dinucleotide (β-NAD^+) into nicotinamide and ADP-ribose and transfer the ADP-ribose moiety to acceptor residues of target proteins (Yelamos et al, 2011). PARPs are involved in different biological functions such as maintaining genomic integrity, transcription, angiogenesis, cell death in oxidative stress related pathologies, and metabolic and immune regulation (Burkle and Virag, 2013;Yelamos et al, 2011).

Overactivation of PARP, which may occur as a result of increased oxidant production, exerts deleterious effects on tissues mainly by depletion of cellular ATP stores that lead to cell dysfunction and death (Ha and Snyder, 1999). Importantly, this mechanism of cell destruction participates in the etiology of conditions such as acute lung and renal injuries (Kiefmann et al, 2004;Vaschetto et al, 2008;Zheng et al, 2005), and sepsis (Jagtap et al, 2002), which is also characterized by severe protein catabolism and muscle wasting. On the other hand, PARP-1 and PARP-2 inhibition was also shown to promote oxidative metabolism in skeletal muscles in two different studies (Bai et al, 2011b;Bai et al, 2011a). These findings may be of potential interest in the treatment of the muscle wasting process associated with chronic conditions including cancer, since pharmacological inhibitors of PARP-1

and -2 are also currently available in clinical settings. However, before a beneficial effect on muscle mass loss and metabolism can be established from the use of those pharmacological inhibitors in patients with severe muscle wasting and cachexia, the role of either PARP-1 or PARP-2 in protein anabolism and catabolism, muscle phenotype and function deserves particular attention in animal models. Furthermore, the specific mechanisms and molecular fingerprints potentially susceptible to be targeted by selective inhibitors of PARP-1 and -2 activities in models of cachexia remain to be identified. Also, whether Parp-1 and -2 deletions may ameliorate muscle metabolism and structure in the main respiratory muscle, the diaphragm, in models of cachexia needs to be elucidated.

On this basis, we hypothesized that specific genetic deletion of Parp-1 and -2 in mice may elicit a beneficial effect on total body and muscle weights and limb force, while inducing an attenuation of muscle protein breakdown and expression of proteolytic pathways, and an improvement in the content of contractile proteins and anabolic markers. Accordingly, the following objectives were established to be analyzed in the diaphragm and gastrocnemius muscles of Parp-$1^{-/-}$ and Parp-$2^{-/-}$ mice exposed to lung cancer cachexia for one month: 1) to assess the effects of PARP -1 and -2 deficiency on body and muscle weights, and limb muscle strength, 2) to explore levels of protein degradation, markers of ubiquitin-proteasome pathway, contractile proteins, and muscle anabolism including mitochondrial biogenesis, 3) to evaluate muscle structural abnormalities and phenotype, and the rate of apoptotic nuclei, and 4) to analyze potential correlations between physiological and molecular variables in cachectic wild type, Parp-$1^{-/-}$ and Parp-$2^{-/-}$ mice.

Materials and Methods (See additional information on all the methodologies in the online supplementary material).

Animal model

Tumor. LP07 is a cell line derived from the transplantable P07 lung tumor that appeared spontaneously in the lung of a BALB/c mouse (Diament et al, 1998). It has also been consistently demonstrated that one month after cellular inoculation, all animals developed lung metastasis, spleen enlargement, and severe cachexia without affecting any other organs (Chacon-Cabrera et al, 2014).

*Mice***.** BALB/c female mice (ten weeks old) were obtained from Harlan *Interfauna Ibérica SL* (Barcelona, Spain). Parp-$1^{-/-}$ and Parp-$2^{-/-}$ female mice (strain 129/Sv x C57BL/6), kindly provided by Dr. de Murcia (de Murcia et al, 1997) (Strasbourg, France), were backcrossed on BALB/c background for twelve generations. Genotyping was performed by PCR analysis using tail DNA as described (Corral et al, 2005). Parp-$1^{-/-}$ and Parp-$2^{-/-}$ knockout animals were also used in another study with the aim to explore epigenetic regulation of muscle wasting (Chacon-Cabrera et al, 2015).

Experimental design and Ethics. In all experimental groups (except for control rodents), LP07 viable

cells ($4x10^5$) resuspended in 0.2 mL minimal essential media (MEM) were subcutaneously inoculated in the left flank of female BALB/c mice on day 1 and were studied for a period of one month. Fifty-eight mice were used in the study, which were further subdivided into the following groups: 1) control wild type (N=12), inoculation of 0.2 mL MEM; 2) LC-cachexia wild type group (N=14), inoculation of LP07 cells in 0.2 mL MEM; 3) control Parp-$1^{-/-}$ (N=8), inoculation of 0.2 mL MEM; 4) LC-cachectic Parp-$1^{-/-}$ mice (N=12), inoculation of LP07 cells in 0.2 mL MEM; 5) control Parp-$2^{-/-}$ (N=6), inoculation of 0.2 mL MEM; and 6) LC-cachectic Parp-$2^{-/-}$ mice (N=6), inoculation of LP07 cells in 0.2 mL MEM. This controlled study was designed in accordance with the ethical standards on animal experimentation (EU 2010/63 CEE, Real Decreto 53/2013 BOE 34, Spain) at PRBB and the Helsinki convention for the use and care of animals. Ethical approval was obtained by the Animal Research Committee (Animal welfare department, Catalonia, EBP-09-1228)

***In vivo* measurements in the mice**

In all the study animals, body weight and food intake were measured every day during the entire duration of the study, whereas limb force (grip strength) was determined on days 0 and 30 in all animals as previously shown (Chacon-Cabrera et al, 2014;Whittemore et al, 2003). Control animals were paired-fed according to the amount of food eaten by the cachectic rodents (3g/24h). As shown in figure E1A, grip strength was assessed in the four limbs at the same time in all mice. Body weight and grip strength gains were calculated as the percentage of the measurements performed at the end of the study period (30 days) with respect to the same measurements obtained at baseline (day 0). In all the animals, body weight and limb strength gains were calculated as follows: (final body weight on day 30 – initial body weight on day 0)/ initial body weight on day 0 x 100, and (grip strength on day 30–grip strength on day 0)/ grip strength on day 0 x 100, respectively.

Sacrifice and sample collection

Mice from all experimental groups were always sacrificed on day 30 post-inoculation of LP07 cells or MEM (control animals), and diaphragm and gastrocnemius muscles were subsequently obtained. In all mice, the weight of each muscle was determined using a high-precision scale immediately after having been excised from the animals. LC-cachectic mice were macroscopically of smaller size than healthy control rodents (Chacon-Cabrera et al, 2014). Frozen tissues were used for immunoblotting and real-time polymerase chain reaction assay (qRT-PCR) techniques, while paraffin-embedded tissues were used for the assessment of muscle structure abnormalities and fiber type morphometry.

Biological analyses

*Muscle DNA isolation***.** Total DNA, including mitochondrial and nuclear DNA, was isolated from diaphragm and gastrocnemius muscles of all mouse experimental groups using QIAmp DNA Mini Kit (QiAgen, GmbH, Germany) (Andreu et al, 2009), following the manufacturer's protocol of DNA

purification from tissues, and without the use of RNase A. Total DNA obtained from muscles was quantified using a spectrophotometer (NanoDrop, Thermo Scientific, Wilmington, Delaware, USA).

Absolute quantification of DNAs. Mitochondrial DNA (mtDNA) copy number was estimated through the quantification of the mtDNA to nuclear DNA (nDNA) ratio (mtDNA/nDNA) by real-time PCR (Andreu et al, 2009;McDermott-Roe et al, 2011).

Immunoblotting of 1D electrophoresis. Protein levels of the different molecular markers analyzed in the study were explored by means of immunoblotting procedures as previously described (Chacon-Cabrera et al, 2014). Glyceraldehyde-3-phosphate dehydrogenase (GAPDH) was used as the loading control for all the immunoblots as shown in the corresponding figures.

Protein catabolism. Protein degradation was explored on the basis of the rate of production of free tyrosine from muscle proteins as previously described (Chacon-Cabrera et al, 2014).

Muscle fiber counts and morphometry. On 3-micrometer muscle paraffin-embedded sections from diaphragms and gastrocnemius muscles of all study groups, MyHC-I and –II isoforms were identified using specific antibodies (Chacon-Cabrera et al, 2014).

Muscle structure abnormalities. The area fraction of normal and abnormal muscle was evaluated on twenty 3-micrometer paraffin-embedded sections of the diaphragm and gastrocnemius of all study groups muscles following previously published methodologies (Chacon-Cabrera et al, 2014) (Fig. E1B).

Terminal deoxynucleotidyl transferase-mediated dUTP nick-end labeling (TUNEL) assay. In muscle paraffin-embedded sections, apoptotic nuclei were identified using the TUNEL assay (Chacon-Cabrera et al, 2014).

Poly(ADP) ribosylation activity. In muscle paraffin-embedded sections, positively nuclei for pADPr were identified using the specific antibody, and following previous published methodologies (Chacon-Cabrera et al, 2014).

Statistical Analysis

Normality of the study variables was checked using the Shapiro-Wilk test. Physiologic, structural, and molecular results are expressed as mean (standard deviation), since the last one represents in a more realistic manner the variability of the sample (Jaykaran, 2010). For the purpose of the study, results obtained in the diaphragm and gastrocnemius muscles were subsequently analyzed as follows: 1) LC-cachectic wild type mice versus their respective non-tumor controls, 2) LC-cachectic Parp-$1^{-/-}$ animals versus their respective knockout non-tumor controls, 3) LC-cachectic Parp-$2^{-/-}$ mice versus their respective knockout non-tumor controls, and 4) any of the non-tumor knockout mice versus non-tumor wild type animals. Comparisons described above were assessed using one-way analysis of

variance (ANOVA), in which *Dunnett's post hoc* analysis was used to adjust for multiple comparisons among the study groups. The existence of potential correlations between different variables was only tested in the LC-cachectic groups of mice (both wild type and knockout mice). Specifically, correlations between physiological and biological variables were explored using the Pearson's correlation coefficient. A level of significance of $P \leq 0.05$ was established. The sample size chosen was based on previous studies (Chacon-Cabrera et al, 2014;Chacon-Cabrera et al, 2015;Fermoselle et al, 2011), where very similar approaches were employed. In addition, statistical power was calculated using specific software (StudySize 2.0, CreoStat HB, Frolunda, Sweden). Body weight gain was selected as the target variable to estimate the statistical power in the study. On the basis of a standard power statistics established at a minimum of 80% and assuming an alpha error of 0.05, the former parameter was sufficiently high to detect a minimum difference of 1.2 points between groups in the sample size (minimum of N=6) and standard deviation.

Results

Physiological characteristics

LC-induced cachexia. Figure 1A illustrates the body weight curves in the animals of all the experimental groups during the 30-day study period. As shown in Figure 1A and Table 1, cachectic wild type mice exhibited a significant reduction in body weight gain compared to their respective controls at the end of the study period (day 30). The weights of diaphragm and gastrocnemius muscles and gain in limb strength were significantly reduced in cachectic wild type mice. Importantly, in Parp-$1^{-/-}$ mice, a statistically significant reduction in these parameters was also observed, but to a much lesser extent that in wild type animals. In cachectic Parp-$2^{-/-}$ mice, no significant differences were observed in body and muscle weights and limb strength between cachectic and non-cachectic mice.

The expression of PARP-1 and PARP-2 was confirmed in the subcutaneous tumors of the wild type and both groups of knockout mice, as previously reported (Chacon-Cabrera et al, 2015;Mateu-Jimenez et al, 2016). Compared to cachectic wild type animals, the weights of the subcutaneous tumors were reduced in both Parp-$1^{-/-}$ and Parp-$2^{-/-}$ LC-cachectic mice (Table 1).

Effects of Parp deletion on non-cachectic control animals. As illustrated in Table 1, non-cachectic knockout animals (Parp-$1^{-/-}$ and Parp-$2^{-/-}$) exhibited a reduction in the weights of their muscles (diaphragm and gastrocnemius) compared to wild type non-tumor animals. However, no significant differences were observed in body weight at baseline and body weight and limb strength gains in either Parp-$1^{-/-}$ or Parp-$2^{-/-}$ control mice compared to non-tumor wild type animals at the end of the study period (Table 1 and Fig. 1A).

Poly-ADP ribosylation in muscles

LC-induced cachexia. Poly-ADPr positive nuclei counts were increased in both diaphragm and gastrocnemius of cachectic wild type mice compared to their respective controls (Figs 1B, 1C, E2A and E2B). In both groups of cachectic knockout mice, no significant differences were seen in poly-ADPr positive nuclei counts in any muscle between cachectic and non-cachectic mice (Figs 1B, 1C, E2A and E2B).

Effects of Parp deletion on non-cachectic control animals. Poly-ADPr positive nuclei counts were reduced in the diaphragm and gastrocnemius of both groups of non-cachectic knockout mice compared to wild type non-tumor bearing rodents (Figs 1B, 1C, E2A and E2B).

Muscle redox balance

LC-induced cachexia. Total protein carbonylation was significantly increased in both diaphragm and gastrocnemius muscles of cachectic wild type mice compared to their respective non-cachectic controls (Figs. 2A, 2B, E3A, and E3B). Total carbonylated proteins did not differ between Parp-$1^{-/-}$ or Parp-$2^{-/-}$ cachectic mice and their respective non-cachectic knockout controls in any of the study muscles (Figs. 2A, 2B, E3A, and E3B). Protein levels of SOD2 were significantly reduced in both diaphragm and gastrocnemius muscles of cachectic wild type mice compared to their respective non-tumor rodents (Figs. 2C, 2D, E3C, and E3D). SOD2 protein content did not differ between any of the cachectic knockout groups of mice and their respective non-cachectic controls (Figs. 2C, 2D, E3C, and E3D). Levels of SOD1 did not differ in any muscle between cachectic and non-cachectic mice in any of the study groups (Figs. 2E, 2F, E3E, and E3F).

Effects of Parp deletion on non-cachectic control animals. Total protein carbonylation, SOD2 and SOD1 levels did not differ between Parp-$1^{-/-}$ or Parp-$2^{-/-}$ non-cachectic controls and non-cachectic wild type rodents in any of the study muscles (Fig. 2A-2F, and E3A-E3F).

Proteolysis in muscles

LC-induced cachexia. Protein degradation, as measured by the release of the amino acid tyrosine, was significantly increased in both diaphragm and gastrocnemius muscles of cachectic wild type mice compared to non-cachectic controls (Fig. 3A and 3B). However, Parp-$1^{-/-}$ and Parp-$2^{-/-}$ cachectic animals did not show any significant difference in protein degradation levels compared to their respective non-cachectic controls in any of the study muscles (Fig. 3A and 3B). Total protein ubiquitination and protein content of 20S proteasome subunit C8 were increased in both respiratory and limb muscles of cachectic wild type mice compared to non-cachectic controls (Figs. 4A-4D, and E4A-E5B). The levels of these proteolytic markers did not differ between any of the cachectic knockout groups of mice and their respective non-cachectic controls (Figs. 4A-4D, and E4A-E5B). Levels of E3 ligases TRIM32 and MURF-1 did not differ in any muscle between cachectic and non-

cachectic mice in any of the study groups (Figs. 5A-5D, and E6A-E7B). Atrogin-1 content was greater in both muscles of the cachectic wild type rodents compared to non-cachectic controls mice, while its levels did not differ in any study muscle between cachectic and non-cachectic knockout animals (Figs. 5E, 5F, E8A, and E8B).

Effects of Parp deletion on non-cachectic control animals. Tyrosine release, total protein ubiquitination, 20S proteasome subunit C8 levels, TRIM32, MURF-1 and atrogin-1 levels did not differ between Parp-$1^{-/-}$ or Parp-$2^{-/-}$ non-cachectic controls and non-cachectic wild type rodents in any of the study muscles (Figs. 3A, 3B, 4A-4D, 5A-5F, and E4A-E8B).

Signaling markers in muscles

LC-induced cachexia. Relative activated NF-kB p50 and NF-kB p65 levels were increased in the diaphragm and gastrocnemius muscles of cachectic wild type mice compared to their non-tumor controls, whereas no significant differences were observed in the same muscles between any of the cachectic knockout mice and their respective non-tumor controls (Figs. 6A-6D, E9A-E10B).

Effects of Parp deletion on non-cachectic control animals. Relative activated NF-kB p50 levels did not significantly differ between either non-cachectic Parp-$1^{-/-}$, or Parp-$2^{-/-}$ and non-cachectic wild type mice in any of the study muscles (Figs. 6A, 6B, E9A, and E9B). Compared to non-cachectic wild type animals, relative activated NF-kB p65 levels were decreased only in the gastrocnemius of non-cachectic Parp-$2^{-/-}$ mice (Figs. 6C, 6D, E10A and E10B).

Muscle anabolism

LC-induced cachexia. Compared to their respective non-cachectic controls, cachectic wild type and Parp-$1^{-/-}$ animals did not show any significant difference in activated Akt muscle levels in any study muscle, while in cachectic Parp-$2^{-/-}$ mice, activated Akt levels were increased in the gastrocnemius but not the diaphragm (Figs. 7A, 7B, E11A, and E11B). Activated mTOR levels were decreased in both muscles of cachectic wild type mice compared to wild type controls (Figs. 7C, 7D, E12A, and E12B). However, an increase in activated mTOR levels was seen in the diaphragm of cachectic Parp-$2^{-/-}$ animals and in the gastrocnemius of cachectic Parp-$1^{-/-}$ mice (Figs. 7C, and 7D, respectively, and Figs. E12A and E12B). Compared to non-cachectic controls, no significant differences were detected in p70S6K levels in the diaphragm of either cachectic wild type or any of the knockout mice (Figs. 7E and E13A). Activated p70S6K levels were decreased in the gastrocnemius of cachectic wild type mice compared to their non-cachectic controls (Figs. 7F and E13B). Cachectic wild type and Parp-$2^{-/-}$ animals showed a reduction in mtDNA/nDNA content in both respiratory and limb muscles compared to their respective non-cachectic controls. However, no differences were seen in mtDNA/nDNA levels in any study muscle of cachectic Parp-$1^{-/-}$ mice compared to the respective non-cachectic controls (Figs. 7G and 7H).

Effects of Parp deletion on non-cachectic control animals. Compared to non-cachectic wild type animals, activated Akt, mTOR and p70S6K levels did not differ in any study muscle among the experimental groups (Figs. 7A-7F and E11A-E13B). The ratio of mtDNA/nDNA did not significantly differ between either non-cachectic Parp-$1^{-/-}$ or Parp-$2^{-/-}$ and non-cachectic wild type mice in any of the study muscles (Figs. 7G and 7H).

Muscle structural proteins

LC-induced cachexia. In diaphragm and gastrocnemius of wild type cachectic mice, protein levels of contractile MyHC were reduced compared to their non-cachectic controls (Figs. 8A, 8B, E14A, and E14B). In cachectic Parp-$1^{-/-}$ mice, MyHC levels also decreased in the diaphragm but not in the gastrocnemius, compared to Parp-$1^{-/-}$ non-cachectic animals (Figs. 8A, 8B, E14A, and E14B). MyHC levels did not significantly differ between cachectic and non-cachectic Parp-$2^{-/-}$ animals in any of the study muscles (Figs. 8A, 8B, E14A, and E14B). Actin levels did not differ in the study muscles between cachectic animals and their respective non-cachectic control rodents in any experimental group (Figs. 8C, 8D, E15A, and E15B).

Effects of Parp deletion on non-cachectic control animals. MyHC and actin levels did not significantly differ among the three non-cachectic groups of animals in any of the study muscles (Figs. 8A-8D and E14A-E15B).

Muscle structure characteristics

LC-induced cachexia. The proportions of type I and II fibers did not differ between cachectic and non-cachectic conditions in any experimental group of mice. The size of both slow- and fast-twitch fibers was significantly reduced in diaphragm and gastrocnemius of cachectic wild type mice compared to their respective non-cachectic controls (Table 2 and Figs. E16A and E16B). However, in both Parp-$1^{-/-}$ and Parp-$2^{-/-}$ mice, the size of type I and type II fibers did not show significantly differed in any study muscle between cachectic and non-cachectic animals (Table 2 and Figs. E16A and E16B). Compared to their respective non-cachectic controls, proportions of abnormal muscle fraction, including inflammatory cell and internal nuclei counts were increased in both respiratory and limb muscles of all study groups (Table 2). A significant correlation was found between proportions of internal nuclei and tyrosine release in the diaphragm of the cachectic wild type mice ($r=0.749$, $p=0.032$), but not in any of the knockout mice ($r=-0.238$, $p=0.457$ and $r=0.784$, $p=0.065$, Parp-$1^{-/-}$ and Parp-$2^{-/-}$ mice, respectively). Compared to their respective non-cachectic controls, TUNEL-stained nuclei counts were increased in respiratory and limb muscles of all the cachectic groups of mice (wild type, Parp-$1^{-/-}$ and Parp-$2^{-/-}$) (Table 2 and Figs. E16C and E16D).

Effects of Parp deletion on non-cachectic control animals. Proportions of type I and type II fibers did

not significantly differ between wild type and either Parp-$1^{-/-}$ or Parp-$2^{-/-}$ non-cachectic controls in any study muscle (Table 2 and Figs. E16A and E16B). The size of slow-twitch fibers was significantly reduced in the gastrocnemius of non-cachectic Parp-$2^{-/-}$ mice compared to non-cachectic wild type animals (Table 2 and Figs. E16A and E16B). Proportions of inflammatory cells were increased only in the diaphragm of Parp-$2^{-/-}$ controls compared to wild type non-cachectic animals (Table 2 and Figs. E16C and E16D).

Discussion

The main findings in the investigation were that compared to non-cachectic control wild type animals, in both diaphragm and gastrocnemius muscles of cancer cachectic wild type mice: 1) body weight gain, muscle weights, limb strength, and the size of slow- and fast-twitch fibers in both diaphragm and gastrocnemius muscles were lower, while structural abnormalities including inflammatory cells and both internal and apoptotic nuclei were greater; 2) protein oxidation, PARP activity and protein breakdown (tyrosine release) were increased; 3) levels of markers of the ubiquitin-proteasome system were greater; 4) contractile myosin content was decreased, 5) NF-κB signaling pathway was induced, and 6) several markers of muscle anabolism were reduced. Specific genetic deletions of Parp-1 and -2 in the cancer cachectic mice induced a reduction in levels of protein oxidation, PARP activity and protein catabolism, markers of ubiquitin-proteasome system, NF-κB signaling pathway, and caused an improvement in levels of protein anabolism, body and muscle weights, limb muscle strength, muscle fiber sizes, and contractile myosin levels. We believe that the results encountered in the present study enhance existing knowledge in the field of muscle wasting and cachexia associated with lung cancer. Moreover, deficiency of either PARP-1 or -2 induced several beneficial effects on the cachectic animals and their muscles that are discussed below.

Muscle protein catabolism as measured by the tyrosine release assay was increased in the diaphragm and gastrocnemius muscles of the cancer cachectic mice. Genetic inhibition of Parp-1 and -2 blunted the rise in protein breakdown in both respiratory muscles of the cachectic animals. In a previous investigation (Chacon-Cabrera et al, 2014), we demonstrated that NF-κB and MAPK are the predominant signaling pathways driving muscle mass loss in this experimental model of cancer cachexia. Additionally, in the same cachectic wild type mice, transcriptional activity of NF-κB was significantly greater in the gastrocnemius muscles than in the non-cachectic control mice (Chacon-Cabrera et al, 2014). In agreement with these findings, in the current investigation, NF-κB signaling pathway was also activated in the diaphragm and gastrocnemius muscles of the cachectic wild type animals. Collectively, it could be assumed that the reduced proteolytic degradation seen in the

muscles of the cachectic knockout animals is likely to be the result of decreased NF-κB transcriptional activity induced by PARP-1 deficiency, as shown to occur in previous studies (Hassa and Hottiger, 1999;Oliver et al, 1999). Importantly, the attenuation of protein degradation may also account for the improvements observed in body and muscle weights and limb muscle strength in Parp-$1^{-/-}$ and Parp-$2^{-/-}$ cachectic mice.

Oxidative stress has been shown to trigger muscle wasting in patients (Barreiro et al, 2008;Barreiro et al, 2010;Fermoselle et al, 2012;Marin-Corral et al, 2010;Puig-Vilanova et al, 2014) and animal models including the current model of cancer cachexia (Chacon-Cabrera et al, 2014;Fermoselle et al, 2011;Fermoselle et al, 2012;Puig-Vilanova et al, 2014) and to induce the activation of PARP in the nucleus (de et al, 1994). On the other hand, it has also been demonstrated that PARP activates the proteasome to degrade oxidative damaged histones (Ullrich et al, 1999). In the current investigation, total protein ubiquitination levels were increased in the cachectic wild type rodents, whereas no differences in this proteolytic marker were detected between cachectic and non-cachectic control Parp-$1^{-/-}$ and Parp-$2^{-/-}$ mice. These findings suggest that both PARP-1 and -2 deficiency blunted the rise in protein ubiquitination seen in the respiratory and limb muscles of the cachectic knockout mice probably by reducing the levels of oxidants, which were previously shown to be increased in diaphragm and gastrocnemius muscles of cancer cachectic mice (Chacon-Cabrera et al, 2014) and quadriceps of cachectic patients with lung tumors (Puig-Vilanova et al, 2014).

Levels of markers of the ubiquitin-proteasome pathway such as the 20S proteasome C8 subunit and that of the E3 ligase atrogin-1 were also significantly increased in the respiratory and limb muscles of the cachectic wild type rodents compared to the non-tumor controls. These findings are in agreement with previous studies, in which markers of this proteolytic system was consistently upregulated in models of muscle wasting (Chacon-Cabrera et al, 2014;Fermoselle et al, 2011) including patients with cachexia (Fermoselle et al, 2012;Puig-Vilanova et al, 2014). Importantly, in both respiratory and limb muscles of Parp-$1^{-/-}$ and Parp-$2^{-/-}$ cachectic mice, levels of those two markers of proteolysis did not differ from the non-cachectic controls. These results imply that PARP-1 and -2 deficiency attenuate protein degradation via the blockade of the ubiquitin-proteasome system at different steps in both respiratory and limb muscles of the cachectic knockout animals. They also suggest that the ubiquitin-proteasome system plays a major role in muscle proteolysis observed in diaphragm and gastrocnemius muscles in this model of cancer cachexia, as previously demonstrated (Chacon-Cabrera et al, 2014). It should also be mentioned that levels of the E3 ligases TRIM-32 and MURF-1 did not significantly differ between cachectic and non-cachectic control mice in any of the study muscles, thus implying that atrogin-1 is the key muscle-specific ligase involved in proteasomal degradation of proteins in the respiratory and limb muscles in this experimental model

of cachexia.

Levels of mTOR were significantly decreased in the diaphragm and gastrocnemius and those of p70SK6 in the latter muscles of the cachectic wild type mice compared to the non-tumor controls. These findings are in agreement with those reported in models of colon cancer cachexia in mice (White et al, 2011) and in muscles from elderly subjects (Fry et al, 2011;White et al, 2011), in which mTOR signaling was suppressed together with a decline in the rate of myofibrilar protein synthesis. Importantly, in cachectic Parp-$1^{-/-}$ and Parp-$2^{-/-}$ mice, the decrease in mTOR levels was attenuated in both muscles, thus suggesting that PARP-1 and -2 may interact with mTOR signaling in this model of muscle wasting, especially in the limb muscle. Indeed, previous studies have shown that pharmacological inhibitors of PARP prevent mTOR inhibition through its role in modulating adenosine monophosphate-activated protein kinase pathways (Ethier et al, 2012).

Furthermore, mitochondrial biogenesis as measured by the ratio of mitochondrial to nuclear DNA was reduced in diaphragm and gastrocnemius muscles of cachectic wild type animals compared to non-cachectic controls. These results are in line with those recently reported in other investigations, in which mitochondrial biogenesis impairment was shown to occur early in the initiation of cachexia (White JP et al, 2012) and in muscles of rats bearing the Yoshida ascites hepatoma (Fontes-Oliveira et al, 2014). Interestingly, in cachectic Parp-$1^{-/-}$ mice, but not Parp-$2^{-/-}$ animals, the reduction in mitochondrial biogenesis was attenuated in respiratory and limb muscles of the cachectic rodents. These findings are in line with previous data showing an improvement in mitochondrial biogenesis upon inhibition of PARP-1, via Sirtuin1 activity (Bai et al, 2015;Rajamohan et al, 2009). Depletion of PARP-2 also resulted in enhanced Sirtuin1 activity and increased mitochondrial biogenesis in several in vitro models (Bai et al, 2011a;Mohamed et al, 2014). Differences between Parp-$1^{-/-}$ and Parp-$2^{-/-}$ cachectic mice in mitochondrial biogenesis observed in this study may be the result of the distinctive interaction of PARP-1 and -2 with Sirtuin1 promoter: while PARP-2 does not modify Sirtuin1 promoter activity, PARP-2 suppresses its activity (Bai et al, 2011b). These findings warrant special attention in further studies in which the specific role of PARP-1 and -2 in mitochondrial remodeling and function should be explored.

Importantly, protein levels of MyHC were significantly decreased in muscles of wild type cachectic mice. These findings are in line with results previously reported by our group on diaphragm (Marin-Corral et al, 2009) and quadriceps muscles of patients with advanced COPD and cancer cachexia (Fermoselle et al, 2012;Puig-Vilanova et al, 2014) as well as in muscles of mice with emphysema-induced cachexia (Fermoselle et al, 2011). A relevant finding in the investigation was the attenuation of such a reduction in MyHC content observed in the study muscles, especially the gastrocnemius, induced by PARP-1 and -2 genetic deletions in the cachectic animals.

Importantly, the reported decrease in the rate of myofibrilar protein synthesis observed in models of cachexia (White JP et al, 2012;White et al, 2011;Toth et al, 2013) and aging (Fry et al, 2011) may partly account for the reduced levels of myosin in the cachectic muscles of wild type animals. Additionally, reductions in myofibrilar protein content may also account for the smaller fiber sizes of slow- and fast-twitch fibers observed in both muscle types of the cachectic wild type mice in the study. Again, previous investigations from our group have also reported similar findings showing that contractile myosin loss, but not actin, is involved in the atrophy of the muscle fibers in patients (Fermoselle et al, 2012;Puig-Vilanova et al, 2014) and animals (Chacon-Cabrera et al, 2014;Marin-Corral et al, 2010) with cachexia.

Interestingly, several structural abnormalities were detected in the diaphragm and gastrocnemius muscles of cachectic wild type animals compared to non-cachectic controls. These results are similar to those encountered in a former investigation from our group (Chacon-Cabrera et al, 2014), suggesting that inflammatory and regenerative events underlie muscle wasting in the animals. Moreover, levels of TUNEL-positive nuclei were also significantly increased in the respiratory and limb muscles of all the cachectic groups of mice as also shown in a previous study (Chacon-Cabrera et al, 2014). In general, structural abnormalities were not modified by selective deletion of either PARP-1 or -2 activities. These findings suggest that PARP does not seem to directly interact with muscle inflammation or regeneration processes taking place in the cancer cachectic muscles.

Study limitations

It is likely that the reduction in tumor burden observed in both groups of knockout mice may have partly contributed to favoring body and muscle mass gain in the mice. In fact, deficiency of both PARP-1 and -2 induced a reduction in tumor weights in the animals, as has recently been demonstrated through several biological mechanisms (Chacon-Cabrera et al, 2015;Mateu-Jimenez et al, 2016).

Another limitation is related to the lack of measurements on the progression of tumor size throughout the study protocol in the tumor-bearing animals. In the study, tumor weights were only available at the time of sacrifice in all experimental groups, partly because the investigation focused on the assessment of the tumor effects on the cachectic muscles. Moreover, the weights of organs such as the liver or heart were not available in all the animals. As no significant differences were detected in body weight gain among the non-tumor control groups of animals, and an improvement was seen in Parp-$1^{-/-}$ and Parp-$2^{-/-}$ cachectic mice compared to their respective non-tumor controls, we believe that it is not a major limitation in the study. Indeed, a major strength in the investigation was that the potential beneficial effects of PARP-1 and PARP-2 genetic deletions have been explored from three different perspectives: 1) whole body and muscle weights and force, 2) muscle fiber sizes,

and 3) biological events involved in muscle catabolism, anabolism, and signaling in an experimental model of LC-induced cachexia.

Future research should focus on the assessment of whether selective pharmacological inhibitors of PARP-1 and -2 exert similar beneficial effects on muscles in models of cancer cachexia including clinical settings.

Conclusions

In respiratory and limb muscles of tumor-bearing mice with cachexia, enhanced protein catabolism through activation of the ubiquitin-proteasome system was blunted by the genetic inhibition of either PARP-1 or PARP-2. The reduction in contractile myosin and atrophy of the fibers was attenuated in respiratory and limb muscles of the cachectic Parp-$1^{-/-}$ or Parp-$2^{-/-}$ mice, while no effects were seen in other structural features. Markers of muscle anabolism partly improved in both diaphragm and gastrocnemius muscles of the cachectic PARP-deficient mice, especially in cachectic Parp-$1^{-/-}$ animals. The pattern of expression of the biological events observed in the study muscles was similar in Parp-$1^{-/-}$ and Parp-$2^{-/-}$ LC-cachectic animals, except for mitochondrial biogenesis. These findings imply that PARP-1 and -2 are likely to play a relevant role in muscle protein catabolism in cancer-induced cachexia. Accordingly, the potential use of selective pharmacological inhibitors in patients with cancer cachexia warrants further attention.

ACKNOWLEDGEMENTS

The authors are thankful to Dr. Juan Martin-Caballero and Mr. Francisco Sanchez for their technical assistance with the animal experiments, to Ms. Maria Cortes-Badia and Ms. Ida Salmela for their support with the muscle structure experiments, and to Ms. Coral Ampurdanes for her contribution to mouse genotyping. The study has been funded by *Instituto de Salud Carlos-III*, contract grant numbers, CIBERES, FIS 11/02029, FIS 14/00713, Catalan Foundation of Pulmonology (FUCAP), contract grant numbers, FUCAP 2011 and 2012, and Fundació La Marató de TV3, contract grant number 2013-4130.

The authors certify that they comply with the ethical guidelines for authorship and publishing of the Journal of Cachexia, Sarcopenia and Muscle (Chacon-Cabrera A, Fermoselle C, García-Arumí E, Andreu AL, Yelamos J, and Barreiro E. Deficiency of either parp-1 or PARP-2 improves protein anabolism and catabolism, phenotype, and function in respiratory and limb muscles of lung cancer cachectic mice. *J Cachexia Sarcopenia Muscle*).

Editorial support: None to declare.

CONFLICT OF INTEREST

The authors declare no conflict of interest in relation to this study.

AUTHOR CONTRIBUTIONS

Alba Chacon-Cabrera: animal experiments, molecular biology and muscle structure experiments, data analyses, and results preparation

Clara Fermoselle: animal and molecular biology experiments

Elena García-Arumí: mitochondrial experiments and analyses

Antoni L. Andreu: mitochondrial experiments and analyses

Jose Yelamos: animal experiments, data interpretation, and manuscript intellectual input

Esther Barreiro: study design, data analyses and interpretation, results preparation, and manuscript writing final version

Literature Cited

Andreu AL, Martinez R, Marti R, Garcia-Arumi E (2009). Quantification of mitochondrial DNA copy number: pre-analytical factors. Mitochondrion 9:242-246.

Bai P, Canto C, Brunyanszki A, Huber A, Szanto M, Cen Y, Yamamoto H, Houten SM, Kiss B, Oudart H, Gergely P, Menissier-de MJ, Schreiber V, Sauve AA, Auwerx J (2011a). PARP-2 regulates SIRT1 expression and whole-body energy expenditure. Cell Metab 13:450-460.

Bai P, Canto C, Oudart H, Brunyanszki A, Cen Y, Thomas C, Yamamoto H, Huber A, Kiss B, Houtkooper RH, Schoonjans K, Schreiber V, Sauve AA, Menissier-de MJ, Auwerx J (2011b). PARP-1 inhibition increases mitochondrial metabolism through SIRT1 activation. Cell Metab 13:461-468.

Bai P, Nagy L, Fodor T, Liaudet L, Pacher P (2015). Poly(ADP-ribose) polymerases as modulators of mitochondrial activity. Trends Endocrinol Metab 26:75-83.

Barreiro E, Peinado VI, Galdiz JB, Ferrer E, Marin-Corral J, Sanchez F, Gea J, Barbera JA (2010). Cigarette smoke-induced oxidative stress: A role in chronic obstructive pulmonary disease skeletal muscle dysfunction. Am J Respir Crit Care Med 182:477-488.

Barreiro E, Schols AM, Polkey MI, Galdiz JB, Gosker HR, Swallow EB, Coronell C, Gea J (2008). Cytokine profile in quadriceps muscles of patients with severe COPD. Thorax 63:100-107.

Burkle A, Virag L (2013). Poly(ADP-ribose): PARadigms and PARadoxes. Mol Aspects Med 34:1046-1065.

Chacon-Cabrera A, Fermoselle C, Salmela I, Yelamos J, Barreiro E (2015). MicroRNA expression and protein acetylation pattern in respiratory and limb muscles of Parp-1(-/-) and Parp-2(-/-) mice with lung cancer cachexia. Biochim Biophys Acta 1850:2530-2543.

Chacon-Cabrera A, Fermoselle C, Urtreger AJ, Mateu-Jimenez M, Diament MJ, De Kier Joffe ED, Sandri M, Barreiro E (2014). Pharmacological strategies in lung cancer-induced cachexia: effects on muscle proteolysis, autophagy, structure, and weakness. J Cell Physiol 229:1660-1672.

Corral J, Yelamos J, Hernandez-Espinosa D, Monreal Y, Mota R, Arcas I, Minano A, Parrilla P, Vicente V (2005). Role of lipopolysaccharide and cecal ligation and puncture on blood coagulation and inflammation in sensitive and resistant mice models. Am J Pathol 166:1089-1098.

de Murcia JM, Niedergang C, Trucco C, Ricoul M, Dutrillaux B, Mark M, Oliver FJ, Masson M, Dierich A, LeMeur M, Walztinger C, Chambon P, de MG (1997). Requirement of poly(ADP-ribose) polymerase in recovery from DNA damage in mice and in cells. Proc Natl Acad Sci U S A 94:7303-7307.

de MG, Schreiber V, Molinete M, Saulier B, Poch O, Masson M, Niedergang C, Menissier de MJ (1994). Structure and function of poly(ADP-ribose) polymerase. Mol Cell Biochem 138:15-24.

Diament MJ, Garcia C, Stillitani I, Saavedra VM, Manzur T, Vauthay L, Klein S (1998). Spontaneous murine lung adenocarcinoma (P07): A new experimental model to study paraneoplastic syndromes of lung cancer. Int J Mol Med 2:45-50.

Diaz MC, Ospina-Tascon GA, Salazar CB (2014). Respiratory muscle dysfunction: a multicausal

entity in the critically ill patient undergoing mechanical ventilation. Arch Bronconeumol 50:73-77.

Ethier C, Tardif M, Arul L, Poirier GG (2012). PARP-1 modulation of mTOR signaling in response to a DNA alkylating agent. PLoS One 7:e47978.

Evans WJ, Morley JE, Argiles J, Bales C, Baracos V, Guttridge D, Jatoi A, Kalantar-Zadeh K, Lochs H, Mantovani G, Marks D, Mitch WE, Muscaritoli M, Najand A, Ponikowski P, Rossi FF, Schambelan M, Schols A, Schuster M, Thomas D, Wolfe R, Anker SD (2008). Cachexia: a new definition. Clin Nutr 27:793-799.

Fearon K, Strasser F, Anker SD, Bosaeus I, Bruera E, Fainsinger RL, Jatoi A, Loprinzi C, MacDonald N, Mantovani G, Davis M, Muscaritoli M, Ottery F, Radbruch L, Ravasco P, Walsh D, Wilcock A, Kaasa S, Baracos VE (2011). Definition and classification of cancer cachexia: an international consensus. Lancet Oncol 12:489-495.

Fermoselle C, Rabinovich R, Ausin P, Puig-Vilanova E, Coronell C, Sanchez F, Roca J, Gea J, Barreiro E (2012). Does oxidative stress modulate limb muscle atrophy in severe COPD patients? Eur Respir J 40:851-862.

Fermoselle C, Sanchez F, Barreiro E (2011). [Reduction of muscle mass mediated by myostatin in an experimental model of pulmonary emphysema]. Arch Bronconeumol 47:590-598.

Fontes-Oliveira CC, Busquets S, Fuster G, Ametller E, Figueras M, Olivan M, Toledo M, Lopez-Soriano FJ, Qu X, Demuth J, Stevens P, Varbanov A, Wang F, Isfort RJ, Argiles JM (2014). A differential pattern of gene expression in skeletal muscle of tumor-bearing rats reveals dysregulation of excitation-contraction coupling together with additional muscle alterations. Muscle Nerve 49:233-248.

Fry CS, Drummond MJ, Glynn EL, Dickinson JM, Gundermann DM, Timmerman KL, Walker DK, Dhanani S, Volpi E, Rasmussen BB (2011). Aging impairs contraction-induced human skeletal muscle mTORC1 signaling and protein synthesis. Skelet Muscle 1:11.

Ha HC, Snyder SH (1999). Poly(ADP-ribose) polymerase is a mediator of necrotic cell death by ATP depletion. Proc Natl Acad Sci U S A 96:13978-13982.

Hassa PO, Hottiger MO (1999). A role of poly (ADP-ribose) polymerase in NF-kappaB transcriptional activation. Biol Chem 380:953-959.

Jagtap P, Soriano FG, Virag L, Liaudet L, Mabley J, Szabo E, Hasko G, Marton A, Lorigados CB, Gallyas F, Jr., Sumegi B, Hoyt DG, Baloglu E, VanDuzer J, Salzman AL, Southan GJ, Szabo C (2002). Novel phenanthridinone inhibitors of poly (adenosine 5'-diphosphate-ribose) synthetase: potent cytoprotective and antishock agents. Crit Care Med 30:1071-1082.

Jaykaran (2010). "Mean +/- SEM" or "Mean (SD)"? Indian J Pharmacol 42:329.

Kiefmann R, Heckel K, Doerger M, Schenkat S, Kupatt C, Stoeckelhuber M, Wesierska-Gadek J, Goetz AE (2004). Role of PARP on iNOS pathway during endotoxin-induced acute lung injury. Intensive Care Med 30:1421-1431.

Leiro-Fernandez V, Mouronte-Roibas C, Ramos-Hernandez C, Botana-Rial M, Gonzalez-Pineiro A, Garcia-Rodriguez E, Represas-Represas C, Fernandez-Villar A (2014). Changes in clinical presentation and staging of lung cancer over two decades. Arch Bronconeumol 50:417-421.

Marin-Corral J, Fontes CC, Pascual-Guardia S, Sanchez F, Olivan M, Argiles JM, Busquets S, Lopez-Soriano FJ, Barreiro E (2010). Redox balance and carbonylated proteins in limb and heart muscles of cachectic rats. Antioxid Redox Signal 12:365-380.

Marin-Corral J, Minguella J, Ramirez-Sarmiento AL, Hussain SN, Gea J, Barreiro E (2009). Oxidised proteins and superoxide anion production in the diaphragm of severe COPD patients. Eur Respir J 33:1309-1319.

Mateu-Jimenez M, Cucarull-Martinez B, Yelamos J, Barreiro E (2016). Reduced tumor burden through increased oxidative stress in lung adenocarcinoma cells of PARP-1 and PARP-2 knockout mice. Biochimie 121:278-286.

McDermott-Roe C, Ye J, Ahmed R, Sun XM, Serafin A, Ware J, Bottolo L, Muckett P, Canas X, Zhang J, Rowe GC, Buchan R, Lu H, Braithwaite A, Mancini M, Hauton D, Marti R, Garcia-Arumi E, Hubner N, Jacob H, Serikawa T, Zidek V, Papousek F, Kolar F, Cardona M, Ruiz-Meana M, Garcia-Dorado D, Comella JX, Felkin LE, Barton PJ, Arany Z, Pravenec M, Petretto E, Sanchis D, Cook SA (2011). Endonuclease G is a novel determinant of cardiac hypertrophy and mitochondrial function. Nature 478:114-118.

Mohamed JS, Hajira A, Pardo PS, Boriek AM (2014). MicroRNA-149 inhibits PARP-2 and promotes mitochondrial biogenesis via SIRT-1/PGC-1alpha network in skeletal muscle. Diabetes 63:1546-1559.

Muscaritoli M, Bossola M, Aversa Z, Bellantone R, Rossi FF (2006). Prevention and treatment of cancer cachexia: new insights into an old problem. Eur J Cancer 42:31-41.

Oliver FJ, Menissier-de MJ, Nacci C, Decker P, Andriantsitohaina R, Muller S, de la Rubia G, Stoclet JC, de MG (1999). Resistance to endotoxic shock as a consequence of defective NF-kappaB activation in poly (ADP-ribose) polymerase-1 deficient mice. EMBO J 18:4446-4454.

Penalver Cuesta JC, Jorda AC, Mancheno FN, Ceron Navarro JA, de Aguiar QK, Arraras MM, Vera Sempere FJ, Padilla Alarcon JD (2015). Prognostic Factors in Non-Small Cell Lung Cancer Less than 3 Centimeters: Actuarial Analysis, Accumulative Incidence and Risk Groups. Arch Bronconeumol.

Puig-Vilanova E, Rodriguez DA, Lloreta J, Ausin P, Pascual-Guardia S, Broquetas J, Roca J, Gea J, Barreiro E (2014). Oxidative stress, redox signaling pathways, and autophagy in cachectic muscles of male patients with advanced COPD and lung cancer. Free Radic Biol Med 79C:91-108.

Rajamohan SB, Pillai VB, Gupta M, Sundaresan NR, Birukov KG, Samant S, Hottiger MO, Gupta MP (2009). SIRT1 promotes cell survival under stress by deacetylation-dependent deactivation of poly(ADP-ribose) polymerase 1. Mol Cell Biol 29:4116-4129.

Rodriguez M, Gomez Hernandez MT, Novoa NM, Aranda JL, Jimenez MF, Varela G (2014). Poorer Survival in Stage IB Lung Cancer Patients After Pneumonectomy. Arch Bronconeumol.

Sanchez dC-E (2015). Prognostic Factors in Stage I Lung Cancer. Arch Bronconeumol 51:427-428.

Sanchez-Salcedo P, Berto J, de-Torres JP, Campo A, Alcaide AB, Bastarrika G, Pueyo JC, Villanueva A, Echeveste JI, Lozano MD, Garcia-Velloso MJ, Seijo LM, Garcia J, Torre W, Pajares MJ, Pio R, Montuenga LM, Zulueta JJ (2015). Lung Cancer Screening: Fourteen Year Experience of the Pamplona Early Detection Program (P-IELCAP). Arch Bronconeumol.

Sebio R, Yanez-Brage MI, Gimenez-Moolhuyzen E, Valenza MC, Reychler G, Cahalin LP (2015). Impact of a pre-operative pulmonary rehabilitation program on functional performance in patients undergoing video-assisted thoracic surgery for lung cancer. Arch Bronconeumol.

Toth MJ, Miller MS, Callahan DM, Sweeny AP, Nunez I, Grunberg SM, Der-Torossian H, Couch ME, Dittus K (2013). Molecular mechanisms underlying skeletal muscle weakness in human cancer: reduced myosin-actin cross-bridge formation and kinetics. J Appl Physiol 114:858-868.

Ullrich O, Reinheckel T, Sitte N, Hass R, Grune T, Davies KJ (1999). Poly-ADP ribose polymerase activates nuclear proteasome to degrade oxidatively damaged histones. Proc Natl Acad Sci U S A 96:6223-6228.

Vaschetto R, Kuiper JW, Chiang SR, Haitsma JJ, Juco JW, Uhlig S, Plotz FB, Della CF, Zhang H, Slutsky AS (2008). Inhibition of poly(adenosine diphosphate-ribose) polymerase attenuates ventilator-induced lung injury. Anesthesiology 108:261-268.

von HS, Anker SD (2010). Cachexia as a major underestimated and unmet medical need: facts and numbers. J Cachexia Sarcopenia Muscle 1:1-5.

White JP, Puppa MJ, Sato S, Gao S, Price RL, Baynes JW, Kostek MC, Matesic LE, Carson JA (2012). IL-6 regulation on skeletal muscle mitochondrial remodeling during cancer cachexia in the ApcMin/+ mouse. Skeletal muscle 2:14.

White JP, Baynes JW, Welle SL, Kostek MC, Matesic LE, Sato S, Carson JA (2011). The regulation of skeletal muscle protein turnover during the progression of cancer cachexia in the Apc(Min/+) mouse. PLoS One 6:e24650.

Whittemore LA, Song K, Li X, Aghajanian J, Davies M, Girgenrath S, Hill JJ, Jalenak M, Kelley P, Knight A, Maylor R, O'Hara D, Pearson A, Quazi A, Ryerson S, Tan XY, Tomkinson KN, Veldman GM, Widom A, Wright JF, Wudyka S, Zhao L, Wolfman NM (2003). Inhibition of myostatin in adult mice increases skeletal muscle mass and strength. Biochem Biophys Res Commun 300:965-971.

Yelamos J, Farres J, Llacuna L, Ampurdanes C, Martin-Caballero J (2011). PARP-1 and PARP-2: New players in tumour development. Am J Cancer Res 1:328-346.

Zheng J, Devalaraja-Narashimha K, Singaravelu K, Padanilam BJ (2005). Poly(ADP-ribose) polymerase-1 gene ablation protects mice from ischemic renal injury. Am J Physiol Renal Physiol 288:F387-F398.

Zhou X, Wang JL, Lu J, Song Y, Kwak KS, Jiao Q, Rosenfeld R, Chen Q, Boone T, Simonet WS, Lacey DL, Goldberg AL, Han HQ (2010). Reversal of cancer cachexia and muscle wasting by ActRIIB antagonism leads to prolonged survival. Cell 142:531-543.

FIGURE LEGENDS

Fig. 1A Mean values and standard deviations of the progression of the actual body weights in mice from all the experimental groups are represented in the graph. Each experimental group is represented by the following signs: non-cachectic control wild type animals (blue diamonds, N=12), LC-cachectic wild type mice (squares, N=14), non-cachectic control Parp-$1^{-/-}$ rodents (triangles, N=8), LC-cachectic Parp-$1^{-/-}$ mice (purple squares, N=12), non-cachectic control Parp-$2^{-/-}$ rodents (green squares, N=6), and LC-cachectic Parp-$2^{-/-}$ animals (open circles, N=6) over the study period (1 month). Statistical significance is represented as follows: *, $p \leq 0.05$, ***, $p \leq 0.001$, and n.s., non-significant differences between either wild type, Parp-$1^{-/-}$, or Parp-$2^{-/-}$ LC-cachectic mice and their respective control (non-tumor) rodents.

Fig. 1B-C Mean values and standard deviation of the percentage of positively-stained nuclei for poly-ADP ribosylation in the diaphragm (panel B) and gastrocnemius (panel C). For statistical analysis purposes, the following animals were used in each group: non-cachectic control wild type (N=8), LC-cachectic wild type (N=8), non-cachectic control Parp-$1^{-/-}$ (N=8), LC-cachectic Parp-$1^{-/-}$ (N=8), non-cachectic control Parp-$2^{-/-}$ (N=6), and LC-cachectic Parp-$2^{-/-}$ (N=6). Non-cachectic control groups are represented in white bars, while LC-cachectic groups are represented in black bars. Definition of abbreviations: LC, Lung cancer; PARP, poly-ADP ribose polymerase; ADPr, ADP ribosylation. Statistical significance is represented as follows: ***, $p \leq 0.001$, and n.s., non-significant differences between either wild type, Parp-$1^{-/-}$, or Parp-$2^{-/-}$ LC-cachectic mice and their respective control (non-tumor) mice*;* †, $p \leq 0.05$, ††, $p \leq 0.01$, †††, $p \leq 0.001$ and n.s., non-significant differences between any of the control knockout animals and control (non-tumor) wild type mice.

Fig. 2A-F Mean values and standard deviation of total carbonylated proteins (panels A and B), SOD2 (panels C and D), and SOD1 (panels E and F) in the diaphragm and gastrocnemius, as measured by optical densities in arbitrary units (OD, a.u.). For statistical analysis purposes, the following animals were used in each group: non-cachectic control wild type (N=7), LC-cachectic wild type (N=8), non-cachectic control Parp-$1^{-/-}$ (N=7), LC-cachectic Parp-$1^{-/-}$ (N=8), non-cachectic control Parp-$2^{-/-}$ (N=3), and LC-cachectic Parp-$2^{-/-}$ (N=5). Non-cachectic control groups are represented in white bars, while LC-cachectic groups are represented in black bars. Definition of abbreviations: LC, Lung cancer; PARP, poly-ADP ribose polymerase; SOD, superoxide dismutase; OD, optical densities; a.u., arbitrary units. Statistical significance is represented as follows: *, $p \leq 0.05$, **, $p \leq 0.01$, and n.s., non-significant differences between either wild type, Parp-$1^{-/-}$, or Parp-$2^{-/-}$ LC-cachectic mice and their respective control (non-tumor) mice.

Fig. 3A-B Mean values and standard deviation of tyrosine release (nmol/mg/2h) in the diaphragm (panel A) and gastrocnemius (panel B) muscles of the following experimental groups: non-cachectic

control wild type (N=10), LC-cachectic wild type (N=10), non-cachectic control Parp-$1^{-/-}$ (N=8), LC-cachectic Parp-$1^{-/-}$ (N=12), non-cachectic control Parp-$2^{-/-}$ (N=6), and LC-cachectic Parp-$2^{-/-}$ (N=6). Non-cachectic control groups are represented in white bars, while LC-cachectic groups are represented in black bars. Statistical significance is represented as follows: *, $p \leq 0.05$, and n.s., non-significant differences between either wild type, Parp-$1^{-/-}$, or Parp-$2^{-/-}$ LC-cachectic mice and their respective control (non-tumor) rodents.

Fig. 4A-D Mean values and standard deviation of total ubiquitinated proteins (panels A and B), and 20S proteasome C8 subunit content (panels C and D) in the diaphragm and gastrocnemius, as measured by optical densities in arbitrary units (OD, a.u.). For statistical analysis purposes, the following animals were used in each group: non-cachectic control wild type (N=7), LC-cachectic wild type (N=8), non-cachectic control Parp-$1^{-/-}$ (N=7), LC-cachectic Parp-$1^{-/-}$ (N=8), non-cachectic control Parp-$2^{-/-}$ (N=3), and LC-cachectic Parp-$2^{-/-}$ (N=5). Non-cachectic control groups are represented in white bars, while LC-cachectic groups are represented in black bars. Definition of abbreviations: LC, Lung cancer; PARP, poly-ADP ribose polymerase; OD, optical densities; a.u., arbitrary units. Statistical significance is represented as follows: *, $p \leq 0.05$, ***, $p \leq 0.001$, and n.s., non-significant differences between either wild type, Parp-$1^{-/-}$, or Parp-$2^{-/-}$ LC-cachectic mice and their respective control (non-tumor) mice.

Fig. 5A-F Mean values and standard deviation of TRIM32 (panels A and B), MURF-1 (panels C and D), and atrogin-1 (panels E and F) protein content in the diaphragm and gastrocnemius, as measured by optical densities in arbitrary units (OD, a.u.). For statistical analysis purposes, the following animals were used in each group: non-cachectic control wild type (N=7), LC-cachectic wild type (N=8), non-cachectic control Parp-$1^{-/-}$ (N=7), LC-cachectic Parp-$1^{-/-}$ (N=8), non-cachectic control Parp-$2^{-/-}$ (N=3), and LC-cachectic Parp-$2^{-/-}$ (N=5). Non-cachectic control groups are represented in white bars, while LC-cachectic groups are represented in black bars. Definition of abbreviations: TRIM32, tripartite motif containing 32; MURF-1, muscle ring finger protein 1; LC, Lung cancer; PARP, poly-ADP ribose polymerase; OD, optical densities; a.u., arbitrary units. Statistical significance is represented as follows: **, $p \leq 0.01$, ***, $p \leq 0.001$, and n.s., non-significant differences between either wild type, Parp-$1^{-/-}$, or Parp-$2^{-/-}$ LC-cachectic mice and their respective control (non-tumor) mice.

Fig. 6A-D Mean values and standard deviation from the p-NF-κB p50/NF-κB p50 (panels A and B), and p-NF-κB p65/NF-κB p65 ratios (panels C and D) are depicted in the diaphragm and gastrocnemius, as measured by optical densities in arbitrary units (OD, a.u.). For statistical analysis purposes, the following animals were used in each group: non-cachectic control wild type (N=7), LC-cachectic wild type (N=8), non-cachectic control Parp-$1^{-/-}$ (N=7), LC-cachectic Parp-$1^{-/-}$ (N=8),

non-cachectic control Parp-$2^{-/-}$ (N=3), and LC-cachectic Parp-$2^{-/-}$ (N=5). Non-cachectic control groups are represented in white bars, while LC-cachectic groups are represented in black bars. Definition of abbreviations: NF-κB p50, nuclear factor-κB p50 subunit; p-NF-κB p50, phosphorylated-NF-κB p50; NF-κB p65, nuclear factor-κB p65 subunit; p-NF-κB p65, phosphorylated-NF-κB p65; LC, Lung cancer; PARP, poly-ADP ribose polymerase; OD, optical densities; a.u., arbitrary units. Statistical significance is represented as follows: *, $p \leq 0.05$, ***, $p \leq 0.001$, and n.s., non-significant differences between either wild type, Parp-$1^{-/-}$, or Parp-$2^{-/-}$ LC-cachectic mice and their respective control (non-tumor) mice; †††, $p \leq 0.001$ between any of the control knockout animals and control (non-tumor) wild type mice.

Fig. 7A-H Mean values and standard deviation from the p-Akt/Akt (panels A and B), p-mTOR/mTOR (panels C and D), and p-p70S6K/p70S6K (panels E and F) ratios, are depicted in the diaphragm and gastrocnemius, as measured by optical densities in arbitrary units (OD, a.u.). For statistical analysis purposes, the following animals were used in each group: non-cachectic control wild type (N=7), LC-cachectic wild type (N=8), non-cachectic control Parp-$1^{-/-}$ (N=7), LC-cachectic Parp-$1^{-/-}$ (N=8), non-cachectic control Parp-$2^{-/-}$ (N=3), and LC-cachectic Parp-$2^{-/-}$ (N=5). Mean values and standard deviation of the mitochondrial DNA copy number in the diaphragm (panel G) and gastrocnemius (panel H), as measured by the mtDNA/mDNA ratio in arbitrary units (a.u.). For statistical analysis purposes, the following animals were used in each group: non-cachectic control wild type (N=8), LC-cachectic wild type (N=8), non-cachectic control Parp-$1^{-/-}$ (N=8), LC-cachectic Parp-$1^{-/-}$ (N=8), non-cachectic control Parp-$2^{-/-}$ (N=6), and LC-cachectic Parp-$2^{-/-}$ (N=6). Non-cachectic control groups are represented in white bars, while LC-cachectic groups are represented in black bars. Definition of abbreviations: Akt, RAC-alpha serine/threonine-protein kinase; p-Akt, phosphorylated-Akt; mTOR, *mammalian target of rapamycin*; p-mTOR, phosphorylated mTOR; p70S6K, p70 S6 kinase; p-70S6K, phosphorylated p70S6K; LC, Lung cancer; PARP, poly-ADP ribose polymerase; OD, optical densities; a.u., arbitrary units. Statistical significance is represented as follows: *, $p \leq 0.05$, **, $p \leq 0.01$, and n.s., non-significant differences between either wild type, Parp-$1^{-/-}$, or Parp-$2^{-/-}$ LC-cachectic mice and their respective control (non-tumor) mice.

Fig. 8A-D Mean values and standard deviation of MyHC (panels A anb B) and actin (panels C and D) protein content in the diaphragm and gastrocnemius, as measured by optical densities in arbitrary units (OD, a.u.). For statistical analysis purposes, the following animals were used in each group: non-cachectic control wild type (N=7), LC-cachectic wild type (N=8), non-cachectic control Parp-$1^{-/-}$ (N=7), LC-cachectic Parp-$1^{-/-}$ (N=8), non-cachectic control Parp-$2^{-/-}$ (N=3), and LC-cachectic Parp-$2^{-/-}$ (N=5). Non-cachectic control groups are represented in white bars, while LC-cachectic groups are represented in black bars. Definition of abbreviations: MyHC, *Myosin Heavy Chain;* LC, Lung

cancer; PARP, poly-ADP ribose polymerase; OD, optical densities; a.u., arbitrary units. Statistical significance is represented as follows: *, $p \leq 0.05$, **, $p \leq 0.01$, ***, $p \leq 0.001$, and n.s., non-significant differences between either wild type, Parp-$1^{-/-}$, or Parp-$2^{-/-}$ LC-cachectic mice and their respective control (non-tumor) mice.

Table 1 Physiological characteristics of wild type, Parp-$1^{-/-}$, and Parp-$2^{-/-}$ mice at the end of the study period

	Wild type mice		Parp-$1^{-/-}$ mice		Parp-$2^{-/-}$ mice	
	Control (N=12)	LC-cachexia (N=14)	Control (N=8)	LC-cachexia (N=12)	Control (N=6)	LC-cachexia (N=6)
Age at baseline (weeks)	10	10, n.s.	10	10, n.s.	10	10, n.s.
Subcutaneous tumor weight (g)		1.86 (0.6)		1.11 (0.3), **		1.21 (0.35), *
Body weight at baseline (g)	19.57 (0.85)	19.52 (0.80), n.s.	19.28 (0.78)	18.61 (0.93), n.s.	19.25 (1.06)	19.89 (0.92), n.s.
Body weight gain (%)	+9.26 (2.63)	-5.39 (9.54), ***	+6.96 (2.23)	+1.55 (3.69), *	+4.34 (2.87)	+3.06 (6.81), n.s.
Diaphragm weight (g)	0.090 (0.01)	0.067 (0.011), ***	0.073 (0.01), ††	0.062 (0.007), *	0.076 (0.012), †	0.086 (0.013), n.s.
Gastrocnemius weight (g)	0.118 (0.006)	0.080 (0.018), ***	0.105 (0.003), †	0.096 (0.007), *	0.096 (0.012), †††	0.098 (0.012), n.s.
Limb strength gain (%)	+9.48 (6.47)	-12.50 (10.52), ***	+12.86 (8.13)	-0.45 (6.08), **	+3.33 (1.99)	+2.10 (5.40), n.s.

Variables are presented as mean (standard deviation).
Definition of abbreviations: Parp-$1^{-/-}$ and Parp-$2^{-/-}$, poly-ADP ribose polymerase-1, and -2 knockout mice, LC, lung cancer; N.A., not applicable.
Statistical significance: *, $p \leq 0.05$, **, $p \leq 0.01$, ***, $p \leq 0.001$, and n.s., non-significant differences between either wild type, Parp-$1^{-/-}$, or Parp-$2^{-/-}$ LC-cachectic mice and their respective control (non-tumor) rodents; †, $p \leq 0.05$, ††, $p \leq 0.01$, and †††, $p \leq 0.001$ between any of the control knockout animals and control (non-tumor) wild type mice. Comparisons were assessed using one-way analysis of variance (ANOVA), in which *Dunnett's post hoc* analysis was used to adjust for multiple comparisons among the study groups.

Table 2 Muscle structural characteristics of wild type, Parp-$1^{-/-}$, and Parp-$2^{-/-}$ mice at the end of the study period

		Wild type mice		Parp-$1^{-/-}$ mice		Parp-$2^{-/-}$ mice	
	Muscle	Control (N=10)	LC-cachexia (N=10)	Control (N=8)	LC-cachexia (N=12)	Control (N=6)	LC-cachexia (N=6)
Fiber type composition							
Type I fibers (%)	Diaphragm	9 (2)	8 (3), n.s.	9 (1)	9 (2), n.s.	7 (2)	9 (2), n.s.
	Gastrocnemius	13 (3)	13 (3), n.s.	13 (2)	13 (2), n.s.	17 (4)	15 (2), n.s.
Type II fibers (%)	Diaphragm	91 (2)	92 (3), n.s.	91 (1)	91 (2), n.s.	92 (3)	90 (2), n.s.
	Gastrocnemius	87 (3)	87 (3), n.s.	87 (2)	87 (2), n.s.	83 (4)	85 (2), n.s.
Type I fibers area (μm^2)	Diaphragm	322 (70)	239 (28), **	325 (77)	289 (58), n.s.	292 (49)	311 (67), n.s.
	Gastrocnemius	965 (107)	673 (121), ***	864 (109)	730 (190), n.s.	775 (128), †	707 (82), n.s.
Type II fibers area (μm^2)	Diaphragm	397 (78)	310 (58), *	384 (80)	371 (76), n.s.	344 (98)	395 (114), n.s.
	Gastrocnemius	924 (134)	714 (135), **	885 (99)	743 (182), n.s.	804 (66)	714 (61), n.s.
Muscle abnormalities							
Abnormal fraction (%)	Diaphragm	8.8 (0.7)	14.3 (3.9), **	9.7 (2.3)	16.1 (4.9), ***	11.5 (2.6)	16 (2.5), *
	Gastrocnemius	3.7 (1.6)	7.9 (1.7), ***	4.4 (1)	7.4 (2.1), **	5.0 (1.8)	8.0 (2.4), *
Inflammatory cells (%)	Diaphragm	3.9 (0.4)	6.3 (1.4), **	6 (1.2), p=0.055	9.7 (2.6), ***	6.6 (1.5), ††	9.7 (0.8), **
	Gastrocnemius	2.1 (1.0)	5.3 (1.8), ***	2.6 (0.6)	4.4 (1.6), *	2.3 (1.1)	4.6 (1.8), *
Internal nuclei (%)	Diaphragm	3.7 (1.0)	7.2 (3.7), **	3.3 (1.5)	5.5 (2.2), *	4.3 (0.7)	5.4 (0.6), *
	Gastrocnemius	1.5 (0.7)	2.3 (0.8), *	1.7 (0.8)	2.8 (0.8), **	2.2 (0.5)	2.8 (0.4), *
TUNEL – positive nuclei (%)	Diaphragm	48.5 (6.7)	65.8 (5.9), ***	49.1 (2.5)	57.5 (1.8), ***	49 (1.8)	59.5 (1.7), ***
	Gastrocnemius	51.6 (5.7)	67.7 (3.8), ***	49 (0.7)	59.5 (2.6), ***	48.6 (1.7)	60.8 (2.4), ***

Values are expressed as mean (standard deviation).
Definition of abbreviations: Parp-$1^{-/-}$ and Parp-$2^{-/-}$, poly-ADP ribose polymerase-1, and -2 knockout mice; LC, lung cancer; µm, micrometer; n.s., non-significant.
Statistical significance: *, $p \leq 0.05$, **, $p \leq 0.01$, ***, $p \leq 0.001$, and n.s., non-significant differences between either wild type, Parp-$1^{-/-}$ or Parp-$2^{-/-}$ LC-cachectic mice and their respective control (non-tumor) rodents; †, $p \leq 0.05$, and ††, $p \leq 0.01$ between any of the control knockout animals and control (non-tumor) wild type mice. Comparisons were assessed using one-way analysis of variance (ANOVA), in which *Dunnett's post hoc* analysis was used to adjust for multiple comparisons among the study groups.

A. Chacon-Cabrera *et al*. Fig. 1

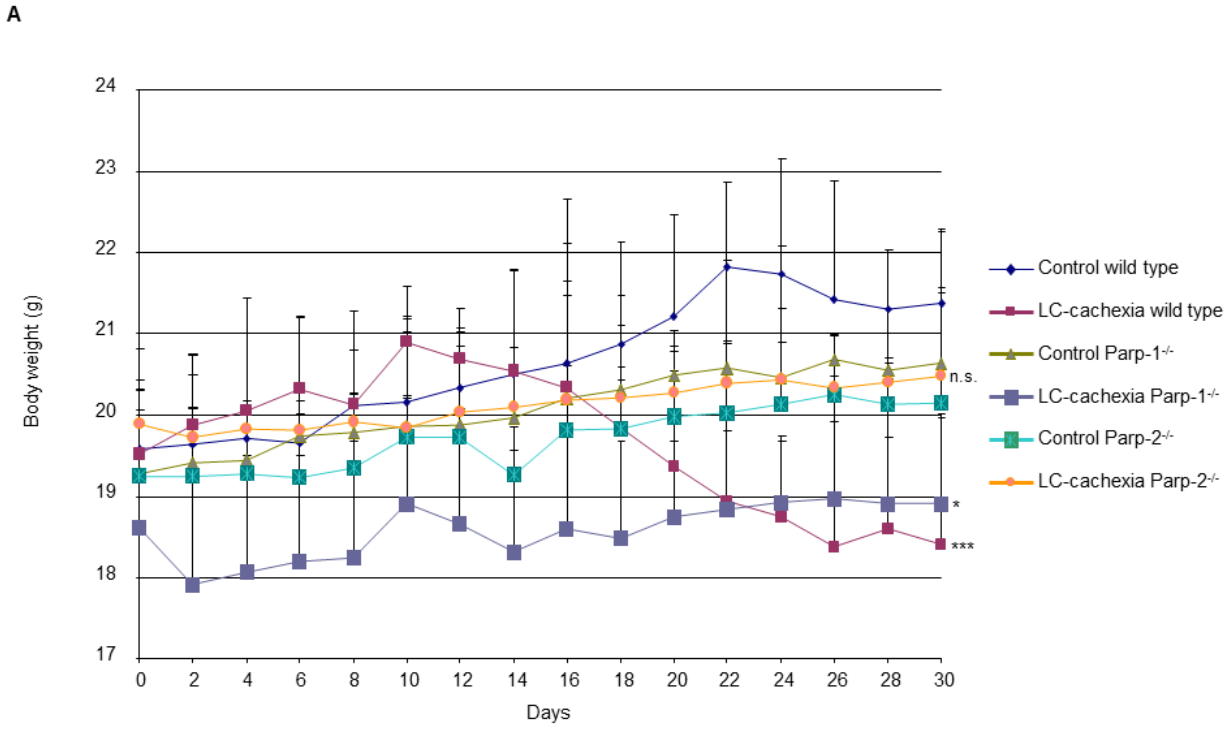

A. Chacon-Cabrera *et al*. Fig. 1

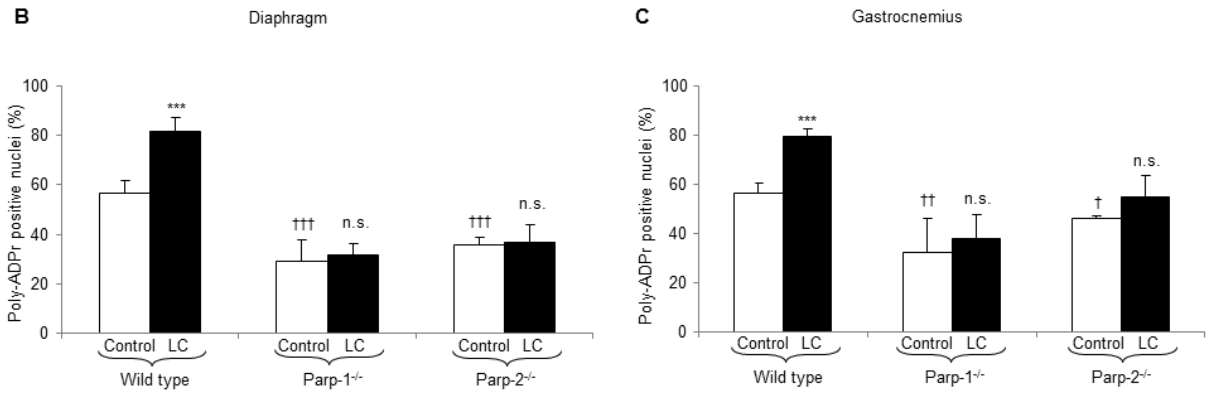

A. Chacon-Cabrera *et al*. Fig. 2

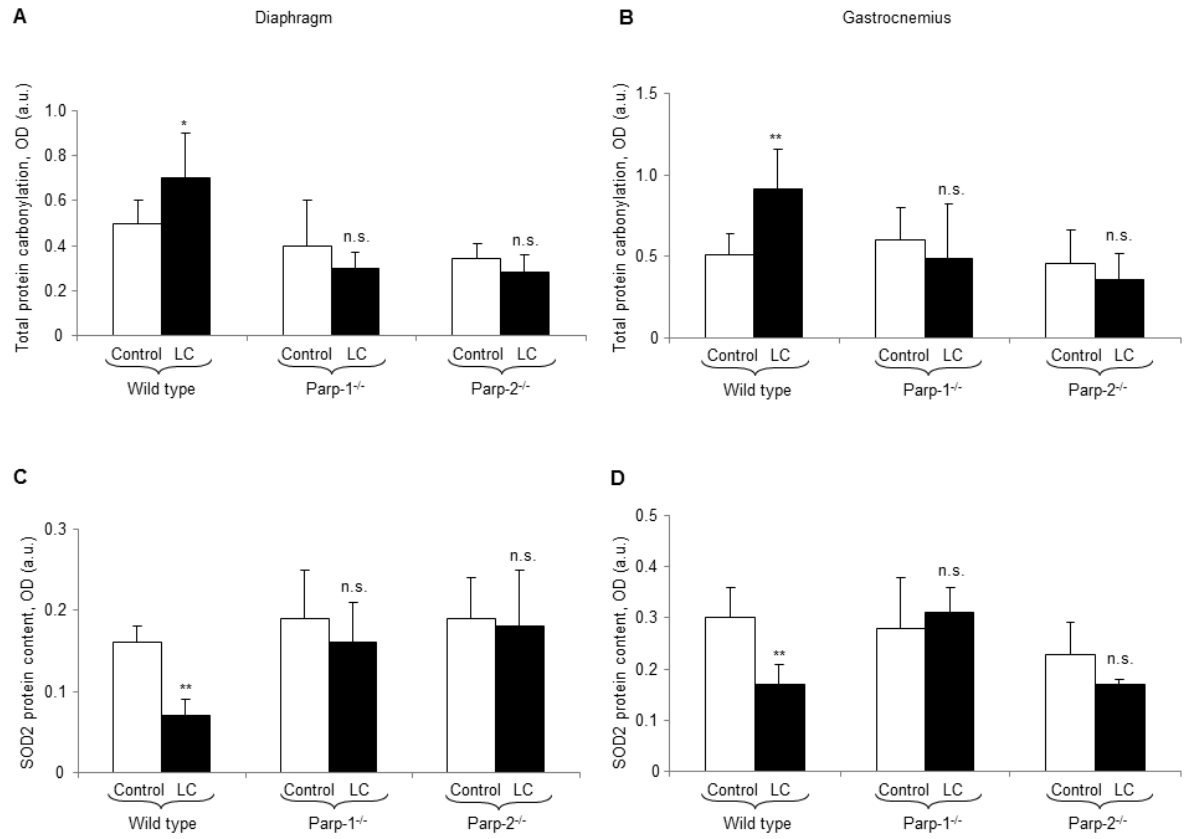

A. Chacon-Cabrera *et al*. Fig. 2

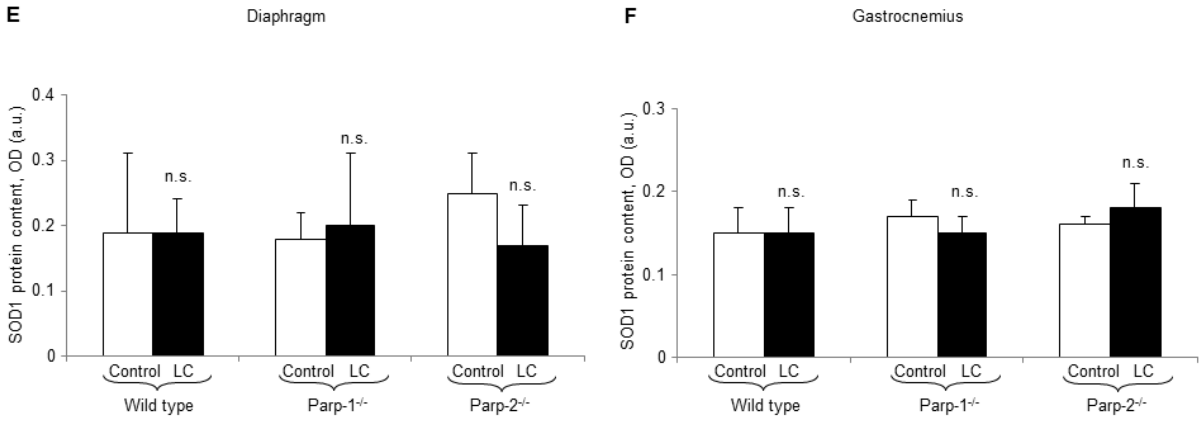

A. Chacon-Cabrera *et al*. Fig. 3

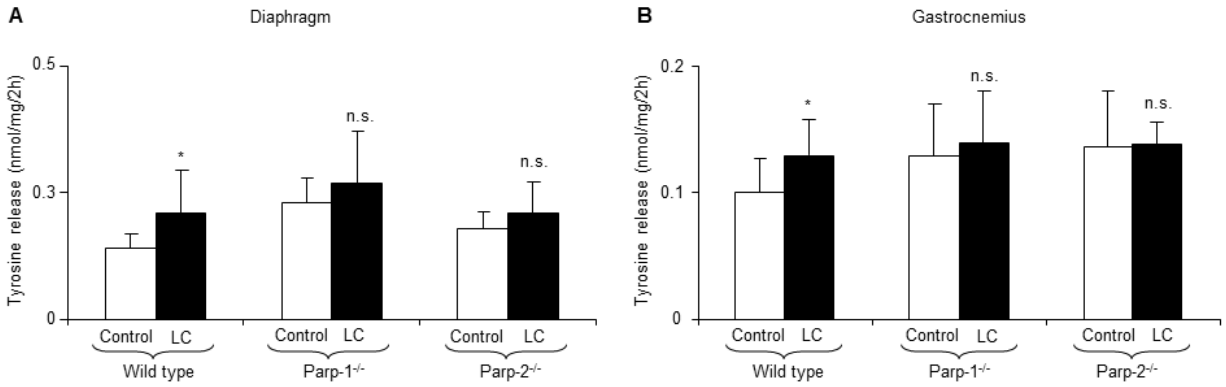

A. Chacon-Cabrera *et al*. Fig. 4

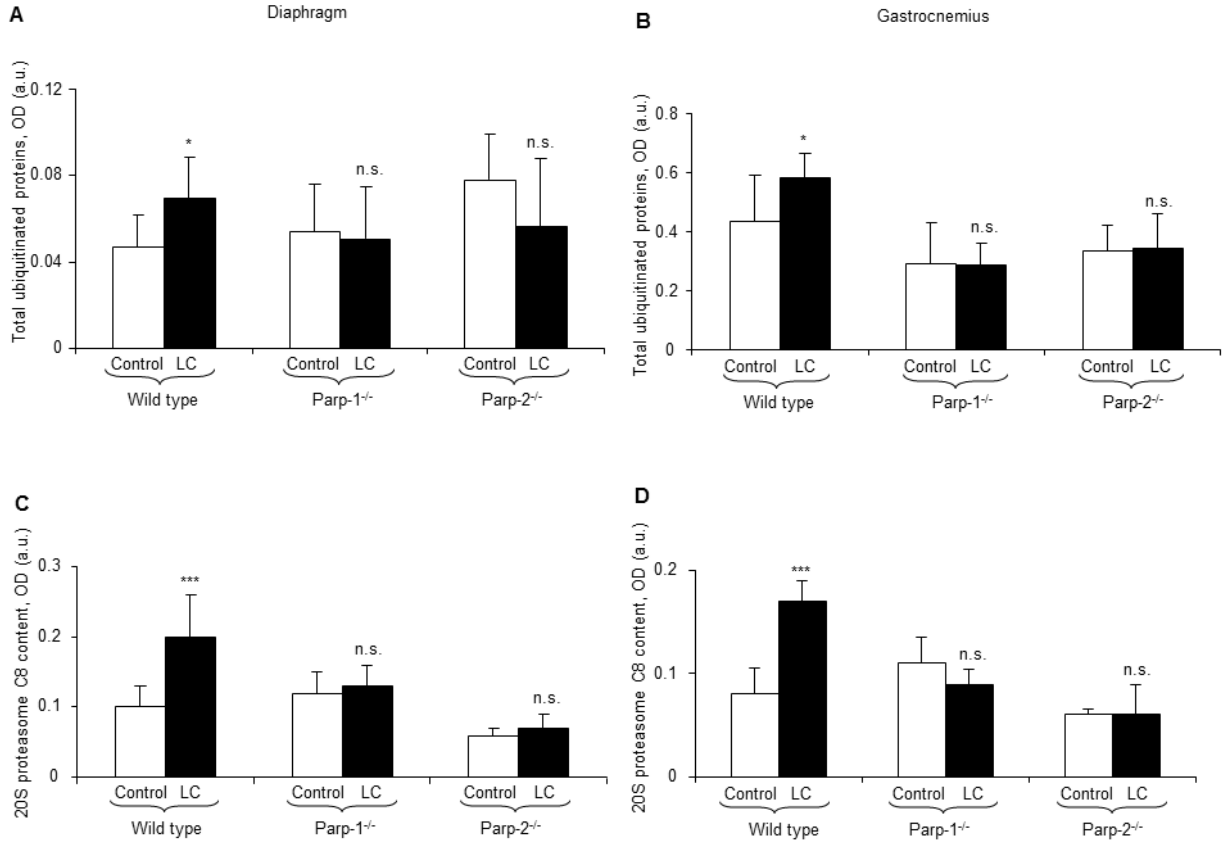

A. Chacon-Cabrera *et al*. Fig. 5

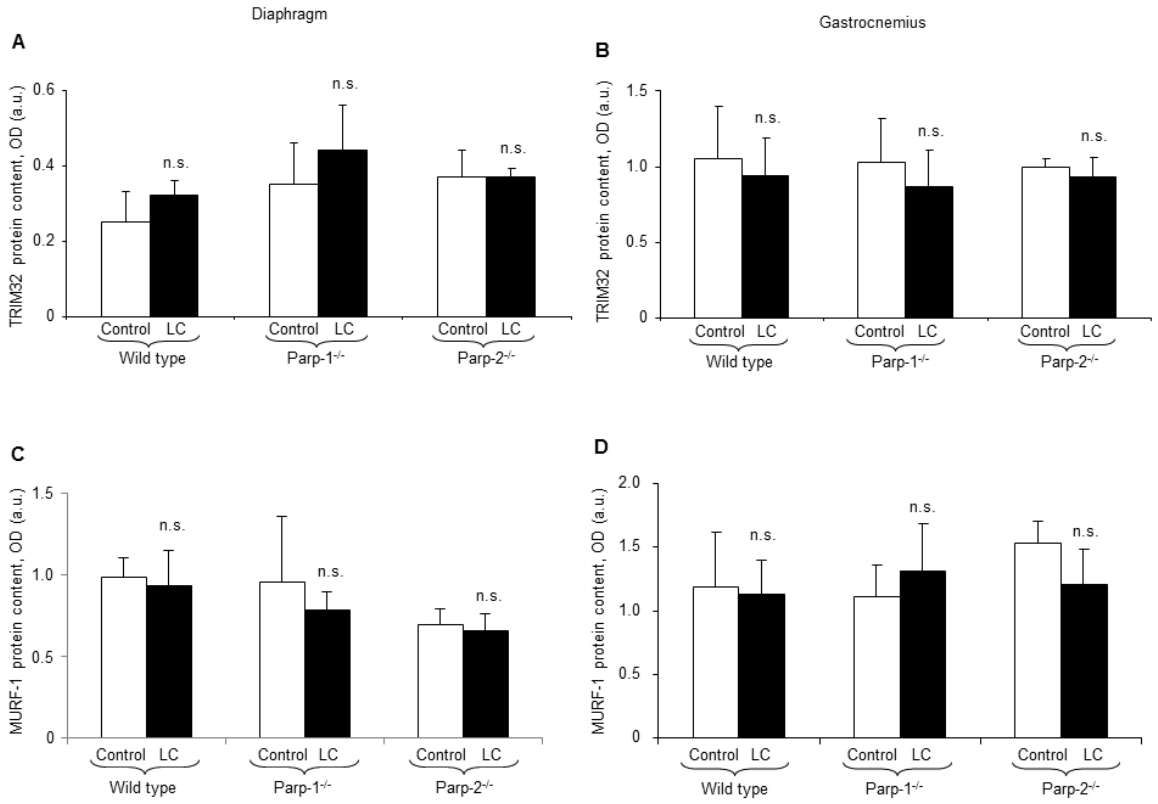

A. Chacon-Cabrera *et al*. Fig. 5

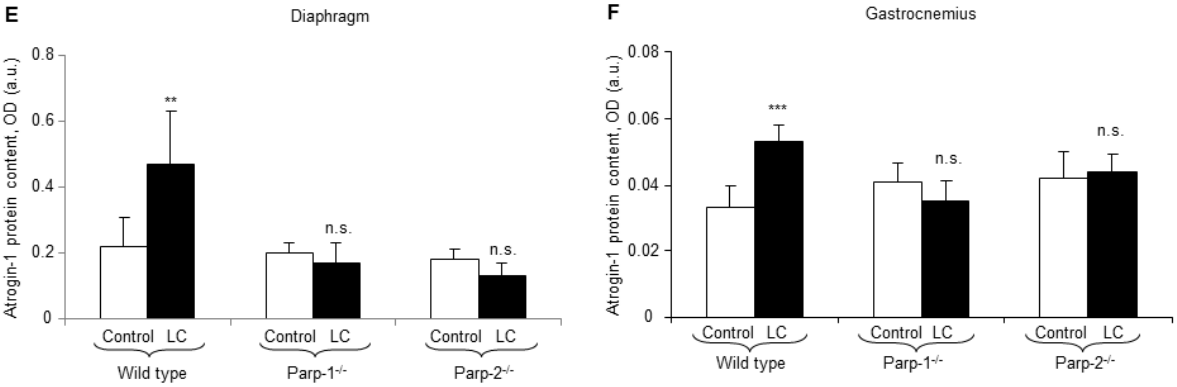

A. Chacon-Cabrera *et al*. Fig. 6

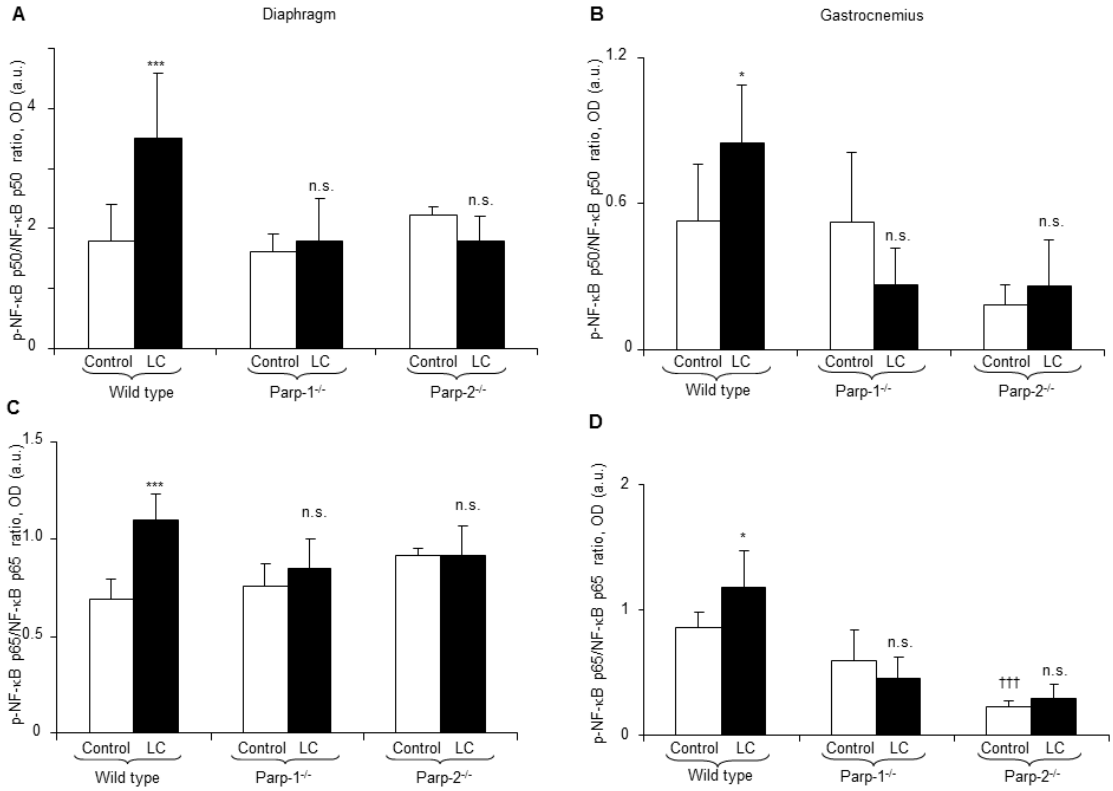

A. Chacon-Cabrera *et al*. Fig. 7

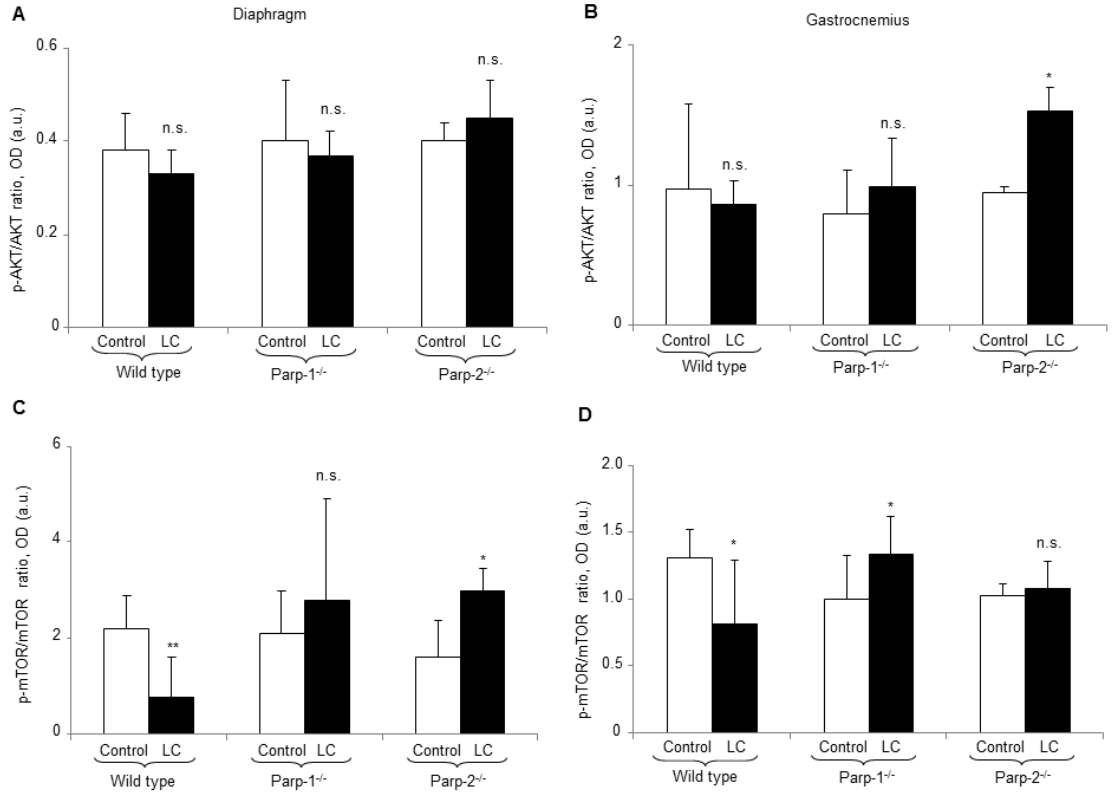

A. Chacon-Cabrera *et al*. Fig. 7

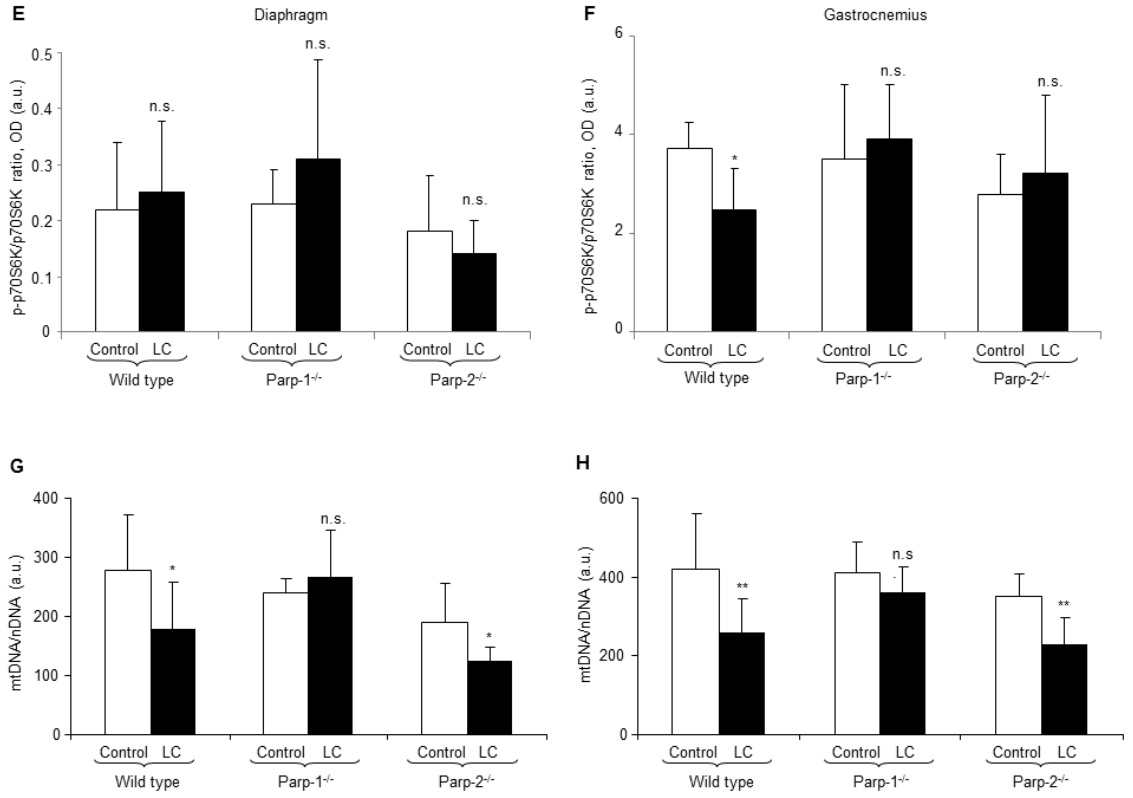

A. Chacon-Cabrera *et al*. Fig. 8

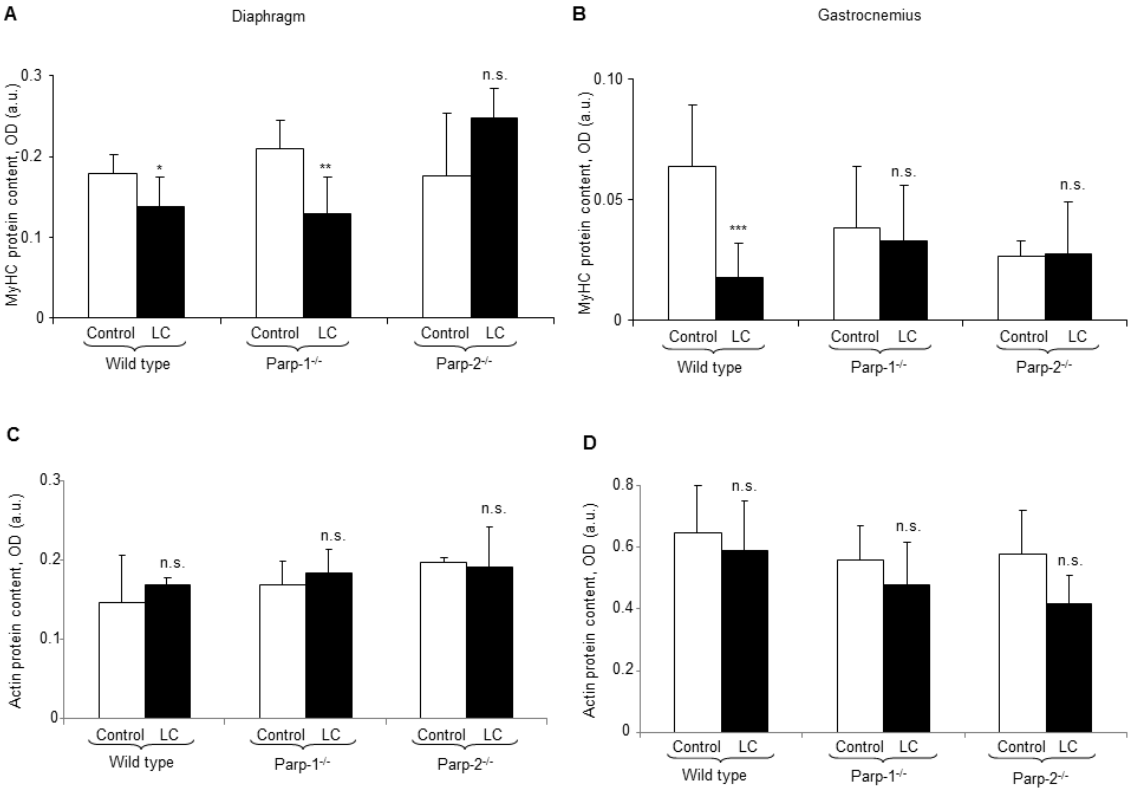

FIGURE LEGENDS ONLINE SUPPLEMENT

Fig. E1 (A) Grip strength was assessed in the four limbs at the same time in all mice. **(B)** Representative examples of 4 grids of 63 point-intercepts extracted from a gastrocnemius of a cachectic mouse (x 400), in which all different categories for point counting were identified. Those categories were defined using a specific number as described in the Methods section above.

Fig. E2 Representative examples of nuclei positively stained (black arrows, brown nuclei) and not stained (red arrows, blue nuclei, hematoxylin counterstaining) for the pADPr assay in the diaphragm (panel A) and gastrocnemius (panel B) of the different study groups of mice (x 400).

Fig. E3 Immunoblots of total carbonylated proteins of different MW, in kilodaltons, SOD2, and SOD1 in the diaphragm (panels A, C, and E) and gastrocnemius (panels B, D, and F) muscles of the following experimental groups: non-cachectic control wild type (N=7), LC-cachectic wild type (N=8), non-cachectic control Parp-$1^{-/-}$ (N=7), LC-cachectic Parp-$1^{-/-}$ (N=8), non-cachectic control Parp-$2^{-/-}$ (N=3), and LC-cachectic Parp-$2^{-/-}$ (N=5). GAPDH is shown as the loading control. Definition of abbreviations: LC, Lung cancer; PARP, poly-ADP ribose polymerase; SOD, superoxide dismutase; GAPDH, glyceraldehyde-3-phospate dehydrogenase; OD, optical densities; a.u., arbitrary units; MW, molecular weights; KDa, kilodaltons.

Fig. E4 Immunoblots of total ubiquitinated proteins of different MW, in kilodaltons, in the diaphragm (panel A) and gastrocnemius (panel B) muscles of the following experimental groups: non-cachectic control wild type (N=7), LC-cachectic wild type (N=8), non-cachectic control Parp-$1^{-/-}$ (N=7), LC-cachectic Parp-$1^{-/-}$ (N=8), non-cachectic control Parp-$2^{-/-}$ (N=3), and LC-cachectic Parp-$2^{-/-}$ (N=5). GAPDH is shown as the loading control. Definition of abbreviations: LC, Lung cancer; PARP, poly-ADP ribose polymerase; GAPDH, glyceraldehyde-3-phospate dehydrogenase; OD, optical densities; a.u., arbitrary units; MW, molecular weights; KDa, kilodaltons.

Fig. E5 Immunoblots of 20S proteasome C8 subunit content in the diaphragm (panel A) and gastrocnemius (panel B) muscles of the following experimental groups: non-cachectic control wild type (N=7), LC-cachectic wild type (N=8), non-cachectic control Parp-$1^{-/-}$ (N=7), LC-cachectic Parp-$1^{-/-}$ (N=8), non-cachectic control Parp-$2^{-/-}$ (N=3), and LC-cachectic Parp-$2^{-/-}$ (N=5). GAPDH is shown as the loading control. Definition of abbreviations: LC, Lung cancer; PARP, poly-ADP ribose polymerase; GAPDH, glyceraldehyde-3-phospate dehydrogenase; OD, optical densities; a.u., arbitrary units; MW, molecular weights; KDa, kilodaltons.

Fig. E6 Immunoblots of TRIM32 protein content in the diaphragm (panel A) and gastrocnemius (panel B) muscles of the following experimental groups: non-cachectic control wild type (N=7), LC-cachectic wild type (N=8), non-cachectic control Parp-$1^{-/-}$ (N=7), LC-cachectic Parp-$1^{-/-}$ (N=8), non-cachectic control Parp-$2^{-/-}$ (N=3), and LC-cachectic Parp-$2^{-/-}$ (N=5). GAPDH is shown as the loading

control. Definition of abbreviations: TRIM32, tripartite motif containing 32; +C, positive control; LC, Lung cancer; PARP, poly-ADP ribose polymerase; GAPDH, glyceraldehyde-3-phospate dehydrogenase; OD, optical densities; a.u., arbitrary units; MW, molecular weights; KDa, kilodaltons.

Fig. E7 Immunoblots of MURF-1 protein content in the diaphragm (panel A) and gastrocnemius (panel B) muscles of the following experimental groups: non-cachectic control wild type (N=7), LC-cachectic wild type (N=8), non-cachectic control Parp-$1^{-/-}$ (N=7), LC-cachectic Parp-$1^{-/-}$ (N=8), non-cachectic control Parp-$2^{-/-}$ (N=3), and LC-cachectic Parp-$2^{-/-}$ (N=5). GAPDH is shown as the loading control. Definition of abbreviations: MURF-1, muscle ring finger protein 1; +C, positive control; LC, Lung cancer; PARP, poly-ADP ribose polymerase; GAPDH, glyceraldehyde-3-phospate dehydrogenase; OD, optical densities; a.u., arbitrary units; MW, molecular weights; KDa, kilodaltons.

Fig. E8 Immunoblots of atrogin-1 protein content in the diaphragm (panel A) and gastrocnemius (panel B) muscles of the following experimental groups: non-cachectic control wild type (N=7), LC-cachectic wild type (N=8), non-cachectic control Parp-$1^{-/-}$ (N=7), LC-cachectic Parp-$1^{-/-}$ (N=8), non-cachectic control Parp-$2^{-/-}$ (N=3), and LC-cachectic Parp-$2^{-/-}$ (N=5). GAPDH is shown as the loading control. Definition of abbreviations: LC, Lung cancer; PARP, poly-ADP ribose polymerase; GAPDH, glyceraldehyde-3-phospate dehydrogenase; OD, optical densities; a.u., arbitrary units; MW, molecular weights; KDa, kilodaltons.

Fig. E9 Immunoblots of NF-κB p50 and p-NF-κB p50 proteins in the diaphragm (panel A) and gastrocnemius (panel B) muscles of the following experimental groups: non-cachectic control wild type (N=7), LC-cachectic wild type (N=8), non-cachectic control Parp-$1^{-/-}$ (N=7), LC-cachectic Parp-$1^{-/-}$ (N=8), non-cachectic control Parp-$2^{-/-}$ (N=3), and LC-cachectic Parp-$2^{-/-}$ (N=5). GAPDH is shown as the loading control. Definition of abbreviations: NF-κB p50, nuclear factor-κB p50 subunit; p-NF-κB p50, phosphorylated-NF-κB p50, LC, Lung cancer; PARP, poly-ADP ribose polymerase; GAPDH, glyceraldehyde-3-phospate dehydrogenase; OD, optical densities; a.u., arbitrary units; MW, molecular weights; KDa, kilodaltons.

Fig. E10 Immunoblots of NF-κB p65 and p-NF-κB p65 proteins in the diaphragm (panel A) and gastrocnemius (panel B) muscles of the following experimental groups: non-cachectic control wild type (N=7), LC-cachectic wild type (N=8), non-cachectic control Parp-$1^{-/-}$ (N=7), LC-cachectic Parp-$1^{-/-}$ (N=8), non-cachectic control Parp-$2^{-/-}$ (N=3), and LC-cachectic Parp-$2^{-/-}$ (N=5). GAPDH is shown as the loading control. Definition of abbreviations: NF-κB p65, nuclear factor-κB p65 subunit; p-NF-κB p65, phosphorylated-NF-κB p65; LC, Lung cancer; PARP, poly-ADP ribose polymerase; GAPDH, glyceraldehyde-3-phospate dehydrogenase; OD, optical densities; a.u., arbitrary units;

MW, molecular weights; KDa, kilodaltons.

Fig. E11 Immunoblots of Akt and p-Akt proteins in the diaphragm (panel A) and gastrocnemius (panel B) muscles of the following experimental groups: non-cachectic control wild type (N=7), LC-cachectic wild type (N=8), non-cachectic control Parp-$1^{-/-}$ (N=7), LC-cachectic Parp-$1^{-/-}$ (N=8), non-cachectic control Parp-$2^{-/-}$ (N=3), and LC-cachectic Parp-$2^{-/-}$ (N=5). GAPDH is shown as the loading control. Definition of abbreviations: Akt, RAC-alpha serine/threonine-protein kinase; p-Akt, phosphorylated-Akt; LC, Lung cancer; PARP, poly-ADP ribose polymerase; GAPDH, glyceraldehyde-3-phospate dehydrogenase; OD, optical densities; a.u., arbitrary units; MW, molecular weights; KDa, kilodaltons.

Fig. E12 Immunoblots of mTOR and p-mTOR proteins in the diaphragm (panel A) and gastrocnemius (panel B) muscles of the following experimental groups: non-cachectic control wild type (N=7), LC-cachectic wild type (N=8), non-cachectic control Parp-$1^{-/-}$ (N=7), LC-cachectic Parp-$1^{-/-}$ (N=8), non-cachectic control Parp-$2^{-/-}$ (N=3), and LC-cachectic Parp-$2^{-/-}$ (N=5). GAPDH is shown as the loading control. Definition of abbreviations: mTOR, *mammalian target of rapamycin*; p-mTOR, phosphorylated mTOR; LC, Lung cancer; PARP, poly-ADP ribose polymerase; GAPDH, glyceraldehyde-3-phospate dehydrogenase; OD, optical densities; a.u., arbitrary units; MW, molecular weights; KDa, kilodaltons.

Fig. E13 Immunoblots of p70S6K and p-p70S6K proteins in the diaphragm (panel A) and gastrocnemius (panel B) muscles of the following experimental groups: non-cachectic control wild type (N=7), LC-cachectic wild type (N=8), non-cachectic control Parp-$1^{-/-}$ (N=7), LC-cachectic Parp-$1^{-/-}$ (N=8), non-cachectic control Parp-$2^{-/-}$ (N=3), and LC-cachectic Parp-$2^{-/-}$ (N=5). GAPDH is shown as the loading control. Definition of abbreviations: p70S6K, p70 S6 kinase; p-70S6K, phosphorylated p70S6K; LC, Lung cancer; PARP, poly-ADP ribose polymerase; GAPDH, glyceraldehyde-3-phospate dehydrogenase; OD, optical densities; a.u., arbitrary units; MW, molecular weights; KDa, kilodaltons.

Fig. E14 Immunoblots of MyHC protein content in the diaphragm (panel A) and gastrocnemius (panel B) muscles of the following experimental groups: non-cachectic control wild type (N=7), LC-cachectic wild type (N=8), non-cachectic control Parp-$1^{-/-}$ (N=7), LC-cachectic Parp-$1^{-/-}$ (N=8), non-cachectic control Parp-$2^{-/-}$ (N=3), and LC-cachectic Parp-$2^{-/-}$ (N=5). GAPDH is shown as the loading control. Definition of abbreviations: MyHC, *Myosin Heavy Chain;* LC, Lung cancer; PARP, poly-ADP ribose polymerase; GAPDH, glyceraldehyde-3-phospate dehydrogenase; OD, optical densities; a.u., arbitrary units; MW, molecular weights; KDa, kilodaltons.

Fig. E15 Immunoblots of actin protein content in the diaphragm (panel A) and gastrocnemius (panel B) muscles of the following experimental groups: non-cachectic control wild type (N=7), LC-

cachectic wild type (N=8), non-cachectic control Parp-$1^{-/-}$ (N=7), LC-cachectic Parp-$1^{-/-}$ (N=8), non-cachectic control Parp-$2^{-/-}$ (N=3), and LC-cachectic Parp-$2^{-/-}$ (N=5). GAPDH is shown as the loading control. Definition of abbreviations: LC, Lung cancer; PARP, poly-ADP ribose polymerase; GAPDH, glyceraldehyde-3-phospate dehydrogenase; OD, optical densities; a.u., arbitrary units; MW, molecular weights; KDa, kilodaltons.

Fig. E16 Representative examples obtained from the diaphragm (panel A) and gastrocnemius (panel B) of the different study groups of animals. Myofibers positively stained with the anti-MyHC type II antibody are stained in brown color (x 200). Type I fibers were not stained (white color). Representative examples of nuclei positively stained (black arrows, brown nuclei) and not stained (red arrows, blue nuclei, hematoxylin counterstaining) for the TUNEL assay in the diaphragm (panel C) and gastrocnemius (panel D) of the different study groups of mice (x 400).

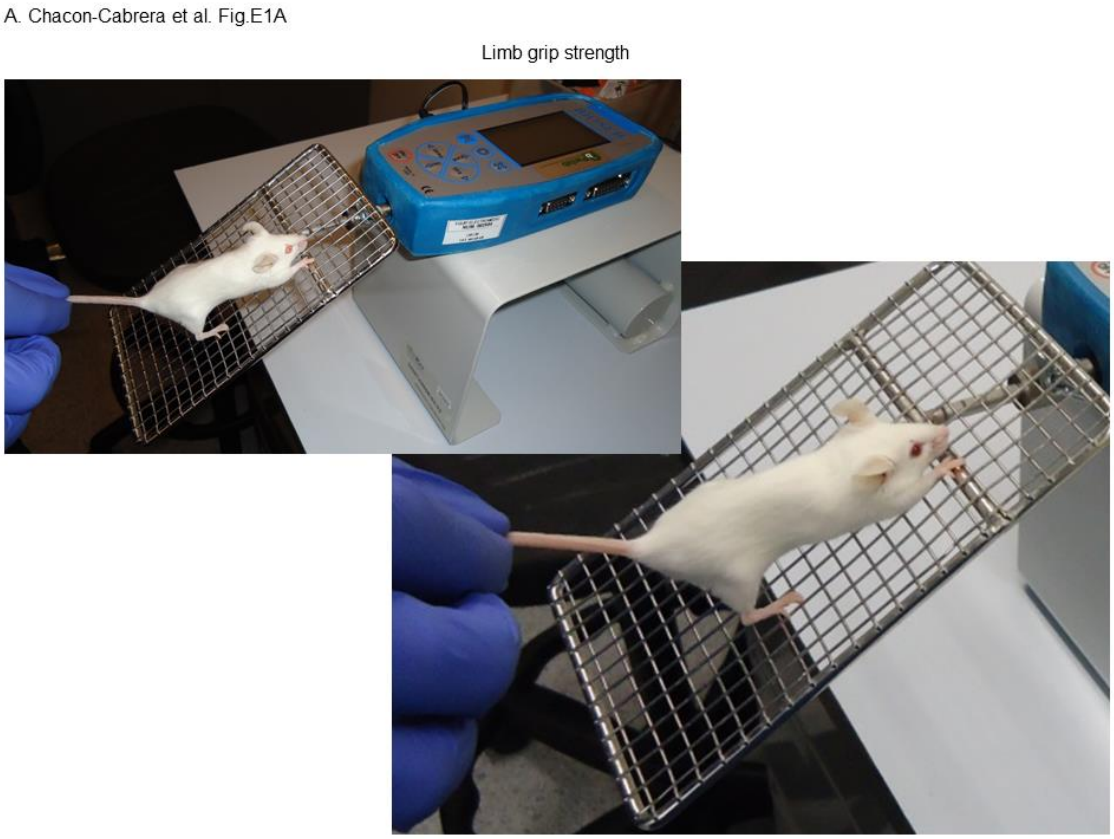

A. Chacon-Cabrera et al. Fig.E1B

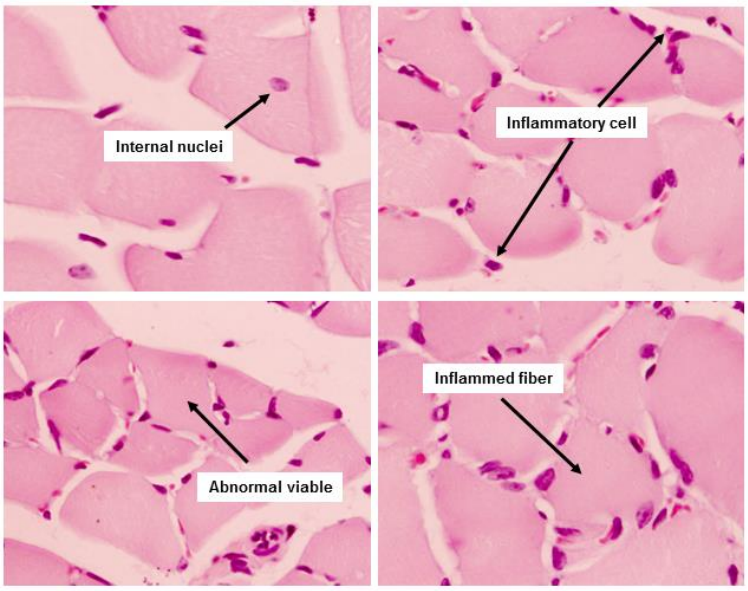

A. Chacon-Cabrera et al. Fig.E2

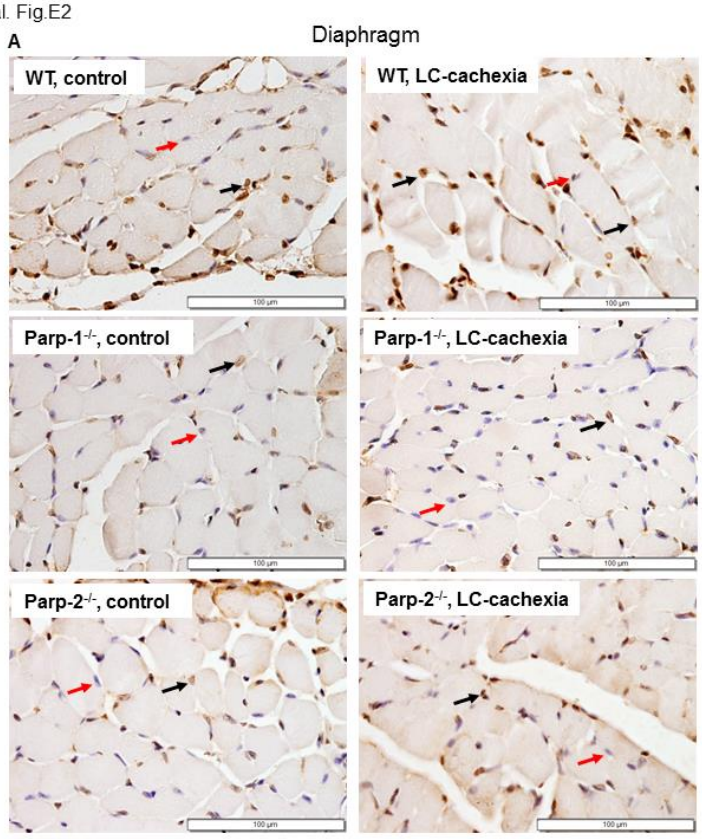

A. Chacon-Cabrera et al. Fig.E2

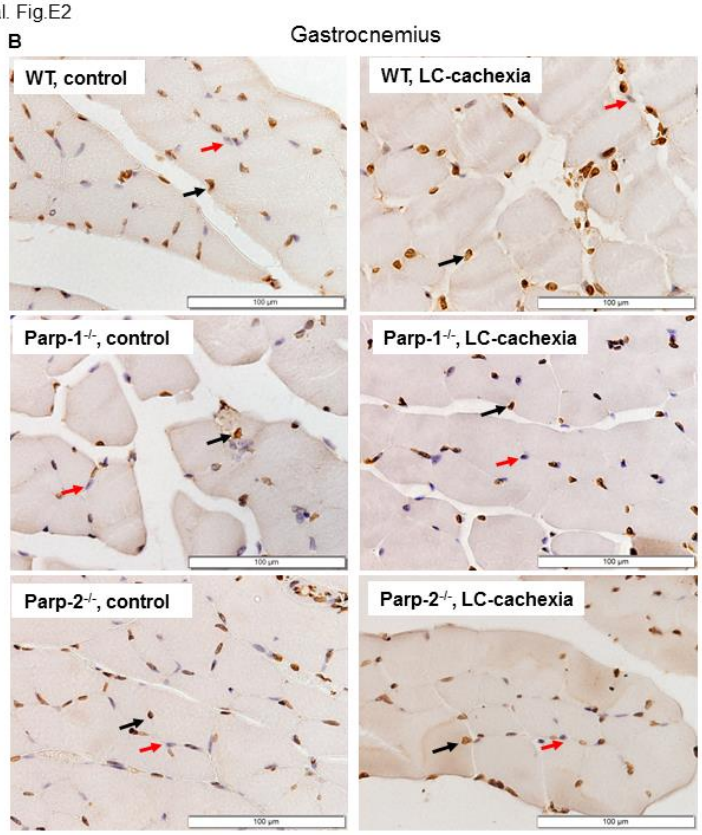

A. Chacon-Cabrera et al. Fig.E3

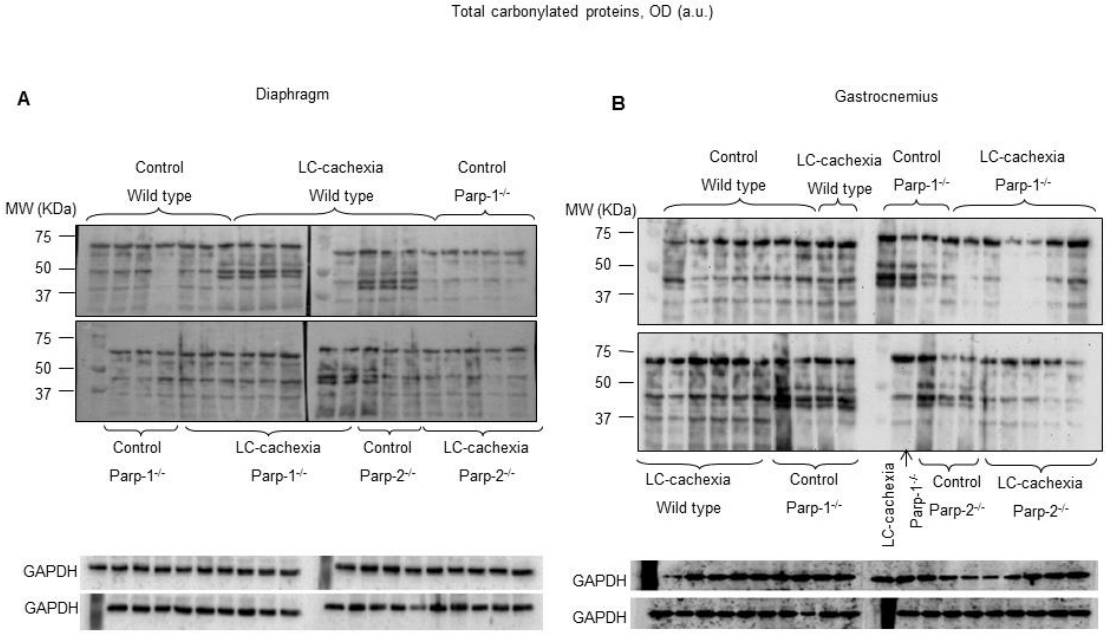

A. Chacon-Cabrera et al. Fig.E3

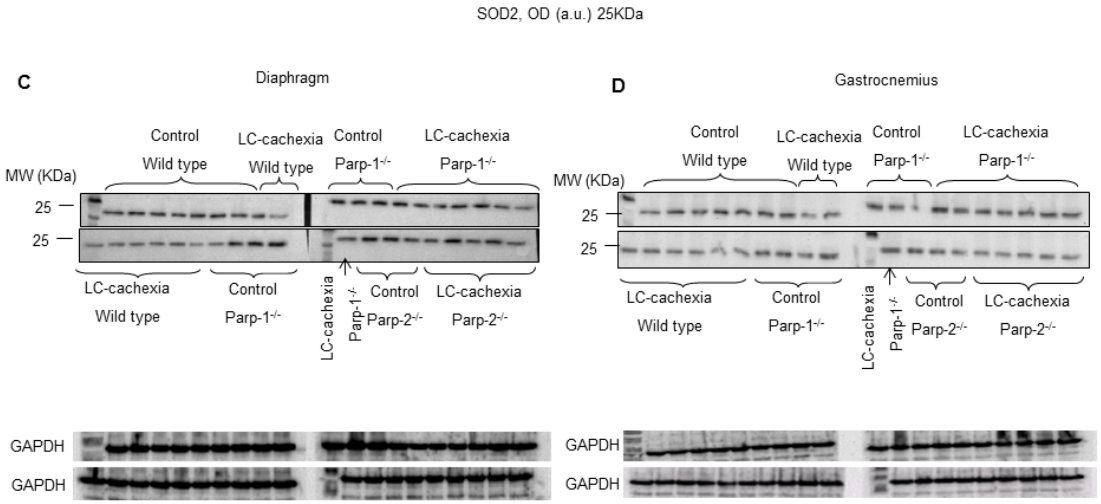

A. Chacon-Cabrera et al. Fig.E3

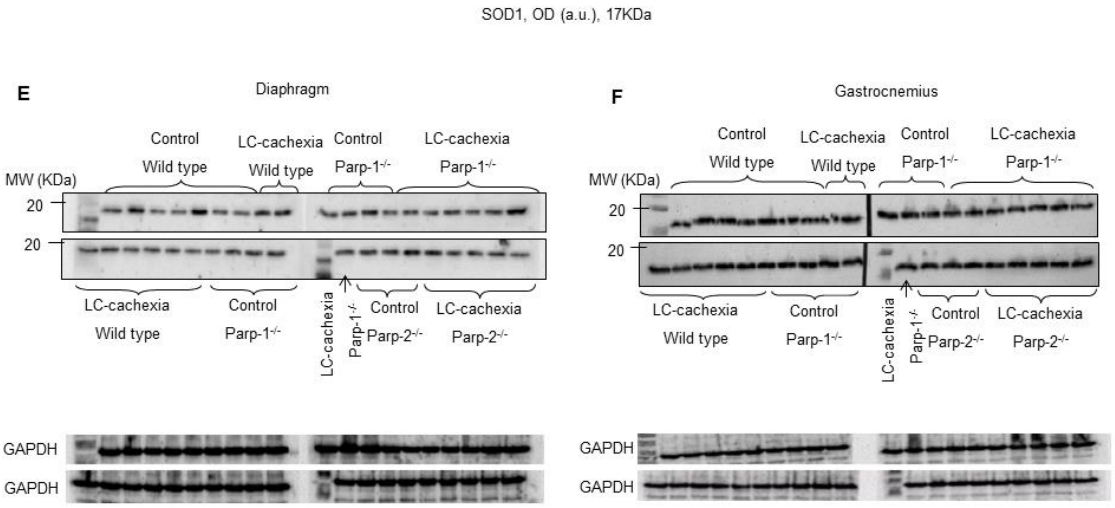

A. Chacon-Cabrera et al. Fig.E4

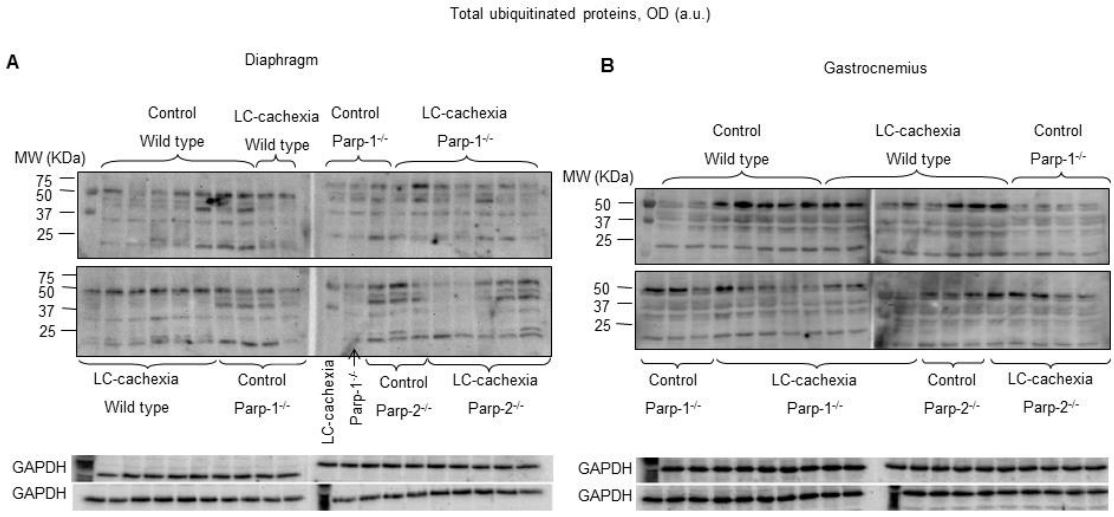

A. Chacon-Cabrera et al. Fig.E5

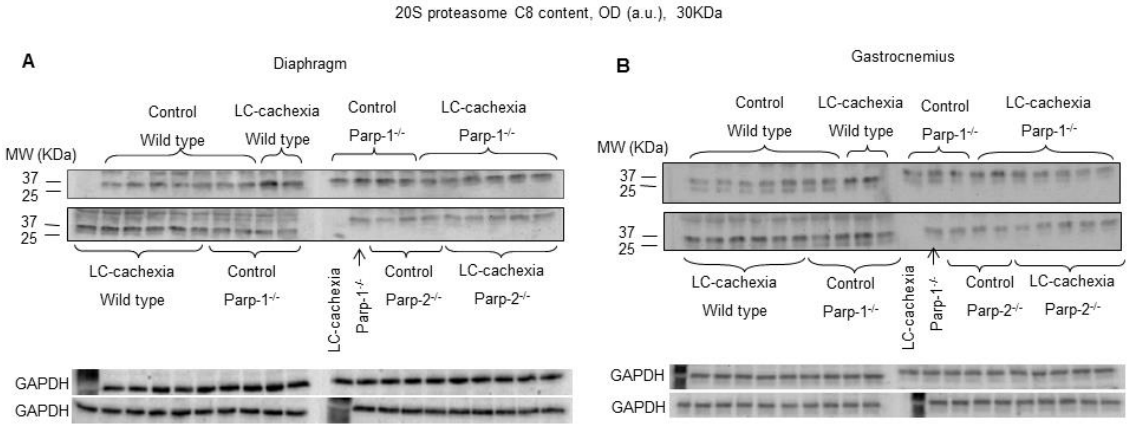

A. Chacon-Cabrera et al. Fig.E6

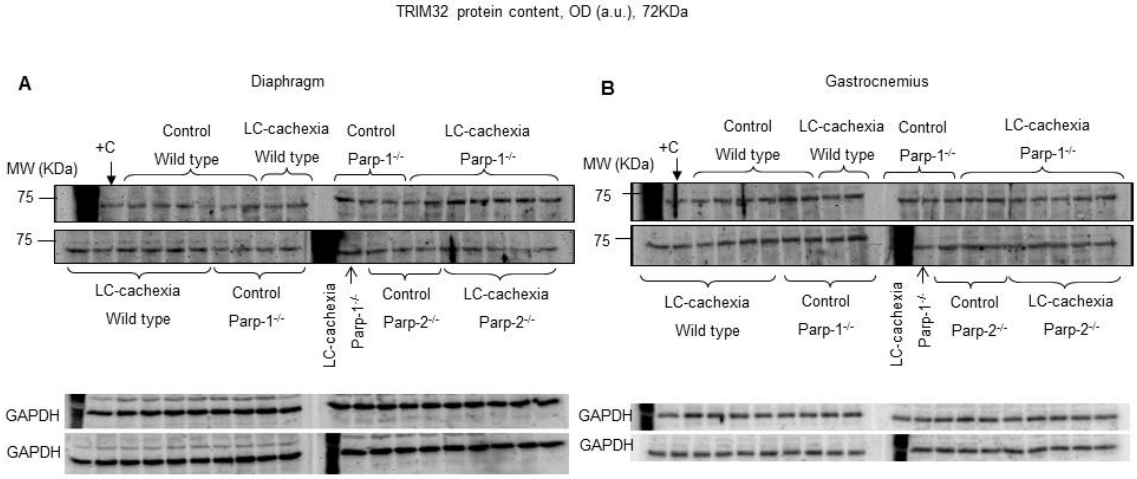

A. Chacon-Cabrera et al. Fig.E7

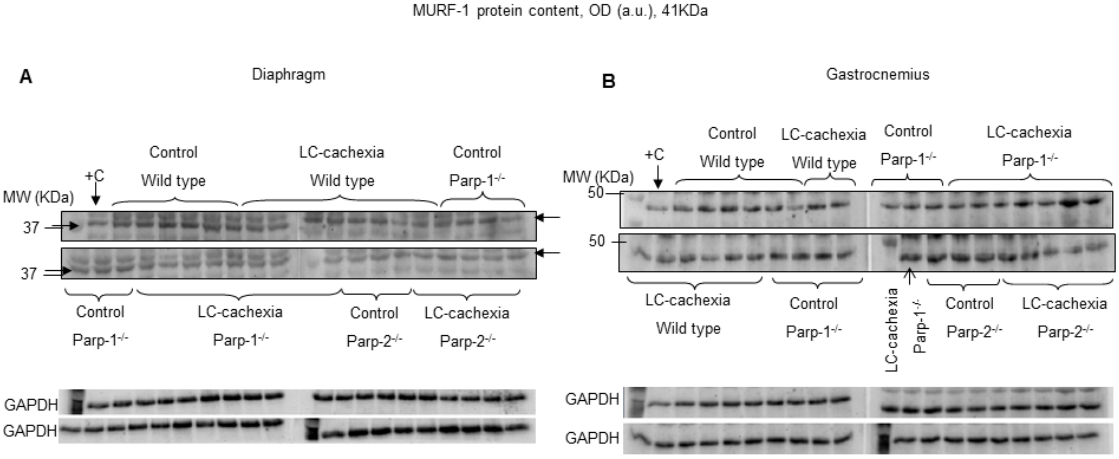

A. Chacon-Cabrera et al. Fig.E8

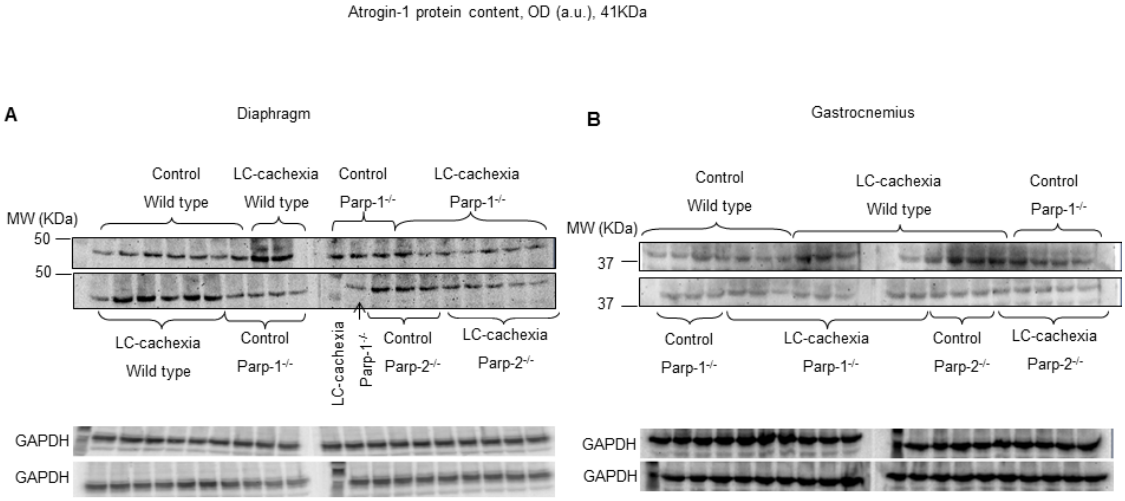

A. Chacon-Cabrera et al. Fig.E9

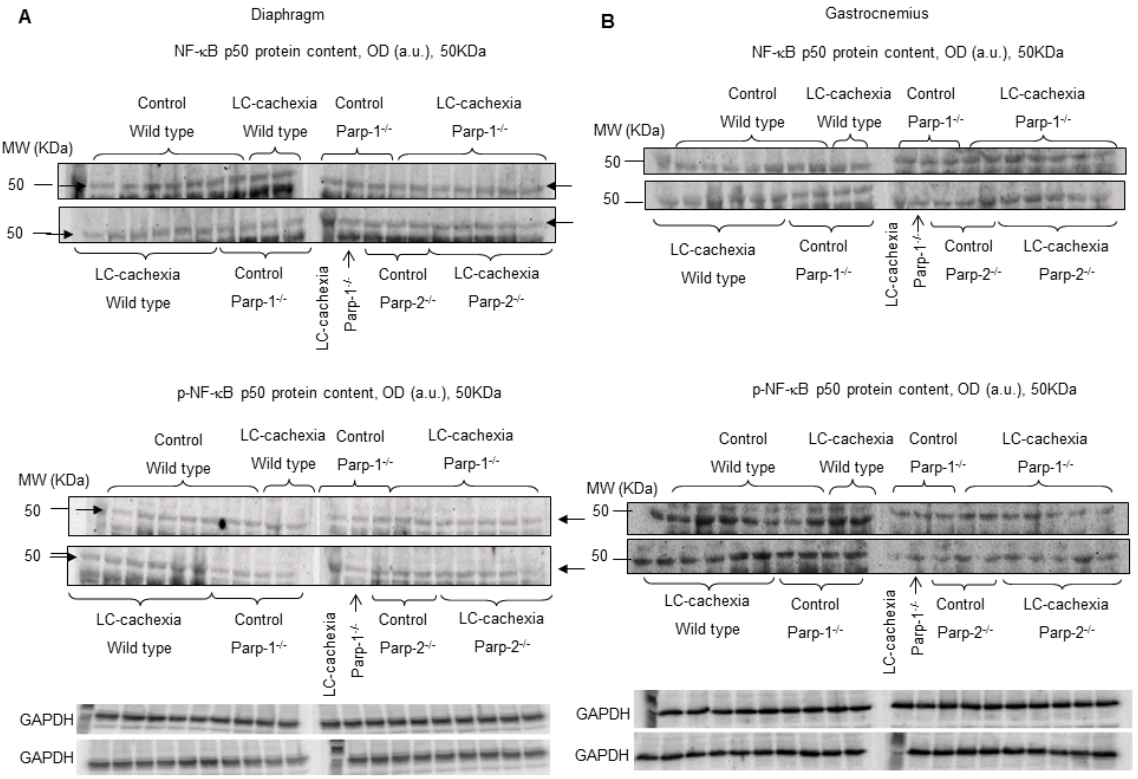

A. Chacon-Cabrera et al. Fig.E10

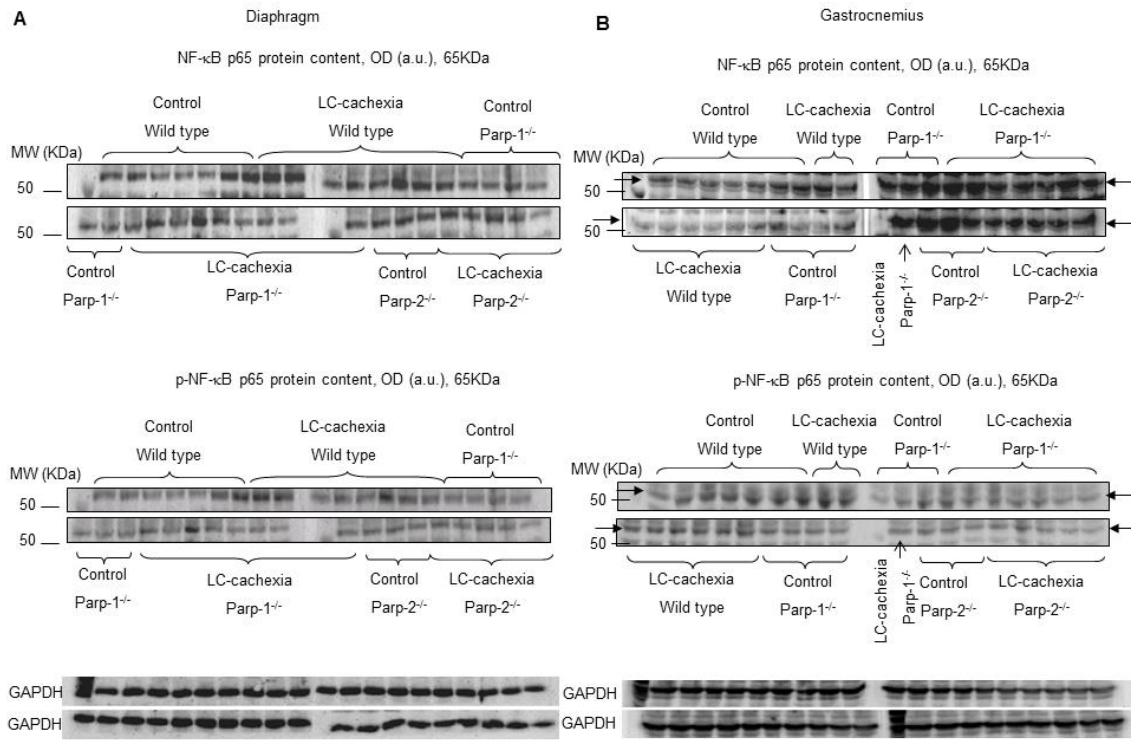

A. Chacon-Cabrera et al. Fig.E11

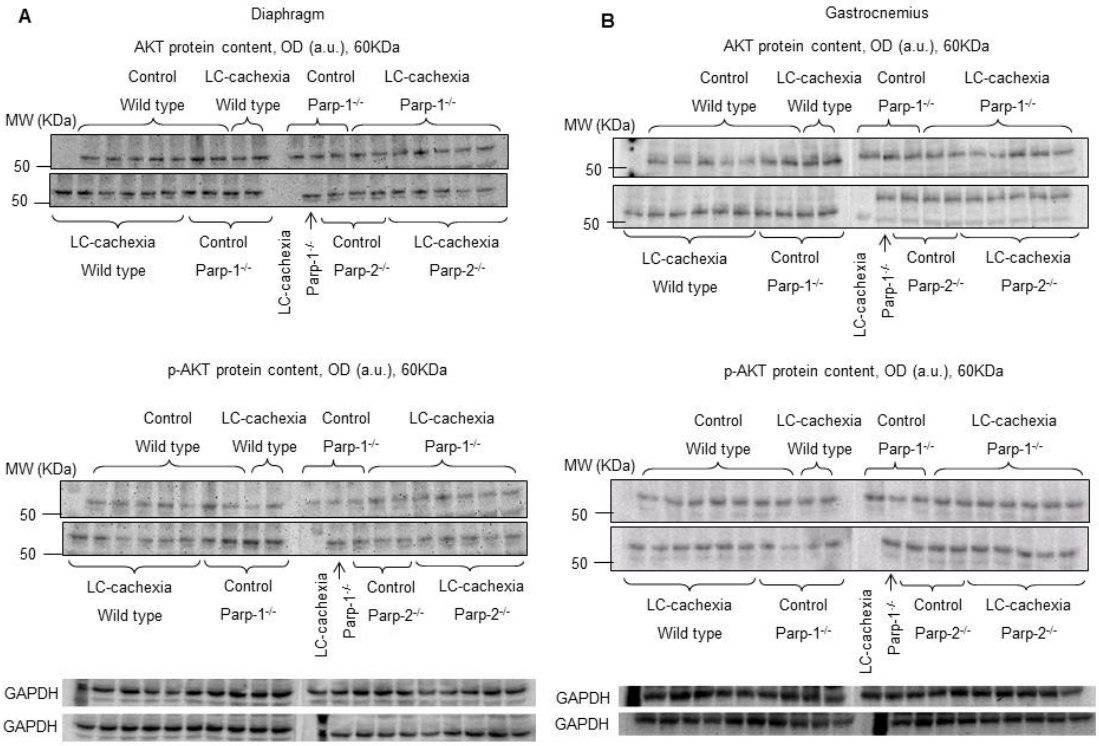

A. Chacon-Cabrera et al. Fig.E12

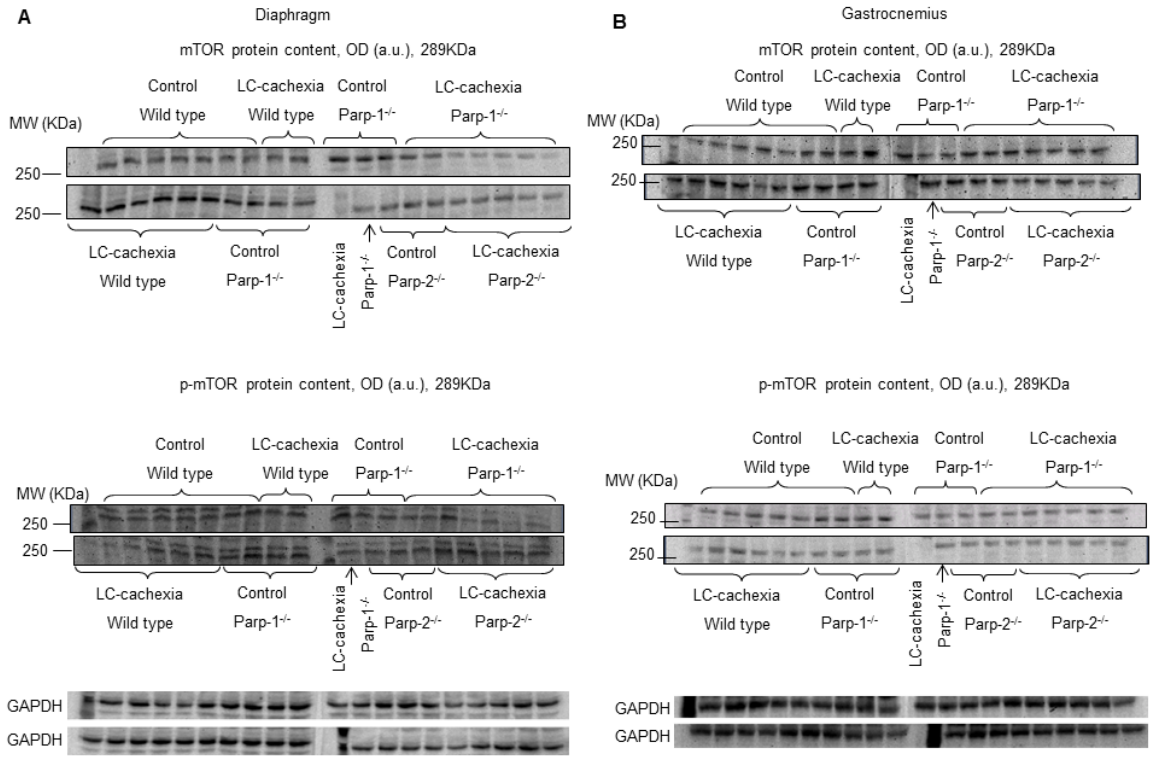

A. Chacon-Cabrera et al. Fig.E13

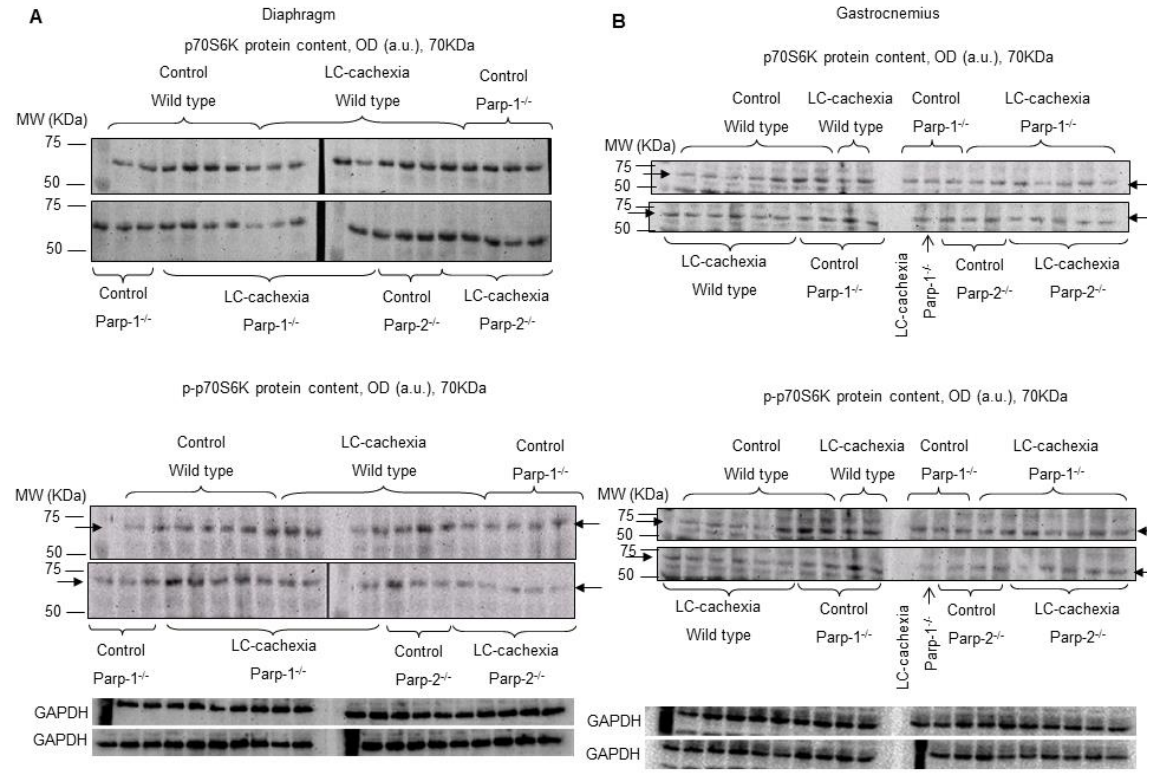

A. Chacon-Cabrera et al. Fig.E14

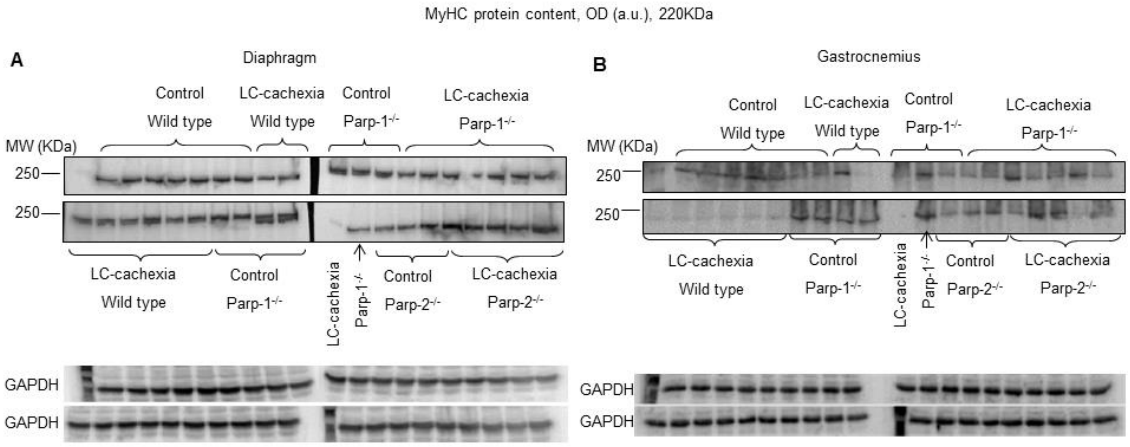

A. Chacon-Cabrera et al. Fig.E15

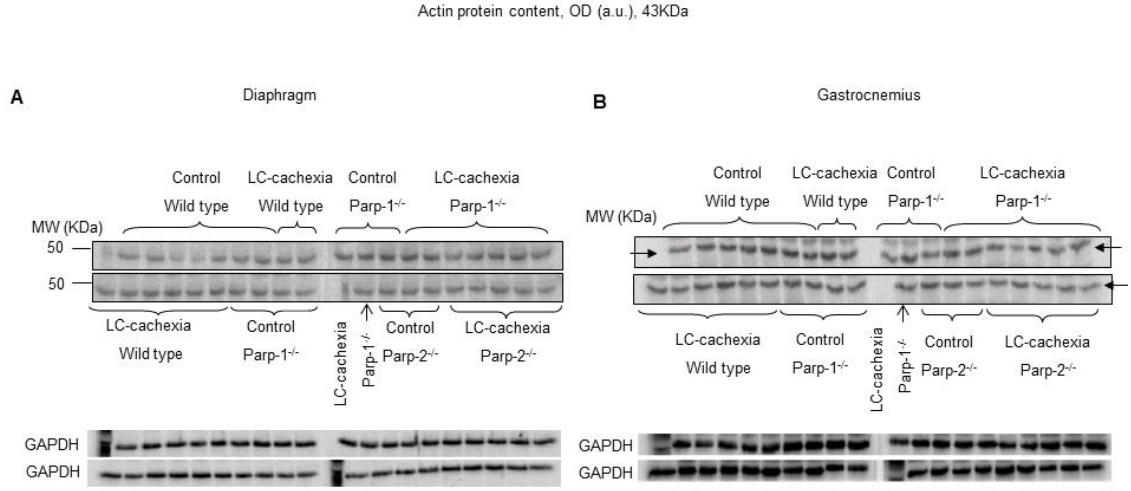

A. Chacon-Cabrera et al. Fig.E16

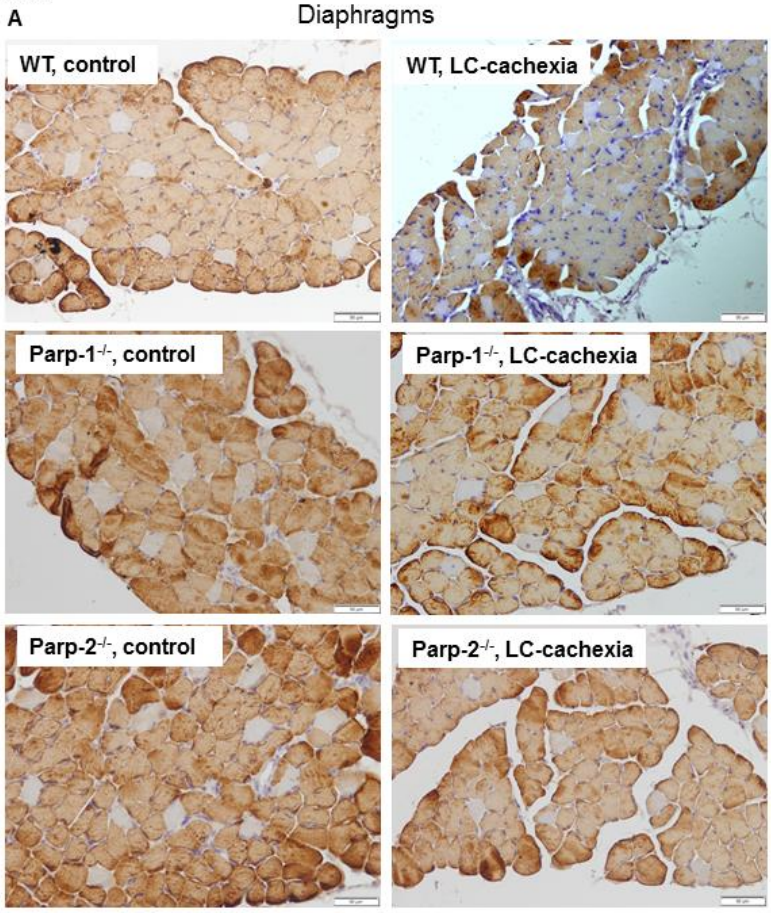

A. Chacon-Cabrera et al. Fig.E16

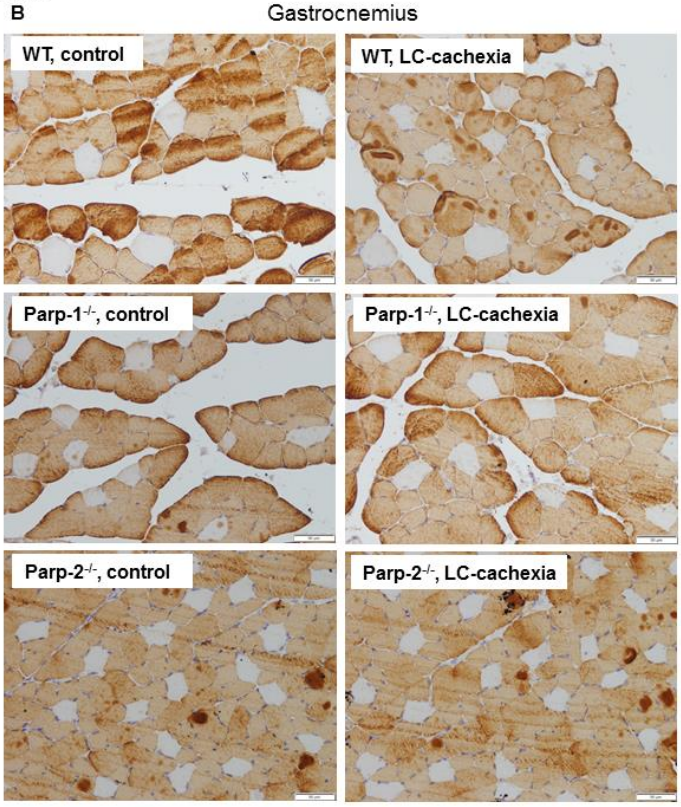

A. Chacon-Cabrera et al. Fig.E16

C

Diaphragms

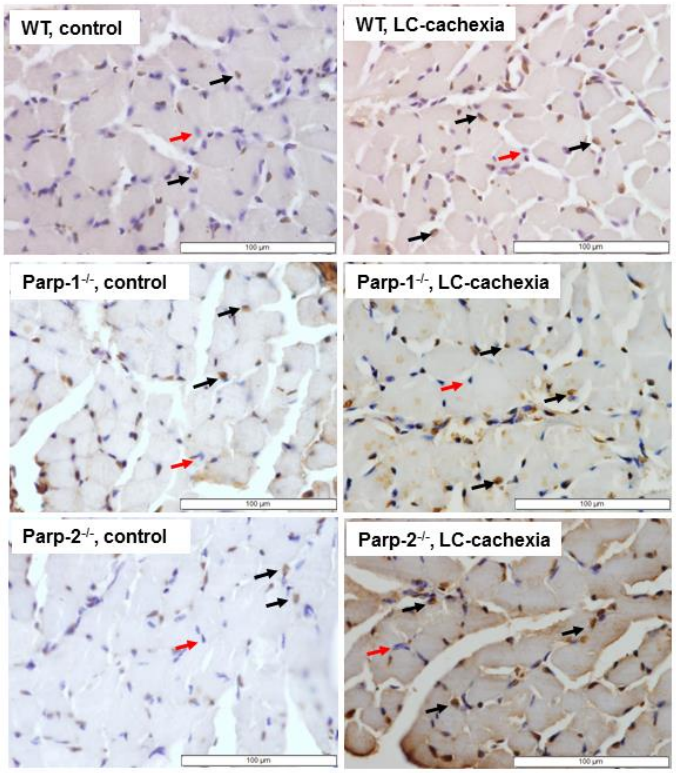

A. Chacon-Cabrera et al. Fig.E16

D

Gastrocnemius

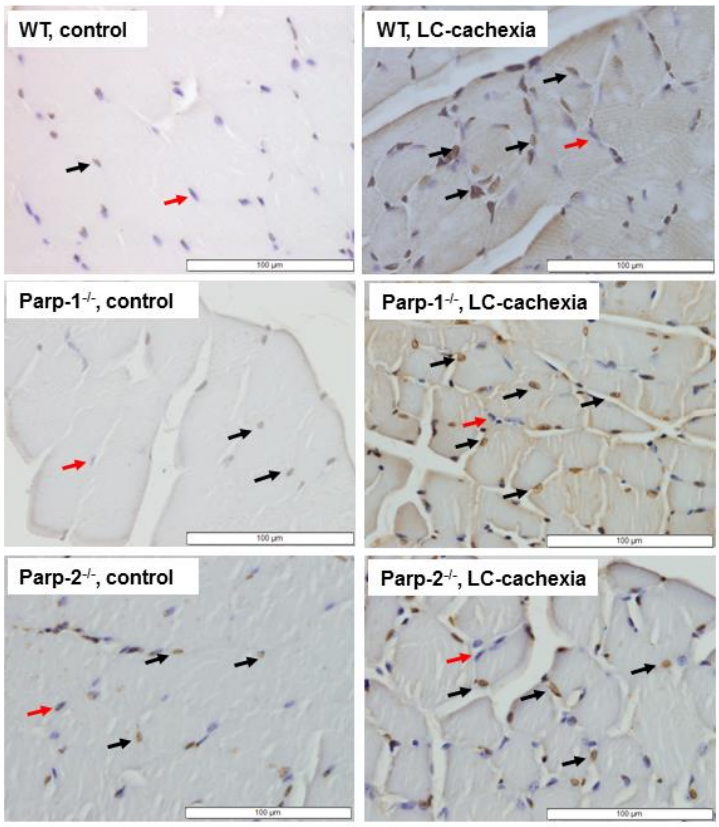

4- Summary of main findings Study #4

In immobilized animals compared to 30-day non-immobilized controls:

Body and muscle weights and muscle function

Total body weight and food intake did not differ between groups.

Change in gastrocnemius muscle weight was reduced from 3- to 30-day I animals. Limb strength gain was decreased in all immobilization groups of animals.

Muscle structure characteristics

Proportions of slow-twitch muscle fibers were significantly reduced, while those of fast-twitch were increased in 15- and 30-day I study groups.

The size of both type I and type II fibers was reduced in the gastrocnemius of 7-, 15-, and 30-day I mice.

Proportions of abnormal muscle fraction and internal nuclei counts were increased in the gastrocnemius of animals immobilized from 3 to 30 days. Inflammatory cells were greater in the gastrocnemius of 7-, 15, and 30-day I animals.

Proteolytic systems

Muscle catabolism, proteasome activity, levels of 20S proteasome subunit C8, total protein ubiquitination, and atrogin-I were increased in the gastrocnemius of 7-, 15-, and 30-day animals.

Protein content of MURF-1 was greater in the gastrocnemius of all immobilization groups of mice.

Levels of TRIM32 and GDF15 did not differ in the gastrocnemius among the study groups.

Muscle structural proteins

Protein levels of MyHC were reduced in the gastrocnemius of 3-, 7-, 15-, and 30-day I animals. Actin protein content did not differ in the gastrocnemius between groups.

Systemic damage

Plasma troponin-I levels were increased in 7-, 15-, and 30-day I animals.

Muscle anabolism

No differences were detected in activated Akt levels in the gastrocnemius of any of the study groups of animals. Activated p70S6K levels were decreased in the

gastrocnemius of 15- and 30-day I mice. The ratio of mtDNA/nDNA was reduced in the gastrocnemius of all immobilized animals.

In recovery groups of animals compared to 7-day immobilized controls:

Body and muscle weights and muscle function

Total body weight and food intake did not differ between groups.

Change in gastrocnemius muscle weight was increased in 15- and 30-day R mice. Limb strength gain was raised as from three and up to thirty days of recovery.

Muscle structure characteristics

Proportions of gastrocnemius type I and type II fibers did not differ between groups. The sizes of slow- and fast-twitch fibers were increased in the gastrocnemius of 7-, 15-, and 30-day R.

Proportions of abnormal muscle fraction and inflammatory cell counts were reduced in the limb muscle of 3-, 7-, 15-, and 30-day R mice. Internal nuclei proportions did not differ between groups.

Proteolytic systems

Muscle catabolism was decreased in all recovery groups of rodents.

In the gastrocnemius, proteasome activity was reduced in 3-, 7-, 15-, and 30-day R animals.

Protein levels of 20S proteasome subunit C8, total protein ubiquitination, and atrogin-1 were lower in the gastrocnemius of 7-, 15-, and 30-day R animals. Levels of MURF-1 were decreased in the gastrocnemius of 3-, 7-, 15-, and 30-day R groups of rodents. Levels of TRIM32 and GDF15 did not differ in the gastrocnemius among the study groups.

Muscle structural proteins

Gastrocnemius MyHC protein levels were increased only in the 30-day R animals. Protein levels of actin did not differ in the gastrocnemius between groups.

Systemic damage

Plasma levels of troponin-I were decreased in 15- and 30-day R animals.

Muscle anabolism

Activated Akt levels did not differ in the gastrocnemius among the different experimental groups. Activated p70S6K levels were increased in the limb muscle of 15- and 30-day R rodents. mtDNA copy number was reduced in the limb muscle of 7-, 15-, and 30-day R animals.

Chacon-Cabrera A, Lund-Palau H, Gea J, Barreiro E. Time-Course of Muscle Mass Loss, Damage, and Proteolysis in Gastrocnemius following Unloading and Reloading:Implications in Chronic Diseases. PLoS One. 2016 Oct 28;11(10):e0164951. doi: 10.1371/journal.pone.0164951. eCollection 2016

5- Summary of main findings Study #5

In immobilized animals compared to 30-day non-immobilized controls:

Body and muscle weights and muscle function

Total body weight and food intake did not differ among groups.

Change in gastrocnemius muscle weight was reduced from 3- to 30-day I animals. Limb strength gain was decreased in all immobilization groups of animals.

Expression microRNA in gastrocnemius

Expression levels of miR-1 and -206 were reduced in the gastrocnemius of 3-, and 7-day I, and 7- and 15-day I cohorts, respectively. Expression of miR-486 was downregulated in the gastrocnemius of 3-, 7-, 15-, and 30-day I animals. Mir-133a expression did not differ between groups.

Myogenic transcription factors

Protein levels of Pax7 were significantly increased in the gastrocnemius of and 3-, 7- 15-, and 30-day I cohorts. Protein levels of MEF2C, MEF2D, and PTEN did not significantly differ among the I study cohorts of mice.

Protein acetylation levels

Total protein acetylation and acetylated H3 levels in the gastrocnemius did not differ between groups.

Histone deacetylase levels

HDAC3 and HDAC6 protein content in the gastrocnemius did not differ between groups. SIRT1 protein levels were decreased in the gastrocnemius of 2-, 3-, 7-, 15-, and 30-day I animals.

Downstream markers of epigenetic regulation

Acetylated levels of Foxo1 and FoxO3 were increased in the limb muscle of 3-, 7-, 15-, and 30-day I animals. Levels of acetylated PGC-1α, and NF-kB did not differ between groups.

Muscle phenotype

Proportions of gastrocnemius type I and type II fibers did not differ between groups. The sizes of slow- and fast-twitch fibers were increased in the gastrocnemius of 7-, 15-, and 30-day I.

Results

In recovery groups of animals compared to 7-day immobilized controls:

Body and muscle weights and muscle function

Total body weight and food intake did not differ between groups.

Change in gastrocnemius muscle weight was increased in 15- and 30-day R mice. Limb strength gain was raised as from three and up to thirty days of recovery.

Expression microRNA in gastrocnemius

Expression levels of miR-1, -206 and -486 were upregulated in the gastrocnemius of 1-, 3-, 7-, 15-, and 30-day R animals. Levels of mir-133a expression did not differ between groups.

Myogenic transcription factors

Protein levels of Pax7 significantly decreased in the gastrocnemius of 3-, 7- , 15-, and 30-day R cohorts of mice. Protein content of MEF2C, MEF2D, and PTEN did not significantly differ among the study groups.

Protein acetylation levels

Total protein acetylation and acetylated H3 levels did not differ between groups in the gastrocnemius.

Histone deacetylase levels

HDAC3 and HDAC6 protein content in the gastrocnemius did not differ between groups. SIRT1 protein levels were increased in the gastrocnemius of 3-, 7-, 15-, and 30-day R animals.

Downstream markers of epigenetic regulation

Acetylated levels of FoxO1 and FoxO3 were decreased in the limb muscle of 3-, 7-, 15- and 30-day R animals. Levels of acetylated PGC-1α and NF-kB did not differ between groups.

Muscle phenotype

Proportions of gastrocnemius type I and type II fibers did not differ between groups. The sizes of slow- and fast-twitch fibers were increased in the gastrocnemius of 7-, 15-, and 30-day R.

Chacon-Cabrera A, Gea J, Barreiro E. Short- and Long-Term Hindlimb Immobilization and Reloading: Profile of Epigenetic Events in Gastrocnemius. J Cell Physiol. 2017 Jun;232(6):1415-1427. doi: 10.1002/jcp.25635

DISCUSSION

Biological events involved in muscle mass loss during cancer-cachexia and disuse muscle atrophy

Muscle wasting and dysfunction are common features of highly prevalent chronic diseases including lung cancer, that lead to a reduced exercise capacity, an impaired quality of life and a reduced survival (28, 188, 189). The physical condition of these patients force them in many cases to be subjected to prolonged bed rest and immobilization, and thus the loss of muscle mass is increased regardless the muscle wasting of the underlying disease (190, 191).

In both animal models (cancer cachexia and disuse), muscle atrophy was confirmed by the reduction observed in muscle weight, MyHC protein content, and muscle fiber sizes, together with increased abnormal muscle fraction. These structural events contributed to the impaired limb force production observed in both muscle wasting conditions. These findings, which are in agreement with earlier investigations conducted in our group on animal models of muscle mass loss (35, 192), suggest that chronic diseases as well as muscle deconditioning contribute in the same fashion to impaired muscle mass and function of the affected muscles.

Importantly, in hindlimb immobilization but not in LC cachexia model, gastrocnemius muscle exhibited a switch to a less fatigue resistant phenotype. These results, which are in the line with those previously reported in other studies of our group performed with cachectic rats (35, 192), indicate that muscle deconditioning is probably the main contributor of slow-to-fast fiber type switch in skeletal muscles of patients with chronic respiratory conditions that impaired their exercise capacity.

In these two animal models, muscle mass loss and dysfunction is the result of the underlying disease (LC), or prolonged muscle inactivity. Despite that cancer cachexia and muscle deconditioning contributes similarly to impair muscle mass and function, biological mechanisms that lead to this process may be different depending on the underlying condition.

Signaling pathways and proteolytic systems

In all study muscles of the two models, similar proteolytic pathways were shown to be involved in the process of muscle mass loss. In LC cachectic mice and in hindlimb immobilized rodents, the ubiquitin proteasome system appears to be the main mechanism of protein degradation in the study muscles. However, signaling regulation of muscle protein breakdown differs between the two models. In LC cachexia mice, NF-kB and MAPK pathways were shown to be the major signaling pathways of muscle mass loss in both muscles. These results are in agreement with previous investigations conducted on cachectic patients (12, 16), and other experimental models of cachexia (192). Nevertheless, in our experimental model of hindlimb immobilization, FoxO signaling pathway appears to regulate protein breakdown in the limb muscle, as previously shown in rodents submitted to denervation (193), and in rats exposed to hindlimb immobilization (194). These findings indicate that in disuse atrophy, FoxO signaling is required to induce the transcription of atrogin-1 and Murf-1 genes, leading to the ubiquitination and degradation of structural proteins via proteasome system. On the contrary, in cancer cachexia, both NF-kB and MAPK pathways are needed for the same purpose. Despite that in our experimental model of hindlimb immobilization, NF-kB pathway was not involved in the signaling muscle protein breakdown, previous studies performed with hindlimb unloading (82) and denervation (195) models in rodents, reported that NF-kB was activated in the slow-twitch muscle soleus. Differences in experimental model design and phenotype of the study muscles may account for the discrepancies among studies.

All these findings lead to the conclusion that during two different muscle wasting conditions (with and without underlying disease), despite the differences in muscle proteolysis signaling, the ubiquitin proteasome system appears to be the main and common proteolytic mechanism involved in the degradation of muscle structural proteins, and thus in the muscle mass loss.

Epigenetic events and post-translational modifications

MyomiR expression was downregulated in the study muscles of both LC cachectic mice and hindlimb immobilized rodents. These findings are in agreement with those reported in previous studies conducted in COPD patients

(156, 186) and in rats exposed to hindlimb unloading (196). Muscle-enriched microRNAs regulate muscle mass loss and repair through different targets in both conditions. In LC cachexia model, reduced miR-1 and -206 levels inhibit the expression of MEF2 transcription factors, thus repressing muscle differentiation, as previously reported in myoblasts (184). Furthermore, in the same model, downregulation of miR-486 expression may induce negative regulation of hypertrophy signaling, such as Akt/mTOR, as previously described (197). In fact, mTOR levels were shown to be reduced in this model of LC cachectic mice. These findings suggest that, in LC cachexia, the negative regulation of MyomiRs impedes regeneration of the affected muscles, thus promoting muscle mass loss. However, in the current model of hindlimb immobilization, the activation of Pax7 (a satellite cells proliferation marker) through the downregulation of mir-1, -206, and -486, indicate that the myogenic program is activated during muscle deconditioning in order to repair muscle damage, as previously reported in other models of denervation and immobilization (22, 198-200). The exact role of satellite cells activation and proliferation during muscle immobilization is poorly understood and remains to be elucidated. Current studies in our group are focus on the assessment of the number of both total and activated satellite cells in the limb muscles of the hindlimb immobilization model. In cancer-induced cachexia, the downregulation of miR-133 prevents myoblast proliferation contributing to muscle mass loss, as previously shown in the diaphragm of COPD patients (156). Conversely, miR-133 seems not to play a relevant role in muscle deconditioning, as reported in a previous investigation conducted on an experimental model of spaceflight (158).

Altogether, these results suggest that despite the important role of the myomiR network in the regulation of muscle mass loss and repair in both models, microRNAs regulate differently the skeletal muscle plasticity depending on the underlying condition.

Hyperacetylation is a post-translational modification of proteins that renders them more prone to degradation thus leading to muscle mass loss. This process is regulated by the action of HDACs and HATs. Concretely, HATs exert ubiquitin ligase activity and stimulate proteasome-dependent proteolysis (163). Results obtained in both animal models indicate that muscle protein

hyperacetylation only plays a relevant role in LC cachexia. Our findings imply that protein hyperacetylation is a potential contributor of muscle mass loss during cancer cachexia, as previously described in other investigations performed in muscle wasting models and in humans (165, 201, 202). Despite that hyperacetylation results in increased degradation of certain proteins, other proteins can be stabilized by increased acetylation, such as FoxO transcription factors which in acetylated state promotes its activity (203-205). Our findings suggest that acetylation of FoxO transcription factors also contribute to muscle protein loss, especially in the diaphragm of LC cachectic rodents, as previously shown in other models (206). Moreover, in the present experimental model of disuse muscle atrophy, histone deacetylase SIRT1 appears to regulate FoxO signaling. Our findings indicate that in gastrocnemius exposed to mechanical unloading, SIRT1 activity results impaired thus favoring the acetylation of FoxO transcription factors, which in this state can promote the transcription of FoxO genes leading to the activation of atrophy-related genes (atrogin-1 and MuRF-1) (170).

Taking together all these findings, hyperacetylation of proteins seems to have a relevant role in the regulation of muscle mass loss accompanied with the underlying disease (cancer), rather than muscle deconditioning. The reasons why hyperacetylation of proteins is more relevant in cancer-induced cachexia model, may be that this mechanism also regulates gene expression in cancer cells, thus impairing apoptosis and facilitating proliferation, which favor the tumor progression (207). However, acetylation/deacetylation of FoxO transcription factors appears to be a common pathway in muscle mass loss during cancer cachexia as well as in muscle deconditioning.

Muscle anabolism

In both LC cachexia and hindlimb immobilization models, the downregulation of markers of muscle anabolism (mTOR, p70S6K, and mitochondrial content) also contributed to the process of muscle mass loss, especially in the limb muscle. These results are in line with those recently reported in other investigations performed in different experimental models of cancer cachexia (108, 131, 208) and muscle disuse (209). Our data suggest that mTOR signaling can be repressed by atrogin-1, thus inhibiting protein

synthesis by the inactivation of p70S6K in both animal models. Different studies have been shown that atrogin-1 seems to control protein synthesis by the ubiquitination and therefore the degradation of the eukariotic translation initiation factor 3 subunit F (eIF3F), thus repressing p70S6K activation by mTOR (104, 210, 211). Future studies should focus in the assessment of whether muscle eIF3F content is degraded in both animal models. These findings indicate that, apart from the increase in protein degradation seen in the muscles of both animal models, a negative regulation of muscle growth may also contribute to the loss of muscle proteins in these two muscle wasting conditions. A number of factors appear to contribute to reduced muscle anabolism during cancer and muscle deconditioning. On the one hand, reduced protein synthesis can be conducted by the systemic inflammatory response associated with cancer. Inflammatory cytokines such as TNF-α, IL-1β and IL-6 are shown to be enhanced in LC patients (16, 212) and have been implicated to impair the anabolic response of the skeletal muscles in experimental models of sepsis (213, 214). On the other hand, alterations in muscle protein turnover during muscle deconditioning can be driven by null physical activity together with decreased levels of IGF-1 (hypertrophic stimuli) (215-217).

Time-course of muscle mass loss following immobilization and recovery

As described above, different molecular and cellular mechanisms are involved in muscle mass loss during deconditioning. However, the temporal sequence of these biological events differs between early and late phases of hindlimb immobilization in mice.

Interestingly, gastrocnemius weight, limb muscle force, as well as MyHC protein content and muscle structural abnormalities were impaired during early phases of hindlimb immobilization (between one and three days), while gastrocnemius muscle fiber CSA and the proportions of slow-twitch muscle fibers were reduced after prolonged time-points of unloading (from seven days of casting). These results are in accordance with previous reports performed in animal models (22, 23) and in humans (218) exposed to mechanical unloading. Conversely, recovery of muscle mass and function following hindlimb immobilization appears to predominate in late phases of muscle reloading (between seven and fifteen days of recovery). All these findings indicate that in

the gastrocnemius, physiological characteristics rather than muscle morphometry are especially susceptible to experience alterations at early stages of muscle disuse. Nonetheless, during muscle recovery following unloading, physiological and structural events seem to be accompanied throughout time.

Importantly, in our model of hindlimb immobilization, epigenetic regulation is shown to be involved in the process of muscle mass loss and repair during early and late time points of muscle disuse (from two to thirty days). Concretely, the downregulation of miR-1, -206, and -486 induced the activation of Pax7 (182). These findings, which are in agreement with those reported in other models of denervation and immobilization (22, 198-200), imply that satellite cells proliferation is promoted during early phases of muscle disuse with the aim to repair muscle damage induced by the unloading. The reduced expression of these myomiRs was rapidly reverted after 1 day of muscle recovery, thus inhibiting Pax7 (from days 3 and 30). These data indicate that after short periods of muscle reloading, a specific pattern of microRNA expression regulates the process of muscle mass repair. Moreover, in response to short-time muscle unloading, reduced SIRT1 activity appears to increase acetylated FoxO levels, leading to the transcription of atrogin-1 and Murf-1 genes. However, despite the early activation of atrophy signaling, muscle proteolysis increased after seven days of immobilization. These findings are in accordance with the reduction on fiber CSA observed in the gastrocnemius after seven days of muscle unloading. Interestingly, muscle proteolysis was mainly reverted during early phases of reloading (between the third and seventh day), leading to the muscle mass recovery after seven days of muscle remobilization. These data are in the line with those previously reported in mice exposed to hindlimb unloading and reloading (219). Taking all these results into consideration, muscle mass loss observed during deconditioning can be explained by reduced levels of SIRT1 in this experimental model of hindlimb immobilization.

During disuse muscle atrophy, markers of muscle anabolism also differed through time. On the one hand, p70S6K regulation seems to be reduced during late phases of muscle unloading (fifteen days) and improved after 15 days of reloading. On the other hand, mitochondrial content decreased in earlier phases of immobilization (one day) and restored after 7-day of reloading period. These

data indicates that muscle mass and structure are likely regulated by p70S6K signaling, while mitochondria regulate limb muscle force. Nonetheless, future studies should assess whether mitochondrial function is impaired in limb muscles exposed to hindlimb immobilization and reloading.

Therapeutic approaches in cancer-induced cachexia

On the basis of the mechanisms involved in muscle mass loss in cancer-cachexia, several strategies of potentially benefit were studied in the LC cachexia animal model. Pharmacological inhibition of NF-kB and MAPK signaling in cancer cachectic mice reduced muscle protein degradation and oxidation, protein ubiquitination levels, myostatin content, and autophagy. Moreover, muscles of cachectic animals treated with these two drugs exhibited an improvement in myogenin and MyHC protein levels. These results may be responsible for the amelioration seen in body and muscles weights, tumor size, and limb muscle force in cachectic animals treated with the NF-kB and MAPK inhibitors. However, despite the improvements in oxidative stress, proteolysis and autophagy seen in study muscles, body and muscles weights, and limb muscle force did not improved in response to the pharmacological inhibition of proteasome. All these findings lead to the conclusion that NF-kB and MAPK pathways play a relevant role in cancer-induced cachexia signaling in this experimental animal model.

The potential beneficial effects of PARP-1 or PARP-2 deficiency on muscle mass and function were also explored in LC cachexia model. Our data showed that oxidative stress act as an activator of PARP activity, which contributed to protein catabolism and muscle mass loss in LC cancer cachexia model. Genetic deletions of Parp-1 and -2 in tumor-bearing animals restored the increased protein oxidation and protein degradation observed in the study muscles of wild type cachectic rodents, through the attenuation of NF-kB signaling and the inhibition of the ubiquitin-proteasome system. Previous studies have demonstrated that PARP-1 also acts as an activator of NF-kB signaling (220). In this regard, our findings indicate that PARP-1 and PARP-2 deficiencies may revert muscle mass loss by reducing both oxidative stress and NF-kB signaling pathway.

Interestingly, markers of muscle anabolism were improved in both muscles of cancer cachectic knockout mice, thus suggesting that PARP-1 and -2 may regulate mTOR signaling pathway in this model of cachexia. In fact, previous studies have shown that pharmacological inhibition of PARP prevents mTOR repression in human embryonic kidney cells (221). Moreover, the improved mitochondrial content observed in the muscles of Parp-1$^{-/-}$ mice may be regulated by SIRT1 signaling, as previously shown in brown adipose tissue and muscle (222, 223). In this regard, PARP-1 deficiency may increase NAD+ availability for SIRT1 activation in this model of cancer cachexia. Indeed, SIRT1 protein content was greater in both muscles of cachectic knockout animals, thus reinforcing this finding.

A novel finding in the present thesis was the interaction between PARP-1 or -2 and muscle microRNAs expression. Our results indicated that PARP-1 and PARP-2 deficiencies improved the expression of muscle-enriched microRNAs, especially in the gastrocnemius of Parp-1$^{-/-}$ cachectic mice. These finding may explain the attenuation of the reduction in myocyte enhancer factor (MEF2) levels seen in the study muscles of cachectic knockout rodents. Further studies are needed to insight into the network between PARP and muscle-enrich microRNAs. Importantly, PARP-1 and -2 deficiencies got better the protein acetylation/deacetylation balance, and concretely reduced the FoxO acetylated levels in both muscles, thus decreasing its activity. Jointly, these data may explain the improvements observed in MyHC content, muscle fiber sizes, and in consequence the amelioration in body and muscle weights, tumor size, and limb muscle force in both Parp-1$^{-/-}$ and Parp-2$^{-/-}$ cachectic animals. These findings may be of potential interest in the treatment of muscle mass loss associated with chronic conditions including lung cancer, since pharmacological inhibitors of PARP-1 and -2 are also currently available for the treatment of several cancer types (153, 154). Nonetheless, future studies should assess if pharmacological inhibition of PARP-1 and -2 has similar therapeutic effects on muscles in cancer cachexia models.

Given the results obtained in the different studies performed in the hindlimb immobilization model, several pharmacological strategies of potentially benefit are need to be studied. Since our results indicate that SIRT1 signaling

contributes to muscle mass loss in this model of disuse muscle atrophy, it could be interesting to explore the effects of pharmacological activation of SIRT1 during muscle disuse and during the recovery process following mechanical unloading. Curcumin is a strong natural antioxidant which is shown to increase SIRT1 activity, thus improving mitochondrial biogenesis in experimental models of exercise training (224, 225). In this regard, new experiments are being conducted in our group, in which animals are being treated with curcumin.

CONCLUSIONS

Two different models of muscle mass loss have been studied in this thesis: 1) cancer-induced cachexia and 2) disuse muscle atrophy in experimental animals. Enhanced proteolysis as a result of activation of ubiquitin-proteasome system was demonstrated in the mouse muscles in both models. The most relevant signaling pathways were NF-kB and MAPK in the cancer cachexia model, and FoxO1 and FoxO3 in the disuse atrophy model. Epigenetic events such as downregulation of miR-1, miR-206, and miR-486 were observed in the mouse muscles in the two models. Protein and histone acetylation, and acetylation of transcription factors were altered in the muscles of mice in the cancer-cachexia model, while only the acetylation of transcription factors was modified in limb muscles of the disuse muscle atrophy model. Increased expression of PARP-1 and -2 was demonstrated in the muscles of the cancer-cachexia mice. Inhibition of NF-kB and MAPK activity ameliorated the process of muscle mass loss and function as well as PARP-1 and -2 genetic deletions.

Collectively, these findings offer novel therapeutic strategies that may be implemented in clinical settings in the near-future.

REFERENCES

1. BD TG. Principles of Anatomy and Physiology. 12th ed ed2009.
2. Hall JE, Guyton AC. Textbook of Medical Physiology. 12th ed2011.
3. Bentzinger CF, Wang YX, Rudnicki MA. Building muscle: molecular regulation of myogenesis. Cold Spring Harbor perspectives in biology. 2012 Feb;4(2).
4. Jones D RJ, de Haan A. Skeletal Muscle: From Molecules to Movement. 1 ed2004.
5. Silverthorn DU. Human Physiology. 5 ed2009.
6. Cooper GM. The Cell. 3 ed2004.
7. Schiaffino S, Reggiani C. Fiber types in mammalian skeletal muscles. Physiol Rev. 2011 Oct;91(4):1447-531.
8. Scott W, Stevens J, Binder-Macleod SA. Human skeletal muscle fiber type classifications. Phys Ther. 2001 Nov;81(11):1810-6.
9. Polla B, D'Antona G, Bottinelli R, Reggiani C. Respiratory muscle fibres: specialisation and plasticity. Thorax. 2004 Sep;59(9):808-17.
10. Villarroya J, Lara MC, Dorado B, Garrido M, Garcia-Arumi E, Meseguer A, et al. Targeted impairment of thymidine kinase 2 expression in cells induces mitochondrial DNA depletion and reveals molecular mechanisms of compensation of mitochondrial respiratory activity. Biochem Biophys Res Commun. 2011 Apr 8;407(2):333-8.
11. Puente-Maestu L, Perez-Parra J, Godoy R, Moreno N, Tejedor A, Gonzalez-Aragoneses F, et al. Abnormal mitochondrial function in locomotor and respiratory muscles of COPD patients. Eur Respir J. 2009 May;33(5):1045-52.
12. Fermoselle C, Rabinovich R, Ausin P, Puig-Vilanova E, Coronell C, Sanchez F, et al. Does oxidative stress modulate limb muscle atrophy in severe COPD patients? Eur Respir J. 2012 Oct;40(4):851-62.
13. Schiaffino S, Gorza L, Sartore S, Saggin L, Ausoni S, Vianello M, et al. Three myosin heavy chain isoforms in type 2 skeletal muscle fibres. J Muscle Res Cell Motil. 1989 Jun;10(3):197-205.
14. Harridge SD, Bottinelli R, Canepari M, Pellegrino MA, Reggiani C, Esbjornsson M, et al. Whole-muscle and single-fibre contractile properties and myosin heavy chain isoforms in humans. Pflugers Arch. 1996 Sep;432(5):913-20.
15. McComas AJ, Thomas HC. Fast and slow twitch muscles in man. J Neurol Sci. 1968 Sep-Oct;7(2):301-7.
16. Puig-Vilanova E, Rodriguez DA, Lloreta J, Ausin P, Pascual-Guardia S, Broquetas J, et al. Oxidative stress, redox signaling pathways, and autophagy in cachectic muscles of male patients with advanced COPD and lung cancer. Free Radic Biol Med. 2014 Nov 18;79C:91-108.
17. Seymour JM, Spruit MA, Hopkinson NS, Natanek SA, Man WD, Jackson A, et al. The prevalence of quadriceps weakness in COPD and the relationship with disease severity. Eur Respir J. 2010 Jul;36(1):81-8.
18. Anker SD, Sharma R. The syndrome of cardiac cachexia. Int J Cardiol. 2002 Sep;85(1):51-66.
19. Sakuma K, Yamaguchi A. Sarcopenia and cachexia: the adaptations of negative regulators of skeletal muscle mass. J Cachexia Sarcopenia Muscle. 2012 Jun;3(2):77-94.

20. Tisdale MJ. Cachexia in cancer patients. Nat Rev Cancer. 2002 Nov;2(11):862-71.
21. Fanzani A, Conraads VM, Penna F, Martinet W. Molecular and cellular mechanisms of skeletal muscle atrophy: an update. J Cachexia Sarcopenia Muscle. 2012 Sep;3(3):163-79.
22. Caron AZ, Drouin G, Desrosiers J, Trensz F, Grenier G. A novel hindlimb immobilization procedure for studying skeletal muscle atrophy and recovery in mouse. J Appl Physiol (1985). 2009 Jun;106(6):2049-59.
23. Lang SM, Kazi AA, Hong-Brown L, Lang CH. Delayed recovery of skeletal muscle mass following hindlimb immobilization in mTOR heterozygous mice. PLoS One. 2012;7(6):e38910.
24. Ratnovsky A, Elad D, Halpern P. Mechanics of respiratory muscles. Respir Physiol Neurobiol. 2008 Nov 30;163(1-3):82-9.
25. Ferlay J SI, Ervik M. Cancer Incidence and Mortality Worldwide: IARC CancerBase No. 11 Lyon, France: International Agency for Research on Cancer; : GLOBOCAN 2012 v1.0; 2013.
26. O'Gorman P, McMillan DC, McArdle CS. Longitudinal study of weight, appetite, performance status, and inflammation in advanced gastrointestinal cancer. Nutr Cancer. 1999;35(2):127-9.
27. Dewys WD, Begg C, Lavin PT, Band PR, Bennett JM, Bertino JR, et al. Prognostic effect of weight loss prior to chemotherapy in cancer patients. Eastern Cooperative Oncology Group. Am J Med. 1980 Oct;69(4):491-7.
28. Fearon K, Strasser F, Anker SD, Bosaeus I, Bruera E, Fainsinger RL, et al. Definition and classification of cancer cachexia: an international consensus. Lancet Oncol. 2011 May;12(5):489-95.
29. Scott HR, McMillan DC, Brown DJ, Forrest LM, McArdle CS, Milroy R. A prospective study of the impact of weight loss and the systemic inflammatory response on quality of life in patients with inoperable non-small cell lung cancer. Lung Cancer. 2003 Jun;40(3):295-9.
30. Fox KM, Brooks JM, Gandra SR, Markus R, Chiou CF. Estimation of Cachexia among Cancer Patients Based on Four Definitions. J Oncol. 2009;2009:693458.
31. Tisdale MJ. Molecular pathways leading to cancer cachexia. Physiology (Bethesda). 2005 Oct;20:340-8.
32. Field-Smith A, Morgan GJ, Davies FE. Bortezomib (Velcadetrade mark) in the Treatment of Multiple Myeloma. Ther Clin Risk Manag. 2006 Sep;2(3):271-9.
33. Porter DR, Sturrock RD. Medical management of rheumatoid arthritis. BMJ. 1993 Aug 14;307(6901):425-8.
34. Fermoselle C, Garcia-Arumi E, Puig-Vilanova E, Andreu AL, Urtreger AJ, de Kier Joffe ED, et al. Mitochondrial dysfunction and therapeutic approaches in respiratory and limb muscles of cancer cachectic mice. Exp Physiol. 2013 Sep;98(9):1349-65.
35. Marin-Corral J, Fontes CC, Pascual-Guardia S, Sanchez F, Olivan M, Argiles JM, et al. Redox balance and carbonylated proteins in limb and heart muscles of cachectic rats. Antioxid Redox Signal. 2010 Mar;12(3):365-80.
36. Adams GR, Caiozzo VJ, Baldwin KM. Skeletal muscle unweighting: spaceflight and ground-based models. J Appl Physiol (1985). 2003 Dec;95(6):2185-201.

37. Booth FW. Effect of limb immobilization on skeletal muscle. J Appl Physiol Respir Environ Exerc Physiol. 1982 May;52(5):1113-8.
38. Thomason DB, Booth FW. Atrophy of the soleus muscle by hindlimb unweighting. J Appl Physiol (1985). 1990 Jan;68(1):1-12.
39. Morey-Holton ER, Globus RK. Hindlimb unloading rodent model: technical aspects. J Appl Physiol (1985). 2002 Apr;92(4):1367-77.
40. Midrio M. The denervated muscle: facts and hypotheses. A historical review. Eur J Appl Physiol. 2006 Sep;98(1):1-21.
41. Frimel TN, Kapadia F, Gaidosh GS, Li Y, Walter GA, Vandenborne K. A model of muscle atrophy using cast immobilization in mice. Muscle Nerve. 2005 Nov;32(5):672-4.
42. Magne H, Savary-Auzeloux I, Migne C, Peyron MA, Combaret L, Remond D, et al. Unilateral hindlimb casting induced a delayed generalized muscle atrophy during rehabilitation that is prevented by a whey or a high protein diet but not a free leucine-enriched diet. PLoS One. 2013;8(8):e70130.
43. Powers SK, Kavazis AN, McClung JM. Oxidative stress and disuse muscle atrophy. J Appl Physiol (1985). 2007 Jun;102(6):2389-97.
44. Rannou F, Pennec JP, Morel J, Gueret G, Leschiera R, Droguet M, et al. Na v1.4 and Na v1.5 are modulated differently during muscle immobilization and contractile phenotype conversion. J Appl Physiol (1985). 2011 Aug;111(2):495-507.
45. Ohira Y, Jiang B, Roy RR, Oganov V, Ilyina-Kakueva E, Marini JF, et al. Rat soleus muscle fiber responses to 14 days of spaceflight and hindlimb suspension. J Appl Physiol (1985). 1992 Aug;73(2 Suppl):51S-7S.
46. Stevens-Lapsley JE, Ye F, Liu M, Borst SE, Conover C, Yarasheski KE, et al. Impact of viral-mediated IGF-I gene transfer on skeletal muscle following cast immobilization. Am J Physiol Endocrinol Metab. 2010 Nov;299(5):E730-40.
47. Reid MB. Nitric oxide, reactive oxygen species, and skeletal muscle contraction. Med Sci Sports Exerc. 2001 Mar;33(3):371-6.
48. Barreiro E, Hussain SN. Protein carbonylation in skeletal muscles: impact on function. Antioxid Redox Signal. 2010 Mar;12(3):417-29.
49. Droge W. Free radicals in the physiological control of cell function. Physiol Rev. 2002 Jan;82(1):47-95.
50. Barreiro E, de la Puente B, Busquets S, Lopez-Soriano FJ, Gea J, Argiles JM. Both oxidative and nitrosative stress are associated with muscle wasting in tumour-bearing rats. FEBS Lett. 2005 Mar 14;579(7):1646-52.
51. Barreiro E, de la Puente B, Minguella J, Corominas JM, Serrano S, Hussain SN, et al. Oxidative stress and respiratory muscle dysfunction in severe chronic obstructive pulmonary disease. Am J Respir Crit Care Med. 2005 May 15;171(10):1116-24.
52. Cheng M, Nguyen MH, Fantuzzi G, Koh TJ. Endogenous interferon-gamma is required for efficient skeletal muscle regeneration. Am J Physiol Cell Physiol. 2008 May;294(5):C1183-91.
53. Marin-Corral J, Minguella J, Ramirez-Sarmiento AL, Hussain SN, Gea J, Barreiro E. Oxidised proteins and superoxide anion production in the diaphragm of severe COPD patients. Eur Respir J. 2009 Jun;33(6):1309-19.
54. Hussain SN, Matar G, Barreiro E, Florian M, Divangahi M, Vassilakopoulos T. Modifications of proteins by 4-hydroxy-2-nonenal in the ventilatory muscles of rats. Am J Physiol Lung Cell Mol Physiol. 2006 May;290(5):L996-1003.

55. Powers SK, Kavazis AN, DeRuisseau KC. Mechanisms of disuse muscle atrophy: role of oxidative stress. Am J Physiol Regul Integr Comp Physiol. 2005 Feb;288(2):R337-44.
56. Kondo H, Miura M, Itokawa Y. Oxidative stress in skeletal muscle atrophied by immobilization. Acta Physiol Scand. 1991 Aug;142(4):527-8.
57. Lawler JM, Song W, Demaree SR. Hindlimb unloading increases oxidative stress and disrupts antioxidant capacity in skeletal muscle. Free Radic Biol Med. 2003 Jul 1;35(1):9-16.
58. Agusti A, Edwards LD, Rennard SI, MacNee W, Tal-Singer R, Miller BE, et al. Persistent systemic inflammation is associated with poor clinical outcomes in COPD: a novel phenotype. PLoS One. 2012;7(5):e37483.
59. Fearon KC, Voss AC, Hustead DS. Definition of cancer cachexia: effect of weight loss, reduced food intake, and systemic inflammation on functional status and prognosis. Am J Clin Nutr. 2006 Jun;83(6):1345-50.
60. Wust RC, Degens H. Factors contributing to muscle wasting and dysfunction in COPD patients. Int J Chron Obstruct Pulmon Dis. 2007;2(3):289-300.
61. Mantovani G, Maccio A, Mura L, Massa E, Mudu MC, Mulas C, et al. Serum levels of leptin and proinflammatory cytokines in patients with advanced-stage cancer at different sites. J Mol Med (Berl). 2000;78(10):554-61.
62. Mantovani G. Serum levels of cytokines and weightloss/anorexia in cancer patients. Support Care Cancer. 1997 Sep;5(5):422-3.
63. Argiles JM, Busquets S, Lopez-Soriano FJ. The pivotal role of cytokines in muscle wasting during cancer. Int J Biochem Cell Biol. 2005 Oct;37(10):2036-46.
64. Argiles JM, Lopez-Soriano FJ, Busquets S. Mechanisms to explain wasting of muscle and fat in cancer cachexia. Curr Opin Support Palliat Care. 2007 Dec;1(4):293-8.
65. Barreiro E, Peinado VI, Galdiz JB, Ferrer E, Marin-Corral J, Sanchez F, et al. Cigarette smoke-induced oxidative stress: A role in chronic obstructive pulmonary disease skeletal muscle dysfunction. Am J Respir Crit Care Med. 2010 Aug 15;182(4):477-88.
66. Barreiro E, Schols AM, Polkey MI, Galdiz JB, Gosker HR, Swallow EB, et al. Cytokine profile in quadriceps muscles of patients with severe COPD. Thorax. 2008 Feb;63(2):100-7.
67. Berridge MJ. Cell signalling. A tale of two messengers. Nature. 1993 Sep 30;365(6445):388-9.
68. Degese MS, Tanos T, Naipauer J, Gringerich T, Chiappe D, Echeverria P, et al. An interplay between the p38 MAPK pathway and AUBPs regulate c-fos mRNA stability during mitogenic stimulation. Biochem J. 2015 Jan 14.
69. Barreiro E, Nowinski A, Gea J, Sliwinski P. Oxidative stress in the external intercostal muscles of patients with obstructive sleep apnoea. Thorax. 2007 Dec;62(12):1095-101.
70. Kramer HF, Goodyear LJ. Exercise, MAPK, and NF-kappaB signaling in skeletal muscle. J Appl Physiol (1985). 2007 Jul;103(1):388-95.
71. McClung JM, Judge AR, Powers SK, Yan Z. p38 MAPK links oxidative stress to autophagy-related gene expression in cachectic muscle wasting. Am J Physiol Cell Physiol. 2010 Mar;298(3):C542-9.
72. Kandarian SC, Jackman RW. Intracellular signaling during skeletal muscle atrophy. Muscle Nerve. 2006 Feb;33(2):155-65.

73. Kyriakis JM, Avruch J. Mammalian mitogen-activated protein kinase signal transduction pathways activated by stress and inflammation. Physiol Rev. 2001 Apr;81(2):807-69.
74. Koyama S, Hata S, Witt CC, Ono Y, Lerche S, Ojima K, et al. Muscle RING-finger protein-1 (MuRF1) as a connector of muscle energy metabolism and protein synthesis. J Mol Biol. 2008 Mar 7;376(5):1224-36.
75. Kim J, Won KJ, Lee HM, Hwang BY, Bae YM, Choi WS, et al. p38 MAPK Participates in Muscle-Specific RING Finger 1-Mediated Atrophy in Cast-Immobilized Rat Gastrocnemius Muscle. Korean J Physiol Pharmacol. 2009 Dec;13(6):491-6.
76. Liu Q, Xu WG, Luo Y, Han FF, Yao XH, Yang TY, et al. Cigarette smoke-induced skeletal muscle atrophy is associated with up-regulation of USP-19 via p38 and ERK MAPKs. J Cell Biochem. 2011 Sep;112(9):2307-16.
77. Chi H, Barry SP, Roth RJ, Wu JJ, Jones EA, Bennett AM, et al. Dynamic regulation of pro- and anti-inflammatory cytokines by MAPK phosphatase 1 (MKP-1) in innate immune responses. Proc Natl Acad Sci U S A. 2006 Feb 14;103(7):2274-9.
78. Shi H, Scheffler JM, Zeng C, Pleitner JM, Hannon KM, Grant AL, et al. Mitogen-activated protein kinase signaling is necessary for the maintenance of skeletal muscle mass. Am J Physiol Cell Physiol. 2009 May;296(5):C1040-8.
79. Johns N, Stephens NA, Fearon KC. Muscle wasting in cancer. Int J Biochem Cell Biol. 2013 Oct;45(10):2215-29.
80. Giordani L, Puri PL. Epigenetic control of skeletal muscle regeneration: Integrating genetic determinants and environmental changes. FEBS J. 2013 Sep;280(17):4014-25.
81. Fermoselle C, Sanchez F, Barreiro E. [Reduction of muscle mass mediated by myostatin in an experimental model of pulmonary emphysema]. Arch Bronconeumol. 2011 Dec;47(12):590-8.
82. Hunter RB, Stevenson E, Koncarevic A, Mitchell-Felton H, Essig DA, Kandarian SC. Activation of an alternative NF-kappaB pathway in skeletal muscle during disuse atrophy. FASEB J. 2002 Apr;16(6):529-38.
83. Delhalle S, Blasius R, Dicato M, Diederich M. A beginner's guide to NF-kappaB signaling pathways. Ann N Y Acad Sci. 2004 Dec;1030:1-13.
84. Jackman RW, Kandarian SC. The molecular basis of skeletal muscle atrophy. Am J Physiol Cell Physiol. 2004 Oct;287(4):C834-43.
85. Gilmore TD. Introduction to NF-kappaB: players, pathways, perspectives. Oncogene. 2006 Oct 30;25(51):6680-4.
86. Salih DA, Brunet A. FoxO transcription factors in the maintenance of cellular homeostasis during aging. Curr Opin Cell Biol. 2008 Apr;20(2):126-36.
87. Birkenkamp KU, Coffer PJ. Regulation of cell survival and proliferation by the FOXO (Forkhead box, class O) subfamily of Forkhead transcription factors. Biochem Soc Trans. 2003 Feb;31(Pt 1):292-7.
88. Glauser DA, Schlegel W. The emerging role of FOXO transcription factors in pancreatic beta cells. J Endocrinol. 2007 May;193(2):195-207.
89. Mammucari C, Milan G, Romanello V, Masiero E, Rudolf R, Del Piccolo P, et al. FoxO3 controls autophagy in skeletal muscle in vivo. Cell Metab. 2007 Dec;6(6):458-71.
90. Zhao J, Brault JJ, Schild A, Cao P, Sandri M, Schiaffino S, et al. FoxO3 coordinately activates protein degradation by the autophagic/lysosomal and

proteasomal pathways in atrophying muscle cells. Cell Metab. 2007 Dec;6(6):472-83.
91. Suzuki N, Motohashi N, Uezumi A, Fukada S, Yoshimura T, Itoyama Y, et al. NO production results in suspension-induced muscle atrophy through dislocation of neuronal NOS. J Clin Invest. 2007 Sep;117(9):2468-76.
92. Langley B, Thomas M, Bishop A, Sharma M, Gilmour S, Kambadur R. Myostatin inhibits myoblast differentiation by down-regulating MyoD expression. J Biol Chem. 2002 Dec 20;277(51):49831-40.
93. Elkina Y, von Haehling S, Anker SD, Springer J. The role of myostatin in muscle wasting: an overview. J Cachexia Sarcopenia Muscle. 2011 Sep;2(3):143-51.
94. Allen DL, Unterman TG. Regulation of myostatin expression and myoblast differentiation by FoxO and SMAD transcription factors. Am J Physiol Cell Physiol. 2007 Jan;292(1):C188-99.
95. Lee SJ, McPherron AC. Regulation of myostatin activity and muscle growth. Proc Natl Acad Sci U S A. 2001 Jul 31;98(16):9306-11.
96. Costelli P, Muscaritoli M, Bonetto A, Penna F, Reffo P, Bossola M, et al. Muscle myostatin signalling is enhanced in experimental cancer cachexia. Eur J Clin Invest. [Research Support, Non-U.S. Gov't]. 2008 Jul;38(7):531-8.
97. Elkina Y, von Haehling S, Anker SD, Springer J. The role of myostatin in muscle wasting: an overview. Journal of cachexia, sarcopenia and muscle. 2011 Sep;2(3):143-51.
98. Yang W, Zhang Y, Li Y, Wu Z, Zhu D. Myostatin induces cyclin D1 degradation to cause cell cycle arrest through a phosphatidylinositol 3-kinase/AKT/GSK-3 beta pathway and is antagonized by insulin-like growth factor 1. The Journal of biological chemistry. [Research Support, Non-U.S. Gov't]. 2007 Feb 9;282(6):3799-808.
99. Reed SA, Sandesara PB, Senf SM, Judge AR. Inhibition of FoxO transcriptional activity prevents muscle fiber atrophy during cachexia and induces hypertrophy. FASEB J. 2012 Mar;26(3):987-1000.
100. Carlson CJ, Booth FW, Gordon SE. Skeletal muscle myostatin mRNA expression is fiber-type specific and increases during hindlimb unloading. The American journal of physiology. [Research Support, U.S. Gov't, Non-P.H.S.

Research Support, U.S. Gov't, P.H.S.]. 1999 Aug;277(2 Pt 2):R601-6.
101. Goldspink DF. The influence of immobilization and stretch on protein turnover of rat skeletal muscle. J Physiol. 1977 Jan;264(1):267-82.
102. Hassa PO, Hottiger MO. The functional role of poly(ADP-ribose)polymerase 1 as novel coactivator of NF-kappaB in inflammatory disorders. Cell Mol Life Sci. 2002 Sep;59(9):1534-53.
103. Hassa PO, Hottiger MO. A role of poly (ADP-ribose) polymerase in NF-kappaB transcriptional activation. Biol Chem. 1999 Jul-Aug;380(7-8):953-9.
104. Schiaffino S, Mammucari C. Regulation of skeletal muscle growth by the IGF1-Akt/PKB pathway: insights from genetic models. Skelet Muscle. 2011;1(1):4.
105. Gallot YS, Durieux AC, Castells J, Desgeorges MM, Vernus B, Plantureux L, et al. Myostatin gene inactivation prevents skeletal muscle wasting in cancer. Cancer Res. 2014 Dec 15;74(24):7344-56.
106. Benny Klimek ME, Aydogdu T, Link MJ, Pons M, Koniaris LG, Zimmers TA. Acute inhibition of myostatin-family proteins preserves skeletal muscle in

mouse models of cancer cachexia. Biochem Biophys Res Commun. 2010 Jan 15;391(3):1548-54.
107. Brunet A, Bonni A, Zigmond MJ, Lin MZ, Juo P, Hu LS, et al. Akt promotes cell survival by phosphorylating and inhibiting a Forkhead transcription factor. Cell. 1999 Mar 19;96(6):857-68.
108. White JP, Baynes JW, Welle SL, Kostek MC, Matesic LE, Sato S, et al. The regulation of skeletal muscle protein turnover during the progression of cancer cachexia in the Apc(Min/+) mouse. PLoS One. 2011;6(9):e24650.
109. Constantinou C, Fontes de Oliveira CC, Mintzopoulos D, Busquets S, He J, Kesarwani M, et al. Nuclear magnetic resonance in conjunction with functional genomics suggests mitochondrial dysfunction in a murine model of cancer cachexia. Int J Mol Med. 2011 Jan;27(1):15-24.
110. Taillandier D, Aurousseau E, Meynial-Denis D, Bechet D, Ferrara M, Cottin P, et al. Coordinate activation of lysosomal, Ca 2+-activated and ATP-ubiquitin-dependent proteinases in the unweighted rat soleus muscle. Biochem J. 1996 May 15;316 (Pt 1):65-72.
111. Adhihetty PJ, O'Leary MF, Chabi B, Wicks KL, Hood DA. Effect of denervation on mitochondrially mediated apoptosis in skeletal muscle. J Appl Physiol (1985). 2007 Mar;102(3):1143-51.
112. Ikemoto M, Nikawa T, Takeda S, Watanabe C, Kitano T, Baldwin KM, et al. Space shuttle flight (STS-90) enhances degradation of rat myosin heavy chain in association with activation of ubiquitin-proteasome pathway. FASEB J. 2001 May;15(7):1279-81.
113. Lecker SH, Solomon V, Mitch WE, Goldberg AL. Muscle protein breakdown and the critical role of the ubiquitin-proteasome pathway in normal and disease states. J Nutr. 1999 Jan;129(1S Suppl):227S-37S.
114. Bodine SC, Latres E, Baumhueter S, Lai VK, Nunez L, Clarke BA, et al. Identification of ubiquitin ligases required for skeletal muscle atrophy. Science. 2001 Nov 23;294(5547):1704-8.
115. Gomes MD, Lecker SH, Jagoe RT, Navon A, Goldberg AL. Atrogin-1, a muscle-specific F-box protein highly expressed during muscle atrophy. Proc Natl Acad Sci U S A. 2001 Dec 4;98(25):14440-5.
116. Kudryashova E, Kudryashov D, Kramerova I, Spencer MJ. Trim32 is a ubiquitin ligase mutated in limb girdle muscular dystrophy type 2H that binds to skeletal muscle myosin and ubiquitinates actin. J Mol Biol. 2005 Nov 25;354(2):413-24.
117. Baumeister W, Walz J, Zuhl F, Seemuller E. The proteasome: paradigm of a self-compartmentalizing protease. Cell. 1998 Feb 6;92(3):367-80.
118. Klionsky DJ. Autophagy: from phenomenology to molecular understanding in less than a decade. Nat Rev Mol Cell Biol. 2007 Nov;8(11):931-7.
119. Wang CW, Klionsky DJ. The molecular mechanism of autophagy. Mol Med. 2003 Mar-Apr;9(3-4):65-76.
120. Penna F, Costamagna D, Pin F, Camperi A, Fanzani A, Chiarpotto EM, et al. Autophagic degradation contributes to muscle wasting in cancer cachexia. Am J Pathol. 2013 Apr;182(4):1367-78.
121. Koh TJ, Tidball JG. Nitric oxide inhibits calpain-mediated proteolysis of talin in skeletal muscle cells. Am J Physiol Cell Physiol. 2000 Sep;279(3):C806-12.

122. Purintrapiban J, Wang MC, Forsberg NE. Degradation of sarcomeric and cytoskeletal proteins in cultured skeletal muscle cells. Comp Biochem Physiol B Biochem Mol Biol. 2003 Nov;136(3):393-401.
123. Tisdale MJ. Mechanisms of cancer cachexia. Physiol Rev. 2009 Apr;89(2):381-410.
124. Talbert EE, Smuder AJ, Min K, Kwon OS, Powers SK. Calpain and caspase-3 play required roles in immobilization-induced limb muscle atrophy. J Appl Physiol (1985). 2013 May 15;114(10):1482-9.
125. Hengartner MO. The biochemistry of apoptosis. Nature. 2000 Oct 12;407(6805):770-6.
126. Norbury CJ, Hickson ID. Cellular responses to DNA damage. Annu Rev Pharmacol Toxicol. 2001;41:367-401.
127. Siu PM, Pistilli EE, Alway SE. Apoptotic responses to hindlimb suspension in gastrocnemius muscles from young adult and aged rats. Am J Physiol Regul Integr Comp Physiol. 2005 Oct;289(4):R1015-26.
128. Alway SE, Degens H, Krishnamurthy G, Chaudhrai A. Denervation stimulates apoptosis but not Id2 expression in hindlimb muscles of aged rats. J Gerontol A Biol Sci Med Sci. 2003 Aug;58(8):687-97.
129. Alway SE, Martyn JK, Ouyang J, Chaudhrai A, Murlasits ZS. Id2 expression during apoptosis and satellite cell activation in unloaded and loaded quail skeletal muscles. Am J Physiol Regul Integr Comp Physiol. 2003 Feb;284(2):R540-9.
130. Busquets S, Figueras MT, Fuster G, Almendro V, Moore-Carrasco R, Ametller E, et al. Anticachectic effects of formoterol: a drug for potential treatment of muscle wasting. Cancer Res. 2004 Sep 15;64(18):6725-31.
131. White JP, Puppa MJ, Sato S, Gao S, Price RL, Baynes JW, et al. IL-6 regulation on skeletal muscle mitochondrial remodeling during cancer cachexia in the ApcMin/+ mouse. Skelet Muscle. 2012;2:14.
132. Puente-Maestu L, Lazaro A, Tejedor A, Camano S, Fuentes M, Cuervo M, et al. Effects of exercise on mitochondrial DNA content in skeletal muscle of patients with COPD. Thorax. 2011 Feb;66(2):121-7.
133. Puente-Maestu L, Tejedor A, Lazaro A, de Miguel J, Alvarez-Sala L, Gonzalez-Aragoneses F, et al. Site of mitochondrial reactive oxygen species production in skeletal muscle of chronic obstructive pulmonary disease and its relationship with exercise oxidative stress. Am J Respir Cell Mol Biol. 2012 Sep;47(3):358-62.
134. Andreu AL, Martinez R, Marti R, Garcia-Arumi E. Quantification of mitochondrial DNA copy number: pre-analytical factors. Mitochondrion. 2009 Jul;9(4):242-6.
135. Bai P, Canto C. The role of PARP-1 and PARP-2 enzymes in metabolic regulation and disease. Cell Metab. 2012 Sep 5;16(3):290-5.
136. Krishnakumar R, Kraus WL. The PARP side of the nucleus: molecular actions, physiological outcomes, and clinical targets. Mol Cell. 2010 Jul 9;39(1):8-24.
137. Yelamos J, Farres J, Llacuna L, Ampurdanes C, Martin-Caballero J. PARP-1 and PARP-2: New players in tumour development. Am J Cancer Res. 2011;1(3):328-46.
138. Burkle A, Virag L. Poly(ADP-ribose): PARadigms and PARadoxes. Mol Aspects Med. 2013 Dec;34(6):1046-65.

139. Sims JL, Berger SJ, Berger NA. Effects of nicotinamide on NAD and poly(ADP-ribose) metabolism in DNA-damaged human lymphocytes. J Supramol Struct Cell Biochem. 1981;16(3):281-8.
140. Ying W, Chen Y, Alano CC, Swanson RA. Tricarboxylic acid cycle substrates prevent PARP-mediated death of neurons and astrocytes. J Cereb Blood Flow Metab. 2002 Jul;22(7):774-9.
141. Yu J, Auwerx J. The role of sirtuins in the control of metabolic homeostasis. Ann N Y Acad Sci. 2009 Sep;1173 Suppl 1:E10-9.
142. Houtkooper RH, Canto C, Wanders RJ, Auwerx J. The secret life of NAD+: an old metabolite controlling new metabolic signaling pathways. Endocr Rev. 2010 Apr;31(2):194-223.
143. Williams CB, Gurd BJ. Skeletal muscle SIRT1 and the genetics of metabolic health: therapeutic activation by pharmaceuticals and exercise. Appl Clin Genet. 2012;5:81-91.
144. Vinciguerra M, Fulco M, Ladurner A, Sartorelli V, Rosenthal N. SirT1 in muscle physiology and disease: lessons from mouse models. Dis Model Mech. 2010 May-Jun;3(5-6):298-303.
145. Bai P, Canto C, Oudart H, Brunyanszki A, Cen Y, Thomas C, et al. PARP-1 inhibition increases mitochondrial metabolism through SIRT1 activation. Cell Metab. 2011 Apr 6;13(4):461-8.
146. Bai P, Canto C, Brunyanszki A, Huber A, Szanto M, Cen Y, et al. PARP-2 regulates SIRT1 expression and whole-body energy expenditure. Cell Metab. 2011 Apr 6;13(4):450-60.
147. Sui H, Shi C, Yan Z, Li H. Combination of erlotinib and a PARP inhibitor inhibits growth of A2780 tumor xenografts due to increased autophagy. Drug Des Devel Ther. 2015;9:3183-90.
148. Tewari KS, Eskander RN, Monk BJ. Development of Olaparib for BRCA-Deficient Recurrent Epithelial Ovarian Cancer. Clin Cancer Res. 2015 Sep 1;21(17):3829-35.
149. Schiewer MJ, Goodwin JF, Han S, Brenner JC, Augello MA, Dean JL, et al. Dual roles of PARP-1 promote cancer growth and progression. Cancer Discov. 2012 Dec;2(12):1134-49.
150. De P, Sun Y, Carlson JH, Friedman LS, Leyland-Jones BR, Dey N. Doubling down on the PI3K-AKT-mTOR pathway enhances the antitumor efficacy of PARP inhibitor in triple negative breast cancer model beyond BRCA-ness. Neoplasia. 2014 Jan;16(1):43-72.
151. Rojo F, Garcia-Parra J, Zazo S, Tusquets I, Ferrer-Lozano J, Menendez S, et al. Nuclear PARP-1 protein overexpression is associated with poor overall survival in early breast cancer. Ann Oncol. 2012 May;23(5):1156-64.
152. Mateu-Jimenez M, Cucarull-Martinez B, Yelamos J, Barreiro E. Reduced tumor burden through increased oxidative stress in lung adenocarcinoma cells of PARP-1 and PARP-2 knockout mice. Biochimie. 2016 Feb;121:278-86.
153. Davar D, Beumer JH, Hamieh L, Tawbi H. Role of PARP inhibitors in cancer biology and therapy. Curr Med Chem. 2012;19(23):3907-21.
154. Postel-Vinay S, Bajrami I, Friboulet L, Elliott R, Fontebasso Y, Dorvault N, et al. A high-throughput screen identifies PARP1/2 inhibitors as a potential therapy for ERCC1-deficient non-small cell lung cancer. Oncogene. 2013 Nov 21;32(47):5377-87.

155. Barreiro E, Sznajder JI. Epigenetic regulation of muscle phenotype and adaptation: a potential role in COPD muscle dysfunction. J Appl Physiol (1985). 2013 May;114(9):1263-72.
156. Puig-Vilanova E, Aguilo R, Rodriguez-Fuster A, Martinez-Llorens J, Gea J, Barreiro E. Epigenetic mechanisms in respiratory muscle dysfunction of patients with chronic obstructive pulmonary disease. PLoS One. 2014;9(11):e111514.
157. Puig-Vilanova E, Ausin P, Martinez-Llorens J, Gea J, Barreiro E. Do epigenetic events take place in the vastus lateralis of patients with mild chronic obstructive pulmonary disease? PLoS One. 2014;9(7):e102296.
158. Allen DL, Bandstra ER, Harrison BC, Thorng S, Stodieck LS, Kostenuik PJ, et al. Effects of spaceflight on murine skeletal muscle gene expression. J Appl Physiol. 2009 Feb;106(2):582-95.
159. Baar K. Epigenetic control of skeletal muscle fibre type. Acta Physiol (Oxf). 2010 Aug;199(4):477-87.
160. McKinsey TA, Zhang CL, Olson EN. Control of muscle development by dueling HATs and HDACs. Curr Opin Genet Dev. 2001 Oct;11(5):497-504.
161. Kouzarides T. Chromatin modifications and their function. Cell. 2007 Feb 23;128(4):693-705.
162. Bannister AJ, Kouzarides T. Regulation of chromatin by histone modifications. Cell Res. 2011 Mar;21(3):381-95.
163. Alamdari N, Aversa Z, Castillero E, Hasselgren PO. Acetylation and deacetylation-novel factors in muscle wasting. Metabolism. 2013 Jan;62(1):1-11.
164. de Ruijter AJ, van Gennip AH, Caron HN, Kemp S, van Kuilenburg AB. Histone deacetylases (HDACs): characterization of the classical HDAC family. Biochem J. 2003 Mar 15;370(Pt 3):737-49.
165. Alamdari N, Smith IJ, Aversa Z, Hasselgren PO. Sepsis and glucocorticoids upregulate p300 and downregulate HDAC6 expression and activity in skeletal muscle. Am J Physiol Regul Integr Comp Physiol. 2010 Aug;299(2):R509-20.
166. Yang H, Wei W, Menconi M, Hasselgren PO. Dexamethasone-induced protein degradation in cultured myotubes is p300/HAT dependent. Am J Physiol Regul Integr Comp Physiol. 2007 Jan;292(1):R337-4.
167. Cohen TJ, Waddell DS, Barrientos T, Lu Z, Feng G, Cox GA, et al. The histone deacetylase HDAC4 connects neural activity to muscle transcriptional reprogramming. J Biol Chem. 2007 Nov 16;282(46):33752-9.
168. Chen L, Fischle W, Verdin E, Greene WC. Duration of nuclear NF-kappaB action regulated by reversible acetylation. Science. 2001 Aug 31;293(5535):1653-7.
169. Williams JP, Phillips BE, Smith K, Atherton PJ, Rankin D, Selby AL, et al. Effect of tumor burden and subsequent surgical resection on skeletal muscle mass and protein turnover in colorectal cancer patients. Am J Clin Nutr. 2012 Nov;96(5):1064-70.
170. Lee D, Goldberg AL. SIRT1 protein, by blocking the activities of transcription factors FoxO1 and FoxO3, inhibits muscle atrophy and promotes muscle growth. J Biol Chem. 2013 Oct 18;288(42):30515-26.
171. Amat R, Planavila A, Chen SL, Iglesias R, Giralt M, Villarroya F. SIRT1 controls the transcription of the peroxisome proliferator-activated receptor-gamma Co-activator-1alpha (PGC-1alpha) gene in skeletal muscle through the

PGC-1alpha autoregulatory loop and interaction with MyoD. J Biol Chem. 2009 Aug 14;284(33):21872-80.
172. Xu J, Li R, Workeneh B, Dong Y, Wang X, Hu Z. Transcription factor FoxO1, the dominant mediator of muscle wasting in chronic kidney disease, is inhibited by microRNA-486. Kidney Int. 2012 Aug;82(4):401-11.
173. Kwon HS, Ott M. The ups and downs of SIRT1. Trends Biochem Sci. 2008 Nov;33(11):517-25.
174. Caron C, Boyault C, Khochbin S. Regulatory cross-talk between lysine acetylation and ubiquitination: role in the control of protein stability. Bioessays. 2005 Apr;27(4):408-15.
175. Rao PK, Kumar RM, Farkhondeh M, Baskerville S, Lodish HF. Myogenic factors that regulate expression of muscle-specific microRNAs. Proc Natl Acad Sci U S A. 2006 Jun 6;103(23):8721-6.
176. Natanek SA, Riddoch-Contreras J, Marsh GS, Hopkinson NS, Man WD, Moxham J, et al. Yin Yang 1 expression and localisation in quadriceps muscle in COPD. Arch Bronconeumol. 2011 Jun;47(6):296-302.
177. Hamilton AJ, Baulcombe DC. A species of small antisense RNA in posttranscriptional gene silencing in plants. Science. 1999 Oct 29;286(5441):950-2.
178. Guller I, Russell AP. MicroRNAs in skeletal muscle: their role and regulation in development, disease and function. J Physiol. 2010 Nov 1;588(Pt 21):4075-87.
179. Reinhart BJ, Slack FJ, Basson M, Pasquinelli AE, Bettinger JC, Rougvie AE, et al. The 21-nucleotide let-7 RNA regulates developmental timing in Caenorhabditis elegans. Nature. 2000 Feb 24;403(6772):901-6.
180. Williams AH, Liu N, van Rooij E, Olson EN. MicroRNA control of muscle development and disease. Curr Opin Cell Biol. 2009 Jun;21(3):461-9.
181. Chen JF, Tao Y, Li J, Deng Z, Yan Z, Xiao X, et al. microRNA-1 and microRNA-206 regulate skeletal muscle satellite cell proliferation and differentiation by repressing Pax7. J Cell Biol. 2010 Sep 6;190(5):867-79.
182. Dey BK, Gagan J, Dutta A. miR-206 and -486 induce myoblast differentiation by downregulating Pax7. Mol Cell Biol. 2011 Jan;31(1):203-14.
183. Liu N, Williams AH, Kim Y, McAnally J, Bezprozvannaya S, Sutherland LB, et al. An intragenic MEF2-dependent enhancer directs muscle-specific expression of microRNAs 1 and 133. Proc Natl Acad Sci U S A. 2007 Dec 26;104(52):20844-9.
184. Chen JF, Mandel EM, Thomson JM, Wu Q, Callis TE, Hammond SM, et al. The role of microRNA-1 and microRNA-133 in skeletal muscle proliferation and differentiation. Nat Genet. 2006 Feb;38(2):228-33.
185. Kim HK, Lee YS, Sivaprasad U, Malhotra A, Dutta A. Muscle-specific microRNA miR-206 promotes muscle differentiation. J Cell Biol. 2006 Aug 28;174(5):677-87.
186. Lewis A, Riddoch-Contreras J, Natanek SA, Donaldson A, Man WD, Moxham J, et al. Downregulation of the serum response factor/miR-1 axis in the quadriceps of patients with COPD. Thorax. 2012 Jan;67(1):26-34.
187. Shi M, Ishikawa M, Kamei N, Nakasa T, Adachi N, Deie M, et al. Acceleration of skeletal muscle regeneration in a rat skeletal muscle injury model by local injection of human peripheral blood-derived CD133-positive cells. Stem Cells. 2009 Apr;27(4):949-60.

188. Barreiro E, Gea J. Epigenetics and muscle dysfunction in chronic obstructive pulmonary disease. Transl Res. 2015 Jan;165(1):61-73.
189. Evans WJ, Morley JE, Argiles J, Bales C, Baracos V, Guttridge D, et al. Cachexia: a new definition. Clin Nutr. 2008 Dec;27(6):793-9.
190. Deitrick JE. The effect of immobilization on metabolic and physiological functions of normal men. Bull N Y Acad Med. 1948 Jun;24(6):364-75.
191. Gibson JN, Halliday D, Morrison WL, Stoward PJ, Hornsby GA, Watt PW, et al. Decrease in human quadriceps muscle protein turnover consequent upon leg immobilization. Clin Sci (Lond). 1987 Apr;72(4):503-9.
192. Barreiro E, Puig-Vilanova E, Marin-Corral J, Chacon-Cabrera A, Salazar-Degracia A, Mateu X, et al. Therapeutic Approaches in Mitochondrial Dysfunction, Proteolysis, and Structural Alterations of Diaphragm and Gastrocnemius in Rats With Chronic Heart Failure. J Cell Physiol. 2016 Jul;231(7):1495-513.
193. Bertaggia E, Coletto L, Sandri M. Posttranslational modifications control FoxO3 activity during denervation. Am J Physiol Cell Physiol. 2012 Feb 1;302(3):C587-96.
194. Senf SM, Dodd SL, Judge AR. FOXO signaling is required for disuse muscle atrophy and is directly regulated by Hsp70. Am J Physiol Cell Physiol. 2010 Jan;298(1):C38-45.
195. Mourkioti F, Kratsios P, Luedde T, Song YH, Delafontaine P, Adami R, et al. Targeted ablation of IKK2 improves skeletal muscle strength, maintains mass, and promotes regeneration. J Clin Invest. 2006 Nov;116(11):2945-54.
196. McCarthy JJ, Esser KA. MicroRNA-1 and microRNA-133a expression are decreased during skeletal muscle hypertrophy. Journal of applied physiology. [Research Support, N.I.H., Extramural]. 2007 Jan;102(1):306-13.
197. Hitachi K, Nakatani M, Tsuchida K. Myostatin signaling regulates Akt activity via the regulation of miR-486 expression. The international journal of biochemistry & cell biology. [Research Support, Non-U.S. Gov't]. 2014 Feb;47:93-103.
198. Ferreira R, Neuparth MJ, Ascensao A, Magalhaes J, Vitorino R, Duarte JA, et al. Skeletal muscle atrophy increases cell proliferation in mice gastrocnemius during the first week of hindlimb suspension. European journal of applied physiology. [Research Support, Non-U.S. Gov't]. 2006 Jun;97(3):340-6.
199. McGeachie JK. Sustained cell proliferation in denervated skeletal muscle of mice. Cell Tissue Res. [Research Support, Non-U.S. Gov't]. 1989 Aug;257(2):455-7.
200. Rodrigues Ade C, Schmalbruch H. Satellite cells and myonuclei in long-term denervated rat muscles. Anat Rec. [Research Support, Non-U.S. Gov't]. 1995 Dec;243(4):430-7.
201. Puig-Vilanova E, Martinez-Llorens J, Ausin P, Roca J, Gea J, Barreiro E. Quadriceps muscle weakness and atrophy are associated with a differential epigenetic profile in advanced COPD. Clin Sci (Lond). 2015 Jun;128(12):905-21.
202. Sadoul K, Boyault C, Pabion M, Khochbin S. Regulation of protein turnover by acetyltransferases and deacetylases. Biochimie. 2008 Feb;90(2):306-12.

203. Motta MC, Divecha N, Lemieux M, Kamel C, Chen D, Gu W, et al. Mammalian SIRT1 represses forkhead transcription factors. Cell. [Research Support, Non-U.S. Gov't

Research Support, U.S. Gov't, P.H.S.]. 2004 Feb 20;116(4):551-63.
204. Perrot V, Rechler MM. The coactivator p300 directly acetylates the forkhead transcription factor Foxo1 and stimulates Foxo1-induced transcription. Molecular endocrinology. 2005 Sep;19(9):2283-98.
205. Yang Y, Hou H, Haller EM, Nicosia SV, Bai W. Suppression of FOXO1 activity by FHL2 through SIRT1-mediated deacetylation. The EMBO journal. [Research Support, U.S. Gov't, Non-P.H.S.

Research Support, U.S. Gov't, P.H.S.]. 2005 Mar 9;24(5):1021-32.
206. Tseng AH, Wu LH, Shieh SS, Wang DL. SIRT3 interactions with FOXO3 acetylation, phosphorylation and ubiquitinylation mediate endothelial cell responses to hypoxia. Biochem J. 2014 Nov 15;464(1):157-68.
207. Minucci S, Pelicci PG. Histone deacetylase inhibitors and the promise of epigenetic (and more) treatments for cancer. Nature reviews Cancer. [Review]. 2006 Jan;6(1):38-51.
208. Fontes-Oliveira CC, Busquets S, Fuster G, Ametller E, Figueras M, Olivan M, et al. A differential pattern of gene expression in skeletal muscle of tumor-bearing rats reveals dysregulation of excitation-contraction coupling together with additional muscle alterations. Muscle Nerve. 2014 Feb;49(2):233-48.
209. Wall BT, Dirks ML, Snijders T, van Dijk JW, Fritsch M, Verdijk LB, et al. Short-term muscle disuse lowers myofibrillar protein synthesis rates and induces anabolic resistance to protein ingestion. Am J Physiol Endocrinol Metab. 2016 Jan 15;310(2):E137-47.
210. Csibi A, Cornille K, Leibovitch MP, Poupon A, Tintignac LA, Sanchez AM, et al. The translation regulatory subunit eIF3f controls the kinase-dependent mTOR signaling required for muscle differentiation and hypertrophy in mouse. PloS one. [Research Support, Non-U.S. Gov't]. 2010;5(2):e8994.
211. Lagirand-Cantaloube J, Offner N, Csibi A, Leibovitch MP, Batonnet-Pichon S, Tintignac LA, et al. The initiation factor eIF3-f is a major target for atrogin1/MAFbx function in skeletal muscle atrophy. The EMBO journal. [Research Support, Non-U.S. Gov't]. 2008 Apr 23;27(8):1266-76.
212. Barreiro E, Fermoselle C, Mateu-Jimenez M, Sanchez-Font A, Pijuan L, Gea J, et al. Oxidative stress and inflammation in the normal airways and blood of patients with lung cancer and COPD. Free radical biology & medicine. [Research Support, Non-U.S. Gov't]. 2013 Dec;65:859-71.
213. Crossland H, Constantin-Teodosiu D, Gardiner SM, Constantin D, Greenhaff PL. A potential role for Akt/FOXO signalling in both protein loss and the impairment of muscle carbohydrate oxidation during sepsis in rodent skeletal muscle. The Journal of physiology. [Research Support, Non-U.S. Gov't]. 2008 Nov 15;586(22):5589-600.
214. Frost RA, Lang CH. Regulation of muscle growth by pathogen-associated molecules. J Anim Sci. [Research Support, N.I.H., Extramural

Review]. 2008 Apr;86(14 Suppl):E84-93.

215. Brooks NE, Myburgh KH. Skeletal muscle wasting with disuse atrophy is multi-dimensional: the response and interaction of myonuclei, satellite cells and signaling pathways. Frontiers in physiology. [Review]. 2014;5:99.
216. Adams GR, Haddad F, Bodell PW, Tran PD, Baldwin KM. Combined isometric, concentric, and eccentric resistance exercise prevents unloading-induced muscle atrophy in rats. Journal of applied physiology. [Research Support, Non-U.S. Gov't]. 2007 Nov;103(5):1644-54.
217. Park S, Brisson BK, Liu M, Spinazzola JM, Barton ER. Mature IGF-I excels in promoting functional muscle recovery from disuse atrophy compared with pro-IGF-IA. Journal of applied physiology. [Comparative Study

Research Support, N.I.H., Extramural]. 2014 Apr 1;116(7):797-806.
218. Dirks ML, Wall BT, Nilwik R, Weerts DH, Verdijk LB, van Loon LJ. Skeletal muscle disuse atrophy is not attenuated by dietary protein supplementation in healthy older men. J Nutr. 2014 Aug;144(8):1196-203.
219. Smith HK, Matthews KG, Oldham JM, Jeanplong F, Falconer SJ, Bass JJ, et al. Translational signalling, atrogenic and myogenic gene expression during unloading and reloading of skeletal muscle in myostatin-deficient mice. PLoS One. 2014;9(4):e94356.
220. Swindall AF, Stanley JA, Yang ES. PARP-1: Friend or Foe of DNA Damage and Repair in Tumorigenesis? Cancers (Basel). 2013;5(3):943-58.
221. Ethier C, Tardif M, Arul L, Poirier GG. PARP-1 modulation of mTOR signaling in response to a DNA alkylating agent. PLoS One. 2012;7(10):e47978.
222. Bai P, Nagy L, Fodor T, Liaudet L, Pacher P. Poly(ADP-ribose) polymerases as modulators of mitochondrial activity. Trends Endocrinol Metab. 2015 Feb;26(2):75-83.
223. Rajamohan SB, Pillai VB, Gupta M, Sundaresan NR, Birukov KG, Samant S, et al. SIRT1 promotes cell survival under stress by deacetylation-dependent deactivation of poly(ADP-ribose) polymerase 1. Mol Cell Biol. 2009 Aug;29(15):4116-29.
224. Higashida K, Kim SH, Jung SR, Asaka M, Holloszy JO, Han DH. Effects of resveratrol and SIRT1 on PGC-1alpha activity and mitochondrial biogenesis: a reevaluation. PLoS biology. [Research Support, N.I.H., Extramural

Research Support, Non-U.S. Gov't]. 2013 Jul;11(7):e1001603.
225. Ray Hamidie RD, Yamada T, Ishizawa R, Saito Y, Masuda K. Curcumin treatment enhances the effect of exercise on mitochondrial biogenesis in skeletal muscle by increasing cAMP levels. Metabolism: clinical and experimental. [Research Support, Non-U.S. Gov't]. 2015 Oct;64(10):1334-47.

ADDENDUM

Besides the scientific publications which collect the results of the current PhD thesis, during my formative stage under the supervision of Dr. Esther Barreiro, I have had the opportunity to collaborate in other studies which have been already published in international journals:

Chacon-Cabrera A, Rojas Y, Martínez-Caro L, Vila-Ubach M, Nin N, Ferruelo A, Esteban A, Lorente JA, Barreiro E. Influence of mechanical ventilation and sepsis on redox balance in diaphragm, myocardium, limb muscles, and lungs. Transl Res. 2014;164(6):477-95.

Barreiro E, Puig-Vilanova E, Marin-Corral J, **Chacon-Cabrera A**, Salazar-Degracia A, Mateu X, Puente-Maestu L, García-Arumí E, Andreu AL, Molina L. Therapeutic Approaches in Mitochondrial Dysfunction, Proteolysis, and Structural Alterations of Diaphragm and Gastrocnemius in Rats With Chronic Heart Failure.
J Cell Physiol. 2016;231(7):1495-513.